NOVA SCHOOL OF SCIENCE & TECHNOLOGY

DEPARTAMENT OF MATERIALS SCIENCE

Inês Esteves dos Santos

BSc in Materials Engineering

Smart and stimuli-responsive materials based on nanocellulose

MASTER IN MATERIALS ENGINEERING

NOVA University Lisbon

October, 2023

NOVA SCHOOL OF SCIENCE & TECHNOLOGY

DEPARTAMENT OF
MATERIALS SCIENCE

Smart and stimuli-responsive materials based on nanocellulose

INÊS ESTEVES DOS SANTOS

BSc in Materials Engineering

Adviser: Doctor Susete Fernandes
Invited Assistant Professor, Materials Science Department, NOVA School of Science and Technology

Co-advisers: Doctor Ana Baptista
Ph.D. Researcher, Materials Science Department, NOVA School of Science and Technology

Examination Committee:

Chair: Doctor João Paulo Miranda Ribeiro Borges,
Cathedratic Professor, Materials Science Department, NOVA School of Science and Technology

Rapporteur: Doctor Ricardo Alexandre Ventura das Chagas,
Technical and Scientific Director, Food4Sustentability

Adviser: Doctor Susete Maria Brazão Nogueira Fernandes,
Invited Assistant Professor, Materials Science Department, NOVA School of Science and Technology

MASTER IN MATERIALS ENGINEERING

NOVA University Lisbon
October, 2023

Smart and stimuli-responsive materials based on nanocellulose

Copyright © Inês Esteves dos Santos, NOVA School of Science and Technology, NOVA University Lisbon, 2023.

The NOVA School of Science and Technology and the NOVA University Lisbon have the right, perpetual and without geographical boundaries, to file and publish this dissertation through printed copies reproduced on paper or in digital form, or by any other means known or that may be invented, and to disseminate through scientific repositories and admit its copying and distribution for non-commercial, educational or research purposes, as long as credit is given to the author and editor.

Aos meus pais, *Victor* e *Mª Lurdes*; e aos meus irmãos, *Vítor* e *Adriana*.

ACKNOWLEDGMENTS

Gostaria de expressar os meus agradecimentos a todos os que apoiaram e contribuíram para a conclusão desta tese. Esta jornada não teria sido possível sem o apoio constante, o incentivo e a inspiração de muitas pessoas e organizações.

Em primeiro lugar, destaco a minha profunda gratidão à minha orientadora. Drª. Susete Fernandes, pela orientação, experiência e paciência ao longo deste projeto. A sua orientação e apoio foram fundamentais para moldar a direção dos meus estudos. Adicionalmente, fico grata pela companhia nas pausas para cafés, lanches e almoços que ofereceu ao longo do projeto. Também agradeço à minha coorientadora, Drª. Ana Baptista, por me ajudar sempre que tive necessidade e por ter uma postura positiva que ajudou a motivar e a apaziguar as ansiedades que tinha relativamente ao trabalho. Especiais agradecimentos aos Professores Drª. Helena Godinho e Dr. João Canejo, que também me auxiliaram com o trabalho no laboratório, sobretudo nas imagens e configuração do microscópio.

Gostaria de reconhecer o apoio e os recursos fornecidos pela Faculdade da NOVA de Lisboa, em particular ao Departamento de Materiais (DCM), sem os quais este trabalho não teria sido possível.

Estendo a minha gratidão aos vários colegas de laboratório: aos alunos de Projeto (Francisco, Tiago, Maria e David) pela ajuda no laboratório na fase inicial, que foi fulcral para ganhar coragem e meter as “mãos na massa”; às alunas de doutoramento Adriana, pela compreensão e palavras amigas, e à Rafaela por me ajudar com a configuração no microscópio. E um especial agradecimento a Annalisa Bracco, Beatriz Silva e Beatriz Calado pelos momentos de entreajuda e descontração que proporcionaram um ambiente agradável no laboratório, ajudando a aliviar o peso do trabalho.

Agradeço especialmente às pessoas amigas: Ana Cruz, Ana Albuquerque, Carolina Bernardes, Gil Ferreira, Mariana Silva e a comité das Alfacinhas Mortíferas pelos pep-talks e tempo de qualidade!

Aos meus pais, Victor e Lurdes, e aos meus irmãos, Vítor e Adriana, que, apesar do distanciamento, demonstraram apoio constante, compreensão e incentivo durante esta jornada académica.

Por fim, dedico este trabalho à busca do conhecimento e à melhoria da nossa sociedade. Desejo que as descobertas desta pesquisa sejam relevantes para o nosso entendimento coletivo.

Obrigado a todos por fazerem parte desta jornada.

Este trabalho é suportado pela Fundação para a Ciência e a Tecnologia, I.P., no âmbito dos projetos LA/P/0037/2020, UIDP/50025/2020 and UIDB/50025/2020 Laboratório Associado Instituto de Nanoestruturas, Nanomodelação e Nanofabricação (I3N).

“The two most powerful warriors are patience and time.”

- Leo Tolstoy.

ABSTRACT

The development of cellulosic materials that respond to external stimuli while maintaining their structural integrity and meeting more sustainable objectives, is one of the current focus of the scientific community. The present thesis aims to produce films that react to stimuli, incorporating a CNC/HPC matrix and a nano-cellulosic derivative of azobenzene, the latter known for its responsive properties to various external stimuli such as light and temperature.

Initially, a cross-linking agent was selected to avoid disintegration of the matrix if in contact with water, which resulted in the choice of citric acid. The chemical-physical, structural analysis, and stimuli-responsi tests carried out on the nanocomposite systems allowed confirming the presence of the chiral nematic structure, and, using the Circular Dichroism technique, the Pitch value of the structure of each film was estimated. The incorporation of HPC/CA promoted an increase in Pitch value, while the increase in AzoCNC solids content caused a decrease. The Thermogravimetric analysis allowed us to observe that higher concentrations of AzoCNC result in greater thermal stability of the films. Additionally, these films showed photosensitivity to temperature and UV light. *Trans* to *cis* isomerization is complete after 8 minutes, and a full reversibility of *cis* to *trans* in the absence of light and a partial reversibility under visible light conditions occurs, although over very long times (>19h). *Cis-trans* backswitch is faster (15 min) if a temperature of 60 ºC is used. Wettability tests were carried out in *cis-trans* states showed minimal variation in samples with low concentrations of AzoCNC, however, the *cis* conformation becomes more hydrophilic for samples with higher concentrations.

The work developed suggests that flexible CNC/HPC/CA/AZO-CNC films, which respond to various external stimuli, present promising properties for use in innovative technologies, particularly in sensor applications that use ultraviolet light and thermal energy.

Keywords: Stimuli-responsive materials, nanocomposite films, cellulose nanocrystals, azobenzene-functionalization, isomerization, wettability.

RESUMO

O desenvolvimento de materiais celulósicos que respondam a estímulos externos, mantendo a sua integridade estrutural e cumprindo objetivos mais sustentáveis, é um dos focos atuais da comunidade científica. A presente tese tem como objetivo produzir membranas que reagem a estímulos, incorporando numa matriz de CNC/HPC e um derivado celulósico de azobenzeno, este último conhecido pelas suas propriedades de resposta a vários estímulos externos como luz e temperatura.

Inicialmente, procedeu-se à seleção de um agente de reticulação de modo a evitar a desintegração da matriz, se em contato com a água, o que resultou na escolha do ácido cítrico. A análise químico-física, estrutural e ensaios de estímulo-resposta efetuada aos sistemas nanocompósito permitiu confirmar a presença da estrutura nemática quiral e, com a técnica de Dicroísmo Circular, foi estimado o valor do passo da estrutura de cada membrana. A incorporação de HPC/CA promoveu um aumento no valor do passo, enquanto o aumento do teor de sólidos de AzoCNC causou uma diminuição. A análise termogravimétrica permitiu observar que concentrações mais elevadas de AzoCNC resultam numa maior estabilidade térmica das membranas. Adicionalmente, estas membranas apresentaram fotossensibilidade à temperatura e à luz UV. A isomerização *trans-cis* é total após 8 minutos, e uma reversibilidade total de *cis-trans* na ausência de luz e uma reversibilidade parcial sob condições de luz visible ocorre, embora em tempos muito longos (>19h). A retroversão *cis-trans* é mais rápida (15 min) se a temperatura de 60 ºC é utilizada. Testes de molhabilidade efetuados nos estados *cis-trans* apresentaram ruma variação mínima em amostras com concentrações baixas de AzoCNC, contudo a conformação *cis* torna-se mais hidrofílica para amostras com teor superiores.

O trabalho desenvolvido sugere que as membranas flexíveis CNC/HPC/CA/AzoCNC, que respondem a vários estímulos externos, apresentam propriedades promissoras a serem usados em tecnologias inovadoras, particularmente nas aplicações de sensores que utilizam luz ultravioleta e energia térmica.

Palavras-chave: Materiais responsivos a estímulos, filmes nanocompósitos, nanocristais de celulose, funcionalização de azobenzeno, isomerização, molhabilidade.

CONTENTS

1 INTRODUCTION 1

1.1 Cellulose and its derivatives 1

1.1.1 Cellulose Nanocrystals 1

1.2 Azobenzene and Azo-derivative systems 2

1.3 State-of-art: Stimuli-Responsive Systems 3

1.3.1 Self-healing nanocomposites 3

1.3.2 Shape memory systems 4

1.3.3 Physically Adaptive Systems 4

1.3.4 Optically adaptable smart systems 5

2 MATERIALS AND METHODS 7

2.1 Preparation of CNC suspensions and AzoCNC suspension. 7

2.2 Production and Characterization of CNC-based films 7

2.3 Stimuli-Response Tests 8

3 RESULTS AND DISCUSSION 9

3.1 System Selection and Production 10

3.1.1 Films Preparation: Cross-linker Selection 10

3.1.2 AzoCNC: Suspension preparation and AzoCNC isomerization 12

3.1.3 Production of the Nanocomposite Films 15

3.2 Stimuli-Response Tests 24

3.2.1 Isomerization phenomenon on the Nanocomposite Films 24

3.2.2 Wettability Tests 29

4 CONCLUSION 31

REFERENCES 33

LIST OF FIGURES

Figure 1.1. — A. Schemes illustrating the photoisomerization of the azobenzene compound, when exposed to UV/Vis light [27]; B1. Representation of the transition of the sol-gel phase of the composite and the three guest interactions between CNC and the grafted polymers, with CB[8] as the cross-linker (Adapted) [28]; B2. Visual demonstration of the hydrogel's self-healing capacities by stretching it, after being split and brought together (Adapted) [28]. 3
Figure 1.2 — A1. Images with a polarizer depicting a 3D-print butterfly made of PUA and CNC-DR1 particles with different printing directions at 0° and 45° angles with the polarizer [38]; A2. Photographs showing the light-driven SME Behavior of CNC-DR1 printed butterfly form, when exposed to a visible blue light - Adapted and reproduced under the term of CC-BY license [38]. Copyright 2022, The Authors, American Chemical Society; B. Pictures of the stretching in parallel directions to the CNC's orientation (left samples and pink arrows as a stretch direction indicator) and perpendicular (right samples and green arrows) showing the gradual color change (observed with crossed polarizers). – Reprinted with permission [44] Copyright 2023, American Chemical Society; C. Wettability test of the CNC-FAzo with a water droplet, exposing the highly hydrophobicity - Adapted and Reproduced under the term of CC-BY license [42] Copyright 2020, The Authors, MDPI. 5
Figure 3.1 — A. Information of the casted films of the composite system of CNC/HPC/CA: composition, solid content (wt.%) and average thickness (n=10); B-D. Photographs with cold white light (Scale bars: 1 cm): B. without polarizer; C. with LCPL; D. RCPL; E POM images evidencing the micro fingerprint (Scale bars: 20 μm). 13
Figure 3.2 — A ATR-FTIR Spectra of AzoCNC with a schematic representation of its possible chemical structure and degree of substitution; B Photograph of the AzoCNC suspension: with some aggregates at the bottom (B1) and after t>12 h since sonication (B2) (Scale bar: 1 cm); C POM photography obtained in transmission mode with cross polarizers(crossed white arrows) of AzoCNC suspension: before (C1) and after (C2) manual stirring (Scale bar: 50 μm). 14
Figure 3.3 — Absorption spectra obtained in time following the photoisomerization process of the AzoCNC suspension from *trans*- to *cis*-conformation when expose to UV light (A) until the maximum of *cis*-conformation was reached, seen in the closedup (A1), evolution of the back switch to *trans*-conformation with visible light (B) and close-up at the region including 450 nm (B1) and in the dark (C). 16

Figure 3.4 — Photographs of the CNC/AzoCNC films obtained with cold white light: with no polarizers (B), with left-handed (C) and right-handed (D) circular polarizers (indicated by the orientation of the arrows). (Scale bar:1 cm); (E) POM photography of the films (Scale bar: 20 µm). 17
Figure 3.5 — A-B Treated control samples at room temperature and after 15h and 60 ºC; C Treated AzoCNC samples after drying at 60 ºC (Scale bar: 5mm). 18
Figure 3.6 — ATR-FTIR spectra of the CNC, CNC/HPC and AzoCNC containing samples, highlighted the vibration bands of cellulose and cross-linker. 19
Figure 3.7 — SEM photography of the cross-section (A) and close-ups (B) of each film : 1- CNC/CA ;2- CNC/HPC/CA; 3 to 8 - CNC/HPC/CA/xAzoCNC (x= 0.1; 0.25; 1; 2.5; 5) (Scale bar: 1 µm). 20
Figure 3.8 — CD spectra normalized graphic representations of the nanocomposite systems in the wavelengths 190-750nm. (ABC); D – estimated pitch value by using the estimated index refractive values of the nanocomposite films and the maximum CD peak wavelength, using the *de Vries* equation. 23
Figure 3.9 — Graphic representations of: A-A2. TGA curve; B. DTG curve; C. DSC curve of the nanocomposite systems, CNC, and AzoCNC. 24
Figure 3.10 — Isomerization from trans- to cis-conformation with UV exposure (ABC) of samples with AzoCNC with the 1%, 2.5 % and 5 % wt.% with close-ups on the right side, respectively. 26
Figure 3.11 — Back switch from cis to trans conformation UV/Vis curves of sample with AZoCNC with 2.5 % AzoCNC (wt.%): in the dark (A) and with visible light (B); of with temperature (C). 27
Figure 3.12 — Back switch from *cis to trans* conformation UV/Vis curves of sample with 5 % AzoCNC (wt.%): in the dark (A); and with visible light (B); of with temperature (C). D. photographs of the UV exposure effect on the appearance of a 5 % wt.% AzoCNC sample. 28
Figure 3.13 — A. Contact Angle measurement of the treated and non-treated control samples and the respective contact angle values. (n=12); B. 5 % AzoCNC sample after 2 cycles of UV/Vis; C. 5 % AzoCNC sample state before UV exposure and after 8 cycles of UV/Vis (Scale bar: 1 mm). 30
Figure 4.1 — Representation of TGA/DSC/DTG curves and the secondary lines (blue dashed lines) for the determination of the onset and offset temperatures values. 1
Figure 4.2 — A. Information of the films casted of the composite system of CNC/CA: composition, solid content (wt.%); B-D. Photographs with cold white light (Scale bar: 1cm): B. without polarizer; C. LCPL (left-handed arrow); D with RCPL (right-handed arrow). 3
Figure 4.3 — A. Information of the films casted of the composite system of CNC/HPC/GA: composition, solid content (wt.%) and average thickness (n=10); B-D. Photographs with cold white light (Scale bar: 1cm): B. without polarizer; C. LCPL (left-handed arrow); D with RCPL (right-handed arrow). 4
Figure 4.4 — Contact angles measurement done in CNC/HPC/CA films containing 1-4 % wt.% of GA (n=8). 5
Figure 4.5 — Static Contact Angle measurements done onto the nanocomposite films with high concentrations of 1~5,1% wt.% AzoCNC.This measurements were done until the 8th cycle, measuring the static contact angle after 20 minutes UV exposure (yellow symbols) and after 20 minutes relaxation of the films, alternatively. 5
Figure 4.6 — Static Contact Angle measurements done onto the nanocomposite films with low concentrations of 0.1 %~0.19 % wt.% AzoCNC.This measurements were done until the 8th cycle,measuring the static contact angle after 20 minutes UV exposure (yellow symbols) and after 20 minutes relaxation of the films, alternatively. 6

Figure 4.7 — UV/Vis spectra of the isomerization study of the nanocomposite films with low concentrations of 0.06 %~0.25 % wt.% AzoCNC. 7
Figure 4.8 — CD spectra from both sides of each sample of CNC, CNC/CA, CNC/HPC/CA and films containing concentrations between 0.06 %~0.19 % wt.% AzoCNC. 8
Figure 4.9 — CD spectra from both sides of each film samples containing between 0.25 %~5.1 % wt.% AzoCNC. 9

LIST OF TABLES

Table 3.1 — Summary of the used temperatures and times that passed the wettability test conditions and the conditions selected for the system selection (in bold). 12
Table 3.2 — Values of the onset, offset, and degradation temperatures from the termogravimetric analysis. The estimation was done by auxiliary lines for the curves of TGA and DTG. 24
Table 4.1 — Estimated *n* values in accordance with the real percentages of each nanocomposite film. By the application of the *de Vries* Equation with the tabled CD maximum peak wavelengths, the estimated pitch values are obtained. 9

ACRONYMS

5CB	4-Cyano-4'-pentylbiphenyl
AFM	Atomic Force Microscopy
ATR- FTIR	Attenuated Total Reflectance Fourier-Transform Infrared
Azo	Azobenzene derivative
CA	Citric Acid
CD	Circular Dichroism
CNC	Cellulose Nanocrystals
DS	Substitution of Degree
EISA	Evaporation-Induced Self-Assembly
GA	Glutaraldehyde
HPC	Hydroxypropyl cellulose
LC	Liquid Crystalline
LCPL	Left-Circularly Polarized Light
M_w	Average Molecular Weight
POM	Polarized Optical Microscope
RCPL	Right-Circularly Polarized Light
SEM	Scanning Electron Microscope
UV/Vis	Ultraviolet – Visible spectroscopy
UVA	Ultraviolet A
TGA	Thermogravimetric Analysis
DTG	Derivative Thermogravimetry
DSC	Differential Scanning Calorimetry

SYMBOLS

^{o}C	Celsius Degrees
θc	Intrinsic contact angle
T	Temperature
t	Time
p	Pitch value
T_{onset}	Onset Temperature
T_{offset}	Offset Temperature
T_{deg}	Degradation Temperature
λ_0	Maximum Wavelength
n	Index refraction

CONTEXT AND MOTIVATION

The continuous demand for sustainable products has arisen due to environmental awareness, leading to the development of new polymeric materials whose properties remarkably change when subjected to external stimuli. When derived from cellulose derivatives, these so-called “smart” polymers have great advantages as they can be sustainable and, eco-friendly products and can be applied to many circumstances.

These materials come in various forms, including copolymers, nanoparticles, gels, and films, making them adaptable to a wide range of uses. They find applications in diverse fields, from drug carrier systems and self-healing hydrogels to smart actuators, sensing technology, smart films, and shape-memory materials.

One standout biomimetic option for creating these smart materials are cellulose nanocrystals (CNC) since it holds a high versatility of physical proprieties- as it can give support and stiffness to the polymer network to sustain the response to the stimuli; chemical properties – for the easy and versatile functionalization of its surface groups; and their optical properties – as a chiral CNC film is a humidity-sensitive material, where swelling can induce a color change.

Other responsive materials involved in smart systems are chromophores, which respond to variations in light and temperature, which leads to an alteration in the physical and/or chemical properties of the material. One illustrative example of such compounds is azobenzene organic dye.

By incorporating azobenzene and CNC-based materials into composite systems, we can create multi-responsive functionality. This positions them as excellent candidates for the development of sustainable products capable of responding to several external stimuli.

The primary objective of this work is to delve into composite systems based on CNC and other cellulosic derivatives. The primary focus is on producing materials functionalized with azo chromophores and their responses to external stimuli, including humidity, light, and temperature. Through this exploration, the aim is to unlock new possibilities for responsive and sustainable materials with potential applications across various industries.

The main objective of this dissertation will be the design of a nanocomposite system composed of nanocrystalline cellulose (CNC), of commercial origin; hydroxypropyl cellulose (HPC), a cross-linker agent and a CNC-functionalized with an azobenzene molecule. The aim intended is to create a stimuli-responsive system, inspired by examples from nature, safer and more secure.

Firstly, the CNC, CNC/HPC, and AzoCNC suspensions were prepared, and the CNC-based films were casted. Also, for the cross-linker selection, preliminary tests were carried out. Secondly, the production of the nanocomposite system films was done. The nanocomposite films underwent chemical and thermal characterization and stimuli-response tests that involved an isomerization study and wettability tests. Finally, the effect of adding AzoCNC to the CNC/HPC matrix on the optical and thermal properties of nanocomposite films was studied and compared with other azobenzene systems.

This dissertation is structured into four chapters. The first corresponds to a theoretical introduction of the fundamental concepts related to CNC and azobenzene and derivatives, the state-of-the-art Stimuli-Responsive Systems that involve azo compounds or AzoCNC. The second comprises the materials and methods carried out in a laboratory environment, followed by the chapter presenting and discussing the results, which are summarized in the last chapter, together with future perspectives for a more in-depth study on this topic.

1

INTRODUCTION

1.1 Cellulose and its derivatives

Cellulose has lately aroused a lot of interest among the scientific community and the industry as an alternative source, mainly for polymers derived from oil, due to being a biocompatible, renewable material. It appears in plants in the form of microfibrils. Because of the crystalline zones interspersed with amorphous zones, it presents rigidity, and mechanical strength, but also flexibility, being denominated a semicrystalline polymer [1]. From cellulose, several derivatives are obtained, by replacing the hydroxyl (OH) groups on the cellobiose unit, used in drugs, textiles, documents, and cars, for example.

1.1.1 Cellulose Nanocrystals

CNC are short highly crystalline nanosized particles (rods) that are products of the hydrolysis of visible cellulosic fibrils, from materials like plants or biomass, and have properties like high crystallinity, high Young's modulus, high specific surface area, lightness, high tensile strength, and high stiffness [2]. With these characteristics, CNC is heavily researched as a reinforcement of polymer matrices [3]. Besides this, CNC colloidal suspensions can present a lyotropic cholesteric liquid-crystalline (LC) behavior. This behavior is described as the transition from a liquid to a LC phase, which occurs with the variation of its concentration in a specific solvent, such as water [4]. A liquid crystal is an intermediate state of matter between the isotropic liquid and the crystalline solid, having the mechanical properties of a liquid (fluidity) and the anisotropic optical properties of a solid matter. In liquid crystals, there are different levels, organized by increasing order, called mesophases. There are variations of the molecular organization in the different mesophases depending on the distribution of defects and the anisotropic shape of the molecules, like smectic, nematic, and chiral nematic (cholesteric) [5]. At low concentrations of CNC in the suspension, the random orientation of the nanorods results in an isotropic phase. However, at higher concentrations, the alignment of the nanorods' direction is favored, transitioning from an isotropic phase to a chiral nematic phase. This LC behavior of CNC is characterized by the alignment of the nanorods along a direction, identified as the director, n, which spatially rotates in a helical structure around an axis, m, to the left. The distance where the direction of the vector is equal to another, that is, it describes a 360º turn is called pitch (p), and it is dimension decreases with the increase of the concentration of CNC [6], [7], [8], [9]. If the evaporation of the solvent occurs in a slow and controlled way, it can be verified that the LC phase is maintained in the solid system, although the pitch value decreases. The CNC films also display water absorption and swelling properties due to abundant hydrophilic (-OH) groups and hydrophobic (-CH) groups, which cause the absorption and clustering of the water on the crystalline surface layers [10]. Moreover, the CNC-based films have an optical property produced from the reflection of light that depends on the orientation, pitch value, and the helix retained in its structure.

Thus, it is possible to fluctuate the refractive indices within the material, causing a structural coloration to appear, iridescence, selectively reflected light of the left-handed circular polarization (LCP), intensifying the coloration observed; and selectively transmitted light of the right-handed circular polarization (RCP), which presents lower intensity in the same spot of the film, showing a darker appearance [4], [11]. Thus, these specific properties have been widely researched for applications in the medical field, nano-carriers, electronics, sensors, and anti-counterfeiting [12]. The CNC's surface can be modified by functionalization with specific groups by chemical functionalization or by adding polymers or molecules to have new, modified, or adjusted properties as a composite material, which enables more versatility for these high-end applications [13]. Additionally, CNC can be integrated with other compounds like chromophores, making them a good candidate to be part of smart hybrid systems[13], [14], [15].

1.2 Azobenzene and Azo-derivative systems

Chromophores are stimuli-responsive molecules that have photo-responsive properties, examples of these compounds are stilbene, spiro-compounds, fulgide, diarylethenes, and azobenzene [16]. The azobenzene (Azo) is composed of 2 phenyl rings linked by a double covalent nitrogen bond (N=N), which enables a variety of functionalized groups as an extension to the molecule (Figure 1.1A) [12]. This compound has two possible conformations, *cis* and *trans*, hence this *trans* conformation being the most stable. When exposed to ultraviolet (UV) irradiation or blue light, an isomerization occurs, that is, the compound changes to the *cis*-conformation. With the cease of the stimulus, the molecule returns to the most stable configuration. Each conformation has different physical and chemical properties like photo-responsive properties, response to the dipole moment, solubility, stability [12], [17], and the photo-isomerization process is reversible and fast [12], [14], [18]. It was also observed that heat can also induce photo-isomerization in azobenzene chromophores due to the thermodynamic stability of the -*trans* isomer [19], [20]. This photo-isomerization reaction can result in not only the visible color of the material but also in its physical and chemical properties. For instance, the integration of azobenzene in thermo-responsive polymeric structures induces a polarity shift when exposed to UV light, which can lead to distinct values of upper critical solution temperature (UCST) and lower critical solution temperature (LCST) of the polymer [16].

Due to these specific characteristics, azobenzene and its derivatives could be potentially applied in information storage devices, biosensors, and nonlinear optical materials [12]. To date, there are several reports that attempt to prepare photo-responsive in liquid crystal networks (LCNs), liquid crystal polymer networks (LCPs), and liquid crystal elastomer networks (LCEs) [21], [22], [23]. Pilz da Cunha et al. fabricated a light-responsive soft robot composed of 4 azobenzene and LCN films that operated as legs and arms, which were connected by polypropylene. The legs were composed of yellow azobenzene derivative, responsible for locomotion while the robotic arms were composed of red azobenzene chromophore, responsible for cargo handling. The arms and legs had different chromophores to achieve selective addressability for locomotion and cargo handling [22].

In recent years, azobenzene has been integrated with other cellulose derivatives to synthesize responsive materials [12]. Fernandes et al. have reported on the synthesis of a thermotropic material that was composed of (acetoxypropyl)cellulose (APC) and azobenzene. The produced nanostructures (Azo-APC Langmuir-Blodgett filaments, multilayers, and lamellae) displayed distinct wettability characteristics, which were determined by the film deposition conditions [24]. While the lamellae kept the predicted light-responsive behavior of Azo-APC, filaments and multilayer films exhibited hydrophilic behavior with no significant alterations. This implies that some assemblies, such as the Langmuir-Blodgett films, trap or restrict the mobility of the azobenzene molecules in the photo-isomerization, which is influenced by the nanostructure of the obtained material [12], [13], [24]. In the same year, Zhang et al. studied the phase transition behavior of 2-azobenzenoxy-ethoxyhydroxpropylcellulose (Azo-EHPC) in aqueous solution by etherifying bromoethoxy-azobenzene (BEA) with polymer hydroxypropylcellulose (HPC) [25]. Similarly, another cellulosic derivative grafted with azobenzene was produced, which gave

rise to a self-healing and photo-responsive hydrogel composed of β-cyclodextrin (CD) and azobenzene-grafted carboxymethyl cellulose (CMC-Azo), exhibiting gel-sol phase transition in response to UV light [26].

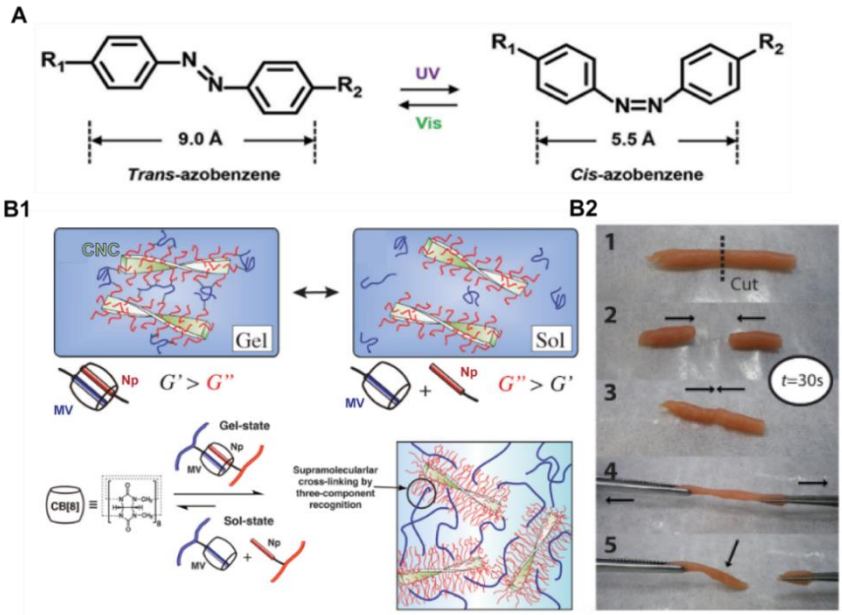

Figure 1.1. — A. Schemes illustrating the photoisomerization of the azobenzene compound, when exposed to UV/Vis light [27]; B1. Representation of the transition of the sol-gel phase of the composite and the three guest interactions between CNC and the grafted polymers, with CB[8] as the cross-linker (Adapted) [28]; B2. Visual demonstration of the hydrogel's self-healing capacities by stretching it, after being split and brought together (Adapted) [28].

1.3 State-of-art: Stimuli-Responsive Systems

The functional hybrid stimuli-responsive systems are considered "smart" since there's a change in their properties when an external stimulus like light, humidity, pH, and temperature is applied [2], [12], [29]. If the base of our system is a cellulosic derivative, like CNC, the smart behavior of these systems is promising due to its biocompatibility and biodegradability, which can address environmental issues [30]. Four categories of smart CNC hybrid systems have been studied lately: CNC-based shape memory polymeric materials and self-healing CNC composites [2], [31], [32]; CNC physically adaptive systems, in which CNC have the functionality needed to support the alteration of the physical properties in response to external stimuli [2], [33]; and optically adaptable systems, in which CNC have been incorporated due to its LC and optical properties [2], [10], [33]. The CNC can have a different and beneficial role that impacts these smart systems' performance. Some examples will be briefly presented.

1.3.1 Self-healing nanocomposites

Self-healing materials like hydrogels [28] and elastomers [34] can repair themselves, improving the functionality and lifetime of the polymer network [2]. CNC can be integrated as a reinforcing filler or an active agent in the polymer network as it improves the stiffness without significantly perturbing the molecular dynamics, which makes them a solution to this incurring issue of these self-healing polymer networks [2]. Similarly, CNC can be applied as a dynamic cross-linking agent to improve self-healing efficiency because of the abundant functional groups (OH) on the CNC's surface, which can be built through either non-covalent or covalent bonds [2], [28], [34]. McKee et al. studied a stiff hydrogel based on non-covalent cross-link interactions: it combined CNC-grafted with polymer brushes such as

naphthyl-functionalized methacrylate (NpMA) and dimethylaminoethyl methacrylate (DMAEMA); then, as a third guest, it was cross-linked with methyl viologen-functionalized poly (vinyl alcohol) (PVA), recurring to cucurbit[8]uril, as the cross-linking agent. The hydrogel got quick self-healing (Figure 1.1B1) and high storage modulus (G') (Figure 1.1B2) because of the specific three-component host-guest interactions [28]. Nevertheless, Cao et al. produced a self-healing, sustainable elastomer with mechanically improved properties based on covalent interactions, from TEMPO-oxidized CNC (TEMPO-CNC), used as a cross-linker and reinforcing agent, with epoxidized visible rubber (ENR), which generated bonds between the interface, consequently enabling topological changes in the elastomer structure, at high temperatures [34].

1.3.2 Shape memory systems

Shape memory polymers (SMPs) are polymers that can deform and return to it is previous shape by a change of pH or upon the effect of light, electric field, and magnetic field [2], [35], [36]. This cycle of mechanical deformation of the material is considered part of "programmable" behavior, known as the shape memory effect (SME) [35]. Additionally, as seen in the photoisomerization of azobenzene, light can increase the SMP temperature over the critical temperature (occurring the transition) and causing shape recovery [36]. This light-sensitive SME has raised interest in soft actuation purposes [27], [30], [37]. Müller et al. 3D-printed photo-responsive CNC-based composites via Direct Ink Writing (DIW) that integrates CNC reinforcing effects with the photo-responsive behavior of azobenzene compounds [38]. A polyurethane acrylate matrix (PUA) was added after the compound azobenzene Disperse Red 1 (DR1) was first grafted onto CNC surfaces. The CNC-DR1 particles influenced the rheology of the ink, making it gel-like and printable. This ink enabled the 3D-printing of a butterfly form, as it is visible in Figure 1.2A1. Also, the printed composite reacted and demonstrated shape memory behavior when exposed to VIS blue light, as shown in the Figure 1.2A2 [38].

1.3.3 Physically Adaptive Systems

Lately, research on multi-stimuli-responsive CNC-based systems has also taken place [2]. Yuan et al. produced a fluorescent nanosensor CNC-based material that reacts to changes in temperature, pH, and UV radiation. This material, CNC-g-P(AzoC6MA-co-DMAEMA), was synthesized recurring to surface-modified CNC with 2-bromoisobutyryl groups (CNC-Br), azobenzene moieties (AzoC6MA) and a pH- and thermo-responsive polymer DMAEMA [2], [12], [13], [39]. This material, due to the presence of the mentioned grafted-brushes, could transition between conformations if the temperature was above LCST or if the pH value was above pKa. When these conditions were met, it resulted in the collapse and accumulation of the grafted brushes [39]. So, this effect leads to a restriction of the isomerization of the azobenzene, contributing to an increase of the compound fluorescence when subjected to UV light. The implementation of the CNC aided the dispersion in water of the fluorescent nanosensor, suggesting potential applications for in-situ detection like keeping track of the temperature and pH of organisms or water [39].

Xu et al. also produced a novel azo-CNC system: a PMMAZO-grafted CNC with 6-[4-(4-methoxyphenyl-azo) phenoxy] hexyl methacrylate (MMAZO) by ATRP, which present thermotropic and lyotropic properties [40]. More recently, Liu et al. added polyurethane to PMMAZO-grafted CNC to produce a nanocomposite film. This photo-responsive and pH-responsive material may be suitable for acid-base detection and reversible optical storage applications [41]. However, this composite system uses an oil-based derivative.

Another azo-cellulosic derivative that has multi-response was fabricated by Xu et al., which involved the production of a hydrophobic hydrogel. This hydrogel was obtained by grafting 9-[4-[2-[4-(trifluorometh) phenyl] diazenyl] phenoxy] nonayl acrylate (FAzo) onto a CNC-functionalized with α-bromoisobutyryl bromide (CNC-Br) via ATRP. Then, the Dimethyl Sulfoxide (DMSO) solvent was used to

disperse the CNC-FAzo particles. These particles demonstrated a high contact angle (above 130º), indicating the hydrophobic behavior of the suspension, as can be seen in Figure 1.2C [42], [43].

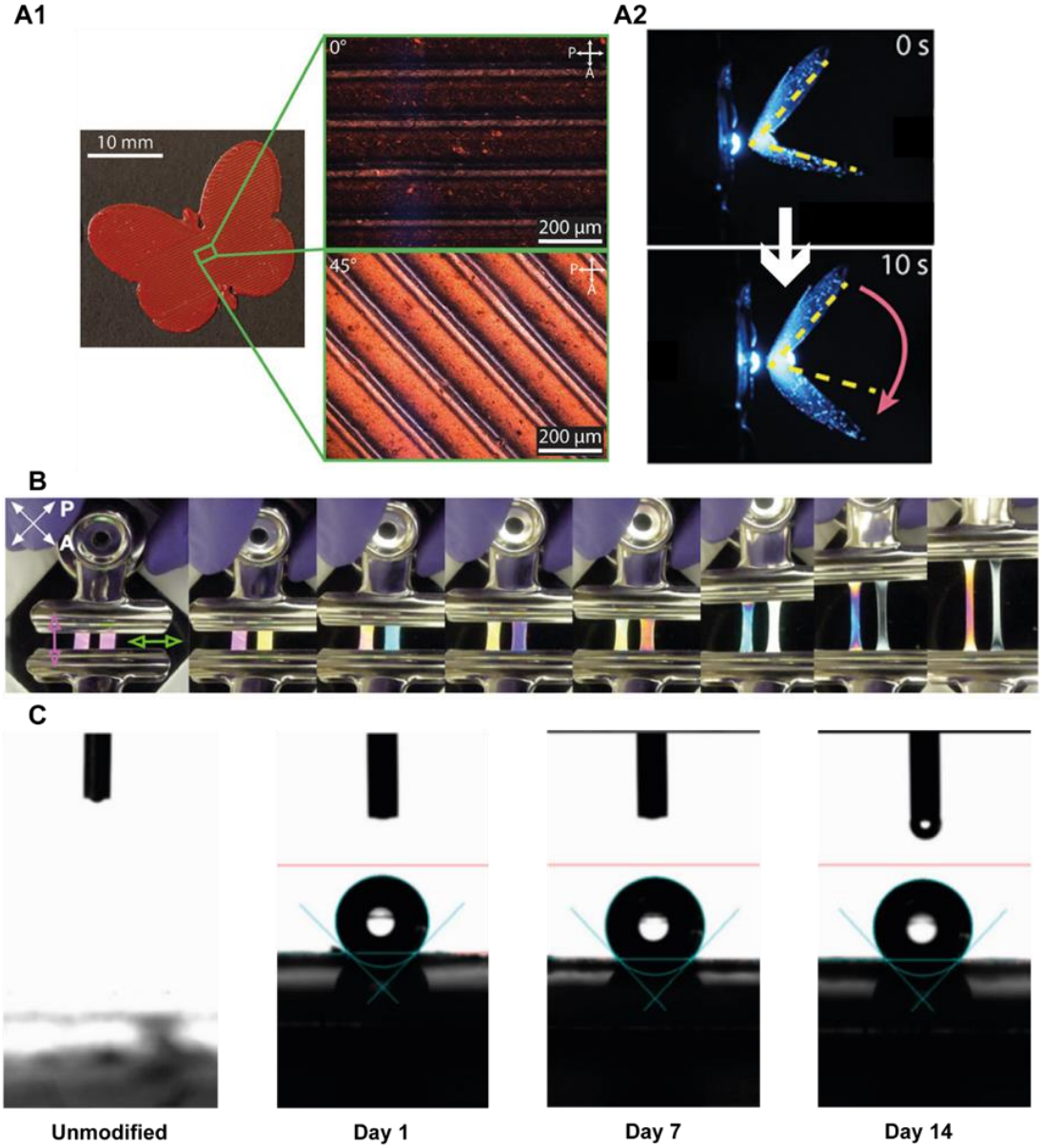

Figure 1.2 — A1. Images with a polarizer depicting a 3D-print butterfly made of PUA and CNC-DR1 particles with different printing directions at 0° and 45° angles with the polarizer [38]; A2. Photographs showing the light-driven SME Behavior of CNC-DR1 printed butterfly form, when exposed to a visible blue light - Adapted and reproduced under the term of CC-BY license [38]. Copyright 2022, The Authors, American Chemical Society; B. Pictures of the stretching in parallel directions to the CNC's orientation (left samples and pink arrows as a stretch direction indicator) and perpendicular (right samples and green arrows) showing the gradual color change (observed with crossed polarizers). – Reprinted with permission [44] Copyright 2023, American Chemical Society; C. Wettability test of the CNC-FAzo with a water droplet, exposing the highly hydrophobicity - Adapted and Reproduced under the term of CC-BY license [42] Copyright 2020, The Authors, MDPI.

1.3.4 Optically adaptable smart systems

CNC have been considered mainly for their structural and mechanical properties, easy surface functionalization, and optical properties, specifically reflectance and birefringence [2]. Nevertheless, to

obtain responsive systems that make use of the CNC's chirality, it has been applied different methodologies, like evaporation-induced self-assembly (EISA), which is one straightforward approach to produce these composites [2], [10]. Also, by taking advantage of CNC's water absorption and swelling properties, humidity-responsive materials have raised interest in humidity-sensing technology applications [2], [10]. As mentioned before, these systems may alter its coloration by a variation of the pitch, which is caused by the water absorption into each nematic layer of the film. One concern with these materials is that it needs a hygroscopic material that confers flexibility, as it shouldn't prevent the diffusion of water particles inside the layers, which remains one of the main challenges in these materials [2]. Nevertheless, other groups have successfully developed sustainable flexible CNC/cellulosic derivative composites adding HPC, while maintaining structural coloration [45], [46]. Currently, several research was done to cover the photonic mechano-responsive CNC systems namely composites, aerogels, and hydrogels [2], [10]. For example, Kose et al. prepared a strain-responsive film composed of CNC and an elastomer (CNC-E) by changing the nematic structure. By drying the combination of CNC and glucose units, the resulting films were soaked with DMSO, which enabled the polymerization of the film when added to poly(ethyl acrylate) (PEA). As a result, it formed a transparent CNC-E composite, which presented different coloration depending on the extent of the uniaxial strain, if the strain was in a parallel direction to the CNC alignment, it would increase the birefringence of the elastomer. On the other hand, if the stretching occurs in the perpendicular direction, it affects CNC orientation, resulting in the loss of birefringence, as seen in Figure 1.2B [44].

In contrast, it has been fewer studies on light-responsive systems that involve CNC photonic properties because of the fixation of the spatial position of the photonic CNC molecules [10]. One of those studies was done by Anusuyadevi et al., which reported on a photo-responsive photonic chiral CNC by drop-casting an azobenzene mesogenic compound 4-Butyl-4'-methoxyazobenzene (BMAB) and the nematic LC 4-Cyano-4′-pentylbiphenyl (5CB) on CNC/glucose film, benefiting of the LC phase transition of the 5CB. This transition from nematic to isotropic is triggered by the BMAB photoisomerization, culminating in a loss or gain of birefringence of the LC layer, depending on the transitioning of the BMAB being from *trans* to *cis* (Induced by the UV irradiation) or from *cis* to *trans* (exposed by VIS light), respectively [47].

From the examples shown above, one can conclude that the combination of CNC, azobenzene, and cellulose derivatives can give rise to a "smart" sustainable material. This work is intended to produce a multi-responsive CNC-based system by adding azobenzene-CNC, obtained via esterification reaction, and a cellulose derivative HPC, as an additive to improve flexibility, to an LC CNC suspension. The produced system is aimed to respond to UV radiation, pH, and humidity with changes in optical behavior.

2

MATERIALS AND METHODS

2.1 Preparation of CNC suspensions and AzoCNC suspension.

The aqueous colloidal suspension of CNC used in this dissertation is of commercial origin (CelluForce, Canada, NCC® NCV100-NAL90, Lot No. C1A21019), designated as CNC-C suspension. The CNC suspensions with sodium counterion (CNC-Na+) were prepared by using the stock suspension. The stock suspension showed a concentration of CNC of 6.04 % wt.% and preparation of the diluted suspension was done by adding ultrapure type II water, to attain around 3.5 % wt.% Two filtrations were proceeded to remove aggregates, first with a 50 µm filter, then with a syringe filter of 1.6 µm. Furthermore, a vortex (VELP Scientifica) was used to homogenize the prepared suspension before undergoing the sonication technique, using the UP400S processor (360 W, 24 kHz, Heilscher Ultrasonics GmbH, with a titanium probe) with 80% amplitude and an 80% pulsed cycle. Each CNC's suspension received 150 J/g suspension. Subsequently, the suspension was stored at room temperature without light exposure to promote the self-organization of the LC phase. The suspension concentration values were obtained by gravimetry, in which 8 aliquots were taken and dried in a chamber at 60 ºC until constant weight.

The CNC-4-(4-methoxyazobenzene-4'-yloxy)butyrate, AzoCNC, was previously synthesized in our lab and prepared under the framework of the project NANOCell2SEC. A suspension was prepared by dispersion of AzoCNC in a mixture of 1,4-dioxane/2-propanol (90/10 v/v), to attain a solid concentration of 0.1 % wt.% AzoCNC. Then, the mixture underwent stirring by using a vortex and sonication, 2.18 KJ/g of suspension, to promote further dispersion. This suspension was diluted to be further analyzed with a UV/Vis spectrophotometer. Multiple spectra were obtained, and for that was prepared a dilution, obtaining a 0.01 % wt.% AzoCNC suspension. The UV exposure (6 W source lamp with λ= 365 nm) was done with an 88 mm distance between the lamp and sample.

2.2 Production and Characterization of CNC-based films

First, the CNC suspensions were allowed to show the LC (isotropic-anisotropic) phase separation (around 1 week). Then HPC (Alfa Aesar, $\overline{Mw}$ =100,000) was added, setting the ratio of 70 %/30 % wt.% (CNC/HPC) followed by HPC dissolution under magnetic stirring for 7 days, at 200 rpm. The suspension was allowed to settle until phase separation was observed. For each cross-linker, different ratios and stirring times were used and adapted from the literature: with glutaraldehyde (GA) (Fluka Analytical, 50 % v/v in H_20, 5.6M). It was prepared a diluted solution of GA (25 % w/v in H_20) addition

was done to attain 1 %, 2 %, 3 % and 4 % wt.% in relation to CNC (wt.%) following magnetic stirring during 2 h [48]; the and for citric acid (CA) (AnalaR NORMAPUR., $\overline{Mw}$= 192.13), a 1 %, 2.5 %, and 5 % wt.% to CNC (wt.%) were added followed by magnetic stirring for 6 h at room temperature [49]. Control samples of CNC and CNC/HPC were also produced.

For the CNC/HPC/CA/AzoCNC (0.06 %~5.1 %: CNC wt.%), AzoCNC was added to the suspension before the selected cross-linker, put under magnetic stirring until homogenization, followed by the cross-linker addition.

Resorting to the solvent evaporation technique, the films were produced by by pouring a specific amount of the abovementioned suspension into polystyrene Petri dishes (Falcon®, 35 mm), and allowed to dry at room temperature or 45 ºC for CA cross-linked films. After drying, the average thickness of the films was measured, using a digital micrometer (Mitutoyo). It was measured in different zones near the central area of each sample. The films were always stored in a desiccator with silica gel beads at room temperature until further use.

The study of the cross-linking temperature and time on the samples containing GA and CA was conducted and assessed with a preliminary water dispersion test. After that, these samples were thoroughly washed with ultrapure water and dried at 60 ºC until constant weight.

The real composition expressed in percentages and film dimensions are presented in the figures of the next chapter. Several other characterization techniques were performed on the casted films, such as ATR-FTIR, TGA/DSC/DTG, POM, UV/Vis Spectrophotometry, SEM, Circular Dichroism, and wettability tests. All the characterization techniques are described in further detail in Annex A.1.

2.3 Stimuli-Response Tests

Photoisomerization and contact angle studies were performed on the samples that were sectionally scissored to obtain samples 7 mm in width.

UV/Vis spectra were obtained by incremental time of UV exposure (distance from the sample and source lamp was 50.8 mm) and relaxation was done in the dark, with visible light and with temperature of 60 ºC.

After undergoing the heat treatment, the CNC-based films and AzoCNC-containing samples were used for wettability tests (Dataphysics Contact Angle System OCA 20, in sessile drop mode) depositing 2 µl droplets of ultrapure water on the surface of each sample, using a micrometric syringe (B. Braun Omnifix 1 mL/1 cc) equipped with a needle with an external diameter of 690 µm inserted in the automatic dosing system. It was possible to acquire the static contact angle measurements by video measuring with a USB camera (model uEye UI-222xSE-M, IDS, GmbH.) and assessed with the Young-Laplace method, in the SCA20 software (version 4.3.12). 12 measurements were taken on different areas of the control samples CNC and CNC/HPC, with both cross-linkers. Additionally, wettability tests were then performed, followed by a 20 min relaxation period, and a 20 min period of UV exposure (6W, 365 nm source, with 50.8 mm between the supporting platform and the UV source), after which a new wettability test was done. To set a relaxation time for the study of the UV response of the AzoCNC suspension and the treated sample, it was captured absorbance spectra using the UV/Vis Spectrophotometer (PG Instruments T90+ Spectrometer, UVWin Version 5.2.0) using the same parameters, as for solid sample it was incremented the time of UV exposure and relaxation time by 20 minutes in each phase.

3

RESULTS AND DISCUSSION

The aim of this dissertation was the production of a nanocomposite system, by solvent evaporation method, of biodegradable films that present properties that change when exposed to external stimuli like UV light and temperature. These materials can be applied in a variety of different applications possible like sensing technology.

Firstly, to achieve this goal the CNC and HPC suspensions were prepared, and each suspension retain the LC phase before use. Then, the process of selecting the optimal cross-linker for the composite system for CNC and HPC, as the composite system is designed to be responsive to environmental stimuli and combines the structural support of CNC and liquid crystalline properties with the flexibility of HPC. The introduction of a cross-linking agent is essential to maintain the structural integrity of this in water, and two cross-linkers, glutaraldehyde (GA) and citric acid (CA), are tested for this purpose. These preliminary tests involved the production of CNC and CNC/HPC-based films with different ratios of each cross-linker and the ideal parameters of time and temperature for the cross-linking reaction on the casted films were assessed.

Meanwhile, the preparation of the AzoCNC suspension was conducted and the AzoCNC's chemical characterization was done. Also, this suspension was characterized by POM in transmission mode to better infer the suspension state before use. Besides this, it was also studied the photoisomerization of a diluted suspension to better characterize the responsive properties of this new material.

After cross-linker selection and AzoCNC suspension preparation, the production of the nanocomposite films was ensued. The produced films had different ratios of AzoCNC to assess the effect of this solid content on the overall system. The films' chemical properties were characterized using ATR-FTIR, and their macroscopic and microscopic characteristics were examined. Macroscopic observations revealed intriguing structural colorations in the films, influenced by AzoCNC concentration and the unique optical properties of the liquid crystalline phase retained in this solid matrix. These observations were further accentuated when viewed under circular polarizers, showing the films' appearance. Then, it was also compared with CD spectroscopy results, as the maximum wavelength reflected by the cholesteric structure is in the UV/Vis region of the electromagnetic spectra, the pitch value increases with HPC addition and there's a decrease of the pitch value with the increment of AzoCNC's concentration on the nanocomposite films. In parallel, the microscopic analysis by POM and SEM provided insights about the nanocomposite system structure due to the "micro-fingerprint" patterns within the films, and the retained chiral nematic structure was also viewed in the cross-section images of the films at the nanoscale. The chemical (ATR-FTIR) and thermal characterization (TGA/DSC) were also conducted. Additionally, the films' responses to heat treatment were examined by macroscopic observation of the appearance and isomerization study, showing a thermal-stimuli response of the samples containing AzoCNC.

Nevertheless, the isomerization study on the films was executed with UV light exposure and backswitch in the dark, with visible light and temperature. Wettability tests were also carried out

measuring the static contact angle and the effect on cyclic experimentation with UV light exposure and relaxation of the films.

3.1 System Selection and Production

As stated before, this study aimed to prepare films with properties that can trigger a response when exposed to external stimuli, whether UV light, temperature, humidity, pH, or even a combination of the lather. As described in the literature review (Chapter 1.3), we can find CNC a good candidate for that, as they provide mechanical support to our films and, due to their versatile chemistry, can be functionalized with stimuli-responsive moieties. Yet, it's known that pristine CNC films lose their physical integrity when in contact with water and are very brittle, compromising its stimuli-response response. For this reason, HPC was introduced to the CNC matrix as it is known for providing flexible mechanical properties while retaining the LC properties and typic cholesteric structure of CNC attained in CNC aqueous suspensions [6]. Since HPC is known for being a water-soluble cellulosic material, this composite system needs a cross-linking agent to avoid structural disintegration of our CNC/HPC matrix [50]. So, before functionalizing the cellulosic nanocomposite with a photo-switching molecule (chromophore), it's important to do a preliminary test to choose an ideal cross-linking agent, which is detailed in the chapter below (Chapter 3.1.1). For this, it was prepared various suspensions of CNC and CNC/HPC and different concentrations of each cross-linker, glutaraldehyde (GA) and citric acid (CA) was added, based on the methods described by Hanif et al. and Verma et al., respectively for CNC films. Both undergo a cross-linking reaction thermally catalyzed, improving CNC properties, in this case, the upholding of water intake without dissolution; and maintaining the cholesteric order of CNC layers [48], [51].

The cross-linker quantity parameter was adopted from Hanif et al. and Verma et al., for GA and CA, respectively. With this in mind, it was produced CNC/GA films with ratios: 0.76 %, 1.52 %, 2.26 %, and 2.96 % wt.%; for CNC/CA films with ratios: 0.78 %, 1.93 %, 3.24 % wt.%. Cross-link temperatures were adapted to the composite mixture, as described in Chapter 2.2 [48], [52].

3.1.1 Films Preparation: Cross-linker Selection

Cellulose nanocrystals, with hydroxypropyl cellulose, were used as a composite system to which CNC functionalized with an azobenzene derivative moiety was added. Since, it is well known that both components, CNC and HPC, can redisperse in water and azobenzene can change the hydrophilic/hydrophobic nature of the matrix and respond to the stimuli of humidity, it was important to stabilize the produced structure. To achieve such stability in water, the use of a cross-linker agent was considered.

The first part of this work aimed the select the appropriate cross-linker, considering that it was important to maintain the liquid crystalline structure retained in the films of CNC/HPC (70 %/30 % wt.%), previously prepared within the group [6]. Glutaraldehyde and critic acid were the tested cross-linkers. Glutaraldehyde (GA) is a molecule used as a cross-linking agent due to its low cost and low reaction times. It's applied for electronic applications, and it has been studied by Hanif et al., who demonstrated that it forms water-stable, flexible CNC photonic films that retain chiral nematic order.[48]. While the Citric Acid (CA) is a non-toxic tricarboxylic acid used in textile applications to improve the materials of cellulosic materials. [53]

Prior to the addition of the cross-linking agent, each suspension of CNC/HPC exhibits the isotropic-anisotropic separation, as reported by Saraiva et al. films of CNC, and CNC/HPC, to be used as controls, and CNC/HPC/GA and CNC/HPC/CA were prepared according to the described methods, by the solvent evaporation technique, cast from a polystyrene Petri dish at room temperature. Photographs

of the obtained structures can be seen in Figure 4.3 and Figure 3.1, for films with GA and CA, respectively. Besides this, it was also possible to obtain photographs of CNC/CA (Figure 4.2).

The samples that were cast with a cross-linker were observed macroscopically and analyzed by polarized optical microscopy. After attaining a dry state, it was measured the thickness in different zones of each film (n=10) with a digital micrometer and photographed with a Canon camera coupled with a macro lens. The photographs, composition, and average thickness are detailed in Figure 3.1A, for CA.

From the macroscopic observation of the films without polarization (Figure 3.1B), it is confirmed that the blue structural coloration is maintained in the CNC/HPC films despite the variation of the concentration of cross-linker agent, which appears to be mostly translucent blue tone. This observed structural coloration derives from a helical arrangement, resulting from the retention of the liquid crystalline phase in the solvent evaporation process, as it is reflected by left-handed circularly polarized light (LCPL) and transmitted with right-handed circularly polarized light (RCPL).

It was also possible to obtain the POM photography in transmission mode, of the central area of each film, where the birefringence is observable in the Figure 3.1E. The micrographs also depict the typical texture of the cholesteric CNC structure, where micro-fingerprint can be seen, resulting from the coalescing of tactoids on the LC phase to a long-range orientational order. The presence of this, at the microscale, may lead to inferring that the cholesteric structure was not completely perpendicular to the film's surface, which means the structure is not totally planar [6]. The same conclusion can be observed in the composite systems of CNC/HPC/GA. These results showed that the presence of HPC, and the fine control of the LC phase in the aqueous suspension, allowed to retain the LC photonic characteristic in the solid structures.

The presence of HPC in our composite system alters the temperatures needed to promote cross-linking. In order to assess the optimal parameters to achieve stability of the films in water, a preliminary test was conducted, which consisted of heating a 16 mm^2 sample of each film at a set temperature and time followed by immersion in ultrapure type II water solution for about ~20-30 min. The experimental parameters were adopted from prior works [54], [55] and followed the method of Dankovich et al.[56] First, the temperature and time parameters for the samples that contained HPC were settled to a temperature of 70 ºC and a time of 120 minutes, as described by Balcerowksi et al and Lam et al. [54], [55] for the samples of HPC/H_2O with GA, however, all our samples, even the control CNC/GA, were dispersed in water. Increments of time and temperature were performed, and an optimized cross-linking temperature and time of 80 ºC, 180 minutes for CNC/GA, and 110ºC and 2520 minutes (48 h) for CNC/HPC/GA samples were attained.

On samples that only contain CNC cross-linked with CA, a thermal treatment was not needed as dispersion in water was not observed, maybe due to drying at 45ºC, 48 h, as observed by Verma et al. [51]. For the CNC/HPC/CA, the same drying parameters were used however, dispersion of the films was observed. The work of Spiliopoulos et al. described the CNC cross-linking mechanism with CA, which involved a first step where the films were placed at 120 ºC for 5 mins for anhydride formation, and a second step at 160 ºC for 10 mins to ensure the cross-linking reaction and then washed with ultrapure type II water to remove the cross-linking byproducts, following frieze dried the samples [57]. This procedure was adopted for our samples with minor adaptations, as the drying was done at 60 ºC. Thus, the dispersion of CNC/CA and CNC/HPC/CA samples was not observed with this adapted procedure. The time and temperature conditions mentioned for each sample can be found in Table 3.1.

Consequently, the most viable composition was CNC/HPC/CA with a ~5 % wt.% of CA (:CNC wt.%), demonstrating water adaptability alongside its environmental-friendly nature and for presenting, when functionalized in nematic CNC, colorimetric properties with different solvents as it induces a change of the pitch value, demonstrated by Verma et al. for CNC films.

Table 3.1 — Summary of the used temperatures and times that passed the wettability test conditions and the conditions selected for the system selection (in bold).

Film Composition	Temperature º C	Time (min.)
CNC/GA	80	180
CNC/HPC/GA	110	2520 (48h)
CNC/CA	45	2520 (48h)
CNC/HPC/CA	**120** **160**	**5** **10**

3.1.2 AzoCNC: Suspension preparation and AzoCNC isomerization

Having selected the cross-linker, the next step would be adding the functionalized CNC, CNC-4-(4-methoxyazobenzene-4'-yloxy)butyrate, AzoCNC to our composite system. For this, it was prepared a suspension of 0.094 % wt.% AzoCNC as described in Chapter 2.1.

The provided azobenzene cellulose nanocrystals were obtained by the functionalization of the cellulosic nanocrystals by esterification with Azo moieties, whereas the carbonyl functional group is responsible for the ester linkage between Azo molecule and CNC, in Figure 3.2A, having associated a substitution degree (DS) of 0.130 (determined by elemental analysis). The functionalization was analyzed by ATR-FTIR spectrum (Figure 3.2A) that was supplied, being evidenced some characteristics bands in Figure 3.2A: 3340 cm^{-1} (OH stretch), 2894 cm^{-1} (C–H stretch), 1740 cm^{-1} (C=O carbonyl ester stretch), 1600-1580 cm^{-1} (aromatic C=C), 1500 cm^{-1} (N=N), 1248 cm^{-1} (C–O ester) and 878 cm^{-1} (aromatic C-H bend).

The yellow powder proved to be difficult to disperse in 2-propanol, even with high energy applied with sonication. The addition of 1,4-dioxane to the suspension allows the production of a more stable suspension, although some aggregates could still be found. In an attempt to further disperse the AzoCNC, it was used higher energy values for the dispersion of the solid aggregates. As seen in Figure 3.2, the difference between the suspension before (Figure 3.2B1) and after its sonication (Figure 3.2B2), getting a homogenous suspension even after resting overnight. In total, it was used 2.18 KJ/g AzoCNC and let it rest until use. So before using for the photoisomerization test, the suspension was analyzed by POM before manual stirring (Figure 3.2C1) and after manual stirring (Figure 3.2C2), and it showed that there was still some aggregation.

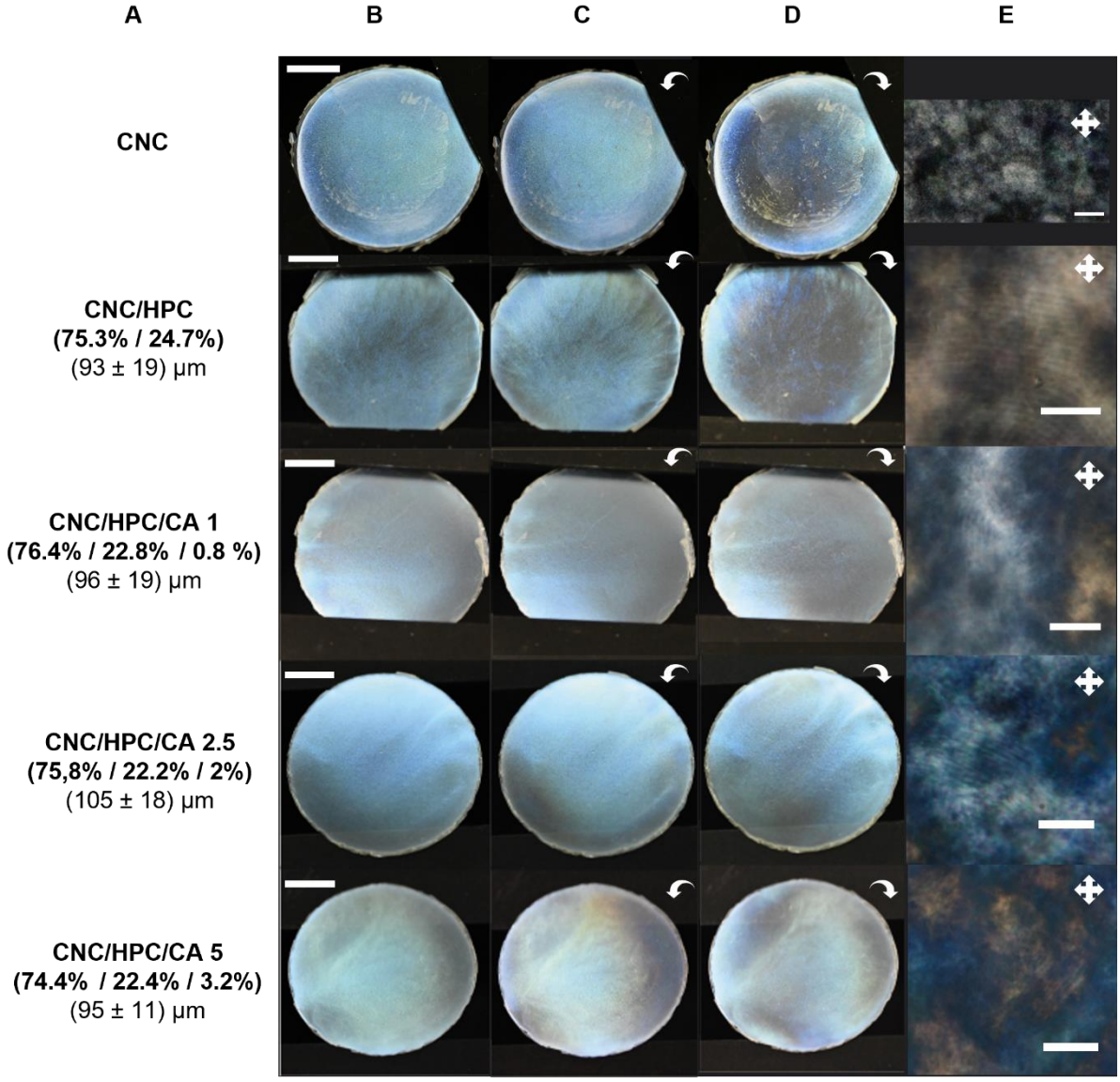

Figure 3.1 — A. Information of the casted films of the composite system of CNC/HPC/CA: composition, solid content (wt.%) and average thickness (n=10); B-D. Photographs with cold white light (Scale bars: 1 cm): B. without polarizer; C. with LCPL; D. RCPL; E POM images evidencing the micro fingerprint (Scale bars: 20 µm).

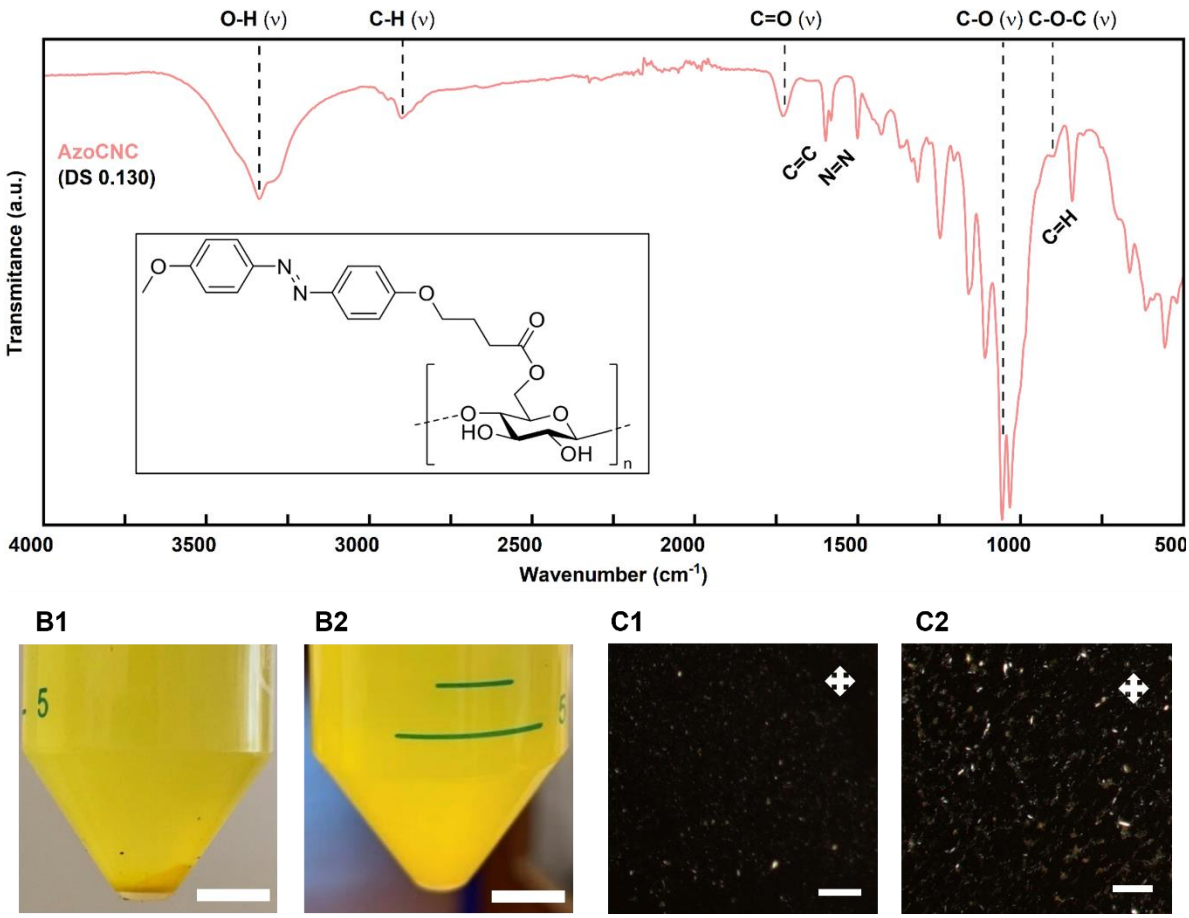

Figure 3.2 — A ATR-FTIR Spectra of AzoCNC with a schematic representation of its possible chemical structure and degree of substitution; B Photograph of the AzoCNC suspension: with some aggregates at the bottom (B1) and after t>12 h since sonication (B2) (Scale bar: 1 cm); C POM photography obtained in transmission mode with cross polarizers(crossed white arrows) of AzoCNC suspension: before (C1) and after (C2) manual stirring (Scale bar: 50 µm).

3.1.2.1 AzoCNC-photoisomerization

Azobenzene exhibits a photoisomerization property, that, when exposed to ultraviolet (UV) light, undergoes a conformational change from the *trans* to *cis* state, while under visible light or heat, causes a reverse transformation from the *cis* to the *trans*-conformation. It is a well-established fact that azobenzene is more energetically stable in the *trans*-state, leading to an inherent bias toward the *trans* isomer when in equilibrium [58].

To study the *trans-cis* photoisomerization of the AzoCNC suspension, and the reversibility of this phenomenon, the absorbance spectra in a wavelength range of 250-550 nm were obtained, using a UV lamp (365 nm, 6 W) as light source and UV/Vis spectrometer, at room temperature. It was observed the response of a diluted AzoCNC suspension with 0.01 % wt.% to UV exposure and measured the relaxation time under dark and under visible light with the aid of a UV source lamp (6 W, with a distance between the UV lamp and samples: 88 mm) and the UV/Vis Spectrophotometer. All spectra present small signal perturbations at 360, 420 and 530 nm, that are imposed by the equipment.

According to the graphic representation in Figure 3.3, all UV/Vis spectra showed the characteristic absorption bands of the azobenzene group, and the photoisomerization from *trans* to *cis*, after UV light exposure and back to *trans* isomer of the AzoCNC suspension. Before UV irradiation, the AzoCNC suspension presents a characteristic maximum absorption band peak at 358 nm, which corresponds to the $\pi \rightarrow \pi^*$ intense band in the UV region (*trans*-conformation), as shown in Figure 3.3AB. After UV exposure, there is a blue shift of the maximum absorption band peak to 310 nm. Additionally, another

absorption band in the visible region is highlighted in the close-ups (Figure 3.3A1-B1), maximum peak wavelength at 450 nm appeared, corresponding to the n-π* transition (*cis*-conformation). This shift proves the change of *trans* to *cis* isomer of the azo-functionalized nanocrystals in the suspension [59]. According to Łukasik et al. study on the isomerization of two novel amides containing photoresponsive azobenzene units, this transition is due to the aromatic double bond nitrogen, more particularly due to its lone electron pairs [60].

As observed, in Figure 3.3A it took 8 minutes of UV light irradiation to switch from *trans*- to *cis*-conformation, while, in the dark, took 24h to go back to the *trans* isomer. Moreover, the back switch was also done in visible light (Figure 3.3B), and it took 18 minutes to reach back the *trans* conformation (Figure 3.3C). With this, the AzoCNC has complete and reversible photoisomerization. The width of the peaks observed in these spectra are quite wide, compared to what is observed for an azobenzene, which may be attributed to the fact that the azobenzene moiety is strongly linked to the cellulose nanocrystals.

From the results obtained, the relaxation time from *cis*- to *trans*-conformation is much faster when the suspension is subject to visible light than when kept in the dark.

3.1.3 Production of the Nanocomposite Films

With our CNC/HPC/CA composite system chosen, it was produced suspensions with different concentrations of AzoCNC (0.06 %~5.1 % wt.%). These suspensions were also solvent casted and underwent the thermal cross-linking. Then the films were washed and dried at 60 ºC.

After casting, the films were characterized with ATR-FTIR observed macroscopically and analyzed microscopically by POM.

From the macroscopic observation without polarization (Figure 3.4B), on the films containing a low solid content of AzoCNC (0.06 %~0.25 % wt.%), the structural coloration is observed and vary almost from a transparent to yellow tone with the increment of AzoCNC solid content, until the 0.25 % wt.% AzoCNC film, becoming more intense green tone. The observed structural coloration derives from the cholesteric arrangement, resulting from the retention of the liquid crystalline phase during the solvent evaporation process, since reflected left circularly polarized light (LCPL) and transmitted right circularly polarized light (RCPL). In the Figure 3.4C-D, it is possible to observe that the difference between the films is the LCPL and RCPL images, as the central area appears to be more transparent in RCPL for films with solid content under the 1 % wt.% AzoCNC. Yet, the periphery of these films in LCPL appears some colors, as in RCPL of the same films appears totally the opposite, appearing color in the central area contrasting the periphery zones. This difference may be due to the walls of the petri dishes that affect the LC organization during the evaporation process. This was, in fact, observed in every sample up to 0.25 % AzoCNC wt.%, while the films with 1 %-5 % AzoCNC wt.% AzoCNC appeared to have a yellow tone. On these films, it is also visible some stretch marks on the films' surface at a macroscale, the reason behind this might be related to some turbulence during the drying period. Comparing to the low AzoCNC concentrations films photographs, the images of 1 %, 2.5 % and 5 % wt.% AzoCNC films were different since there was no evident change between the images of these samples observed with RCPL and LCPL (Figure 3.4CD). However, the strong yellow coloration dominates the appearance of the films with higher AzoCNC content.

Additionally, in the POM images in transmission mode, the "micro-fingerprint" was also noticeable at low concentrations of AzoCNC (0.06 %~0.25 % wt.%) in the Figure 3.4E. While the films with higher AzoCNC solid content, this was not observed. Comparing between those images of 1 %-5 % wt.% AzoCNC films, the 5 % AzoCNC wt.% films presented the most homogeneous texture (Figure 3.4E).

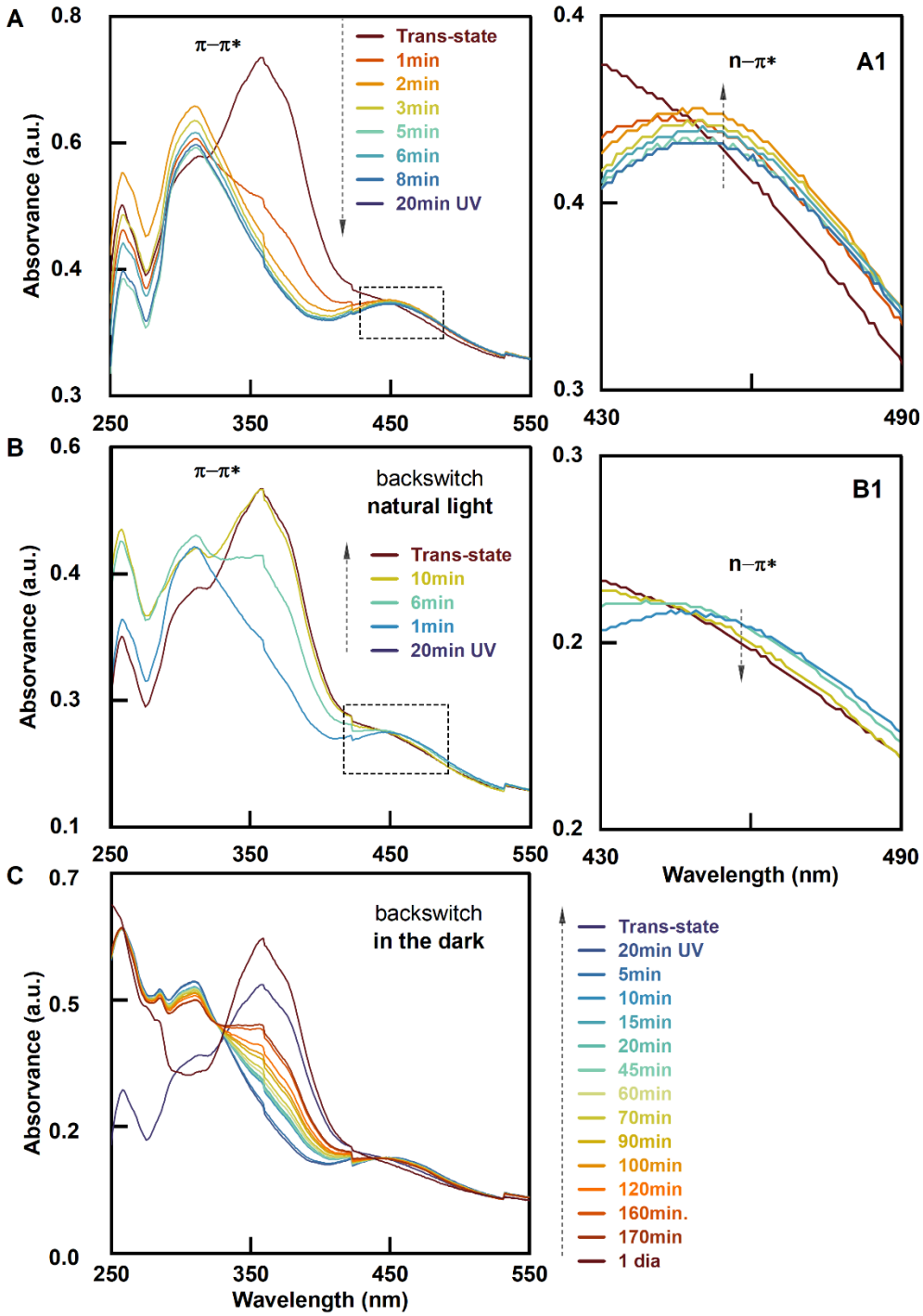

Figure 3.3 — Absorption spectra obtained in time following the photoisomerization process of the AzoCNC suspension from *trans*- to *cis*-conformation when expose to UV light (A) until the maximum of *cis*-conformation was reached, seen in the closedup (A1), evolution of the back switch to *trans*-conformation with visible light (B) and close-up at the region including 450 nm (B1) and in the dark (C).

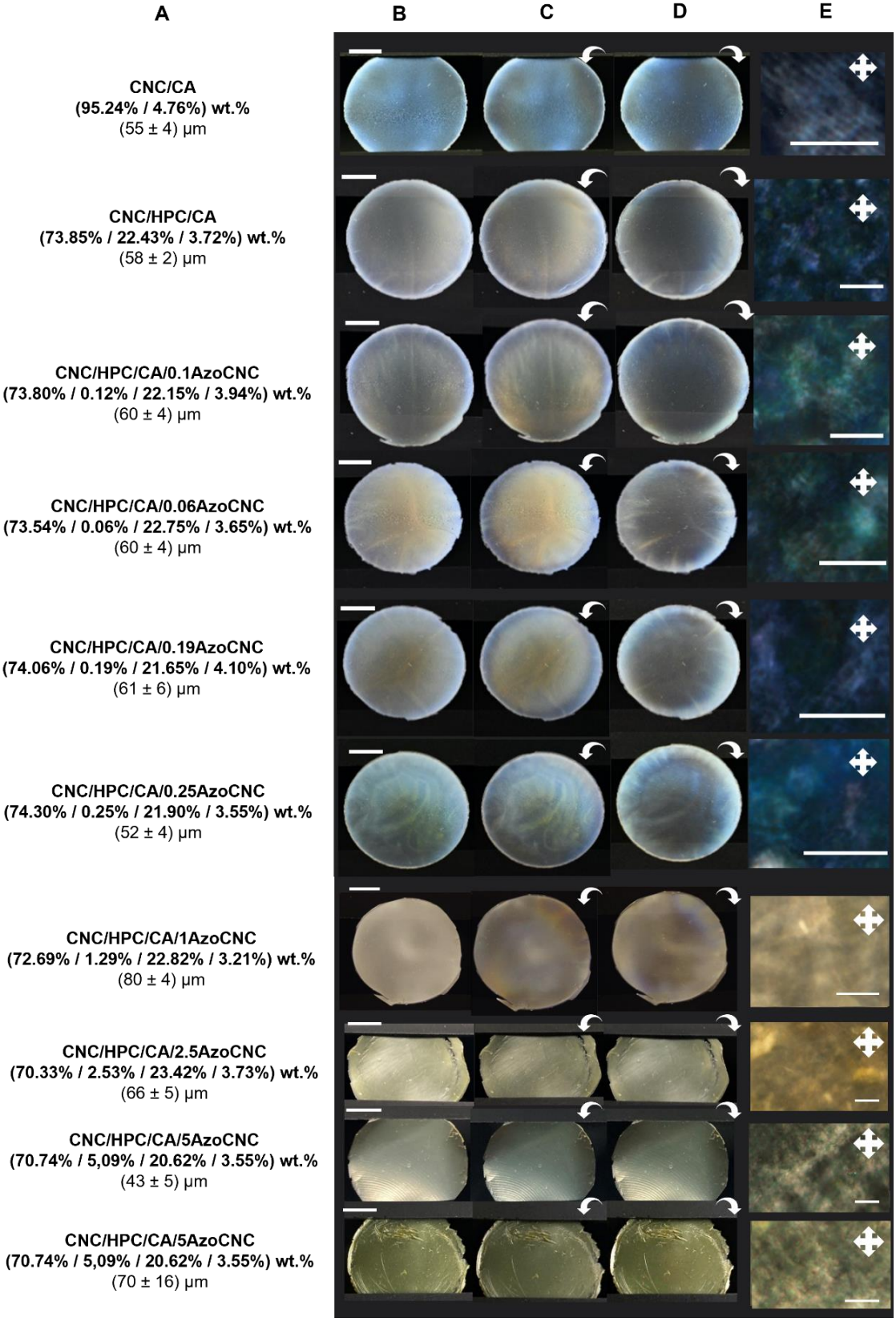

Figure 3.4 — Photographs of the CNC/AzoCNC films obtained with cold white light: with no polarizers (B), with left-handed (C) and right-handed (D) circular polarizers (indicated by the orientation of the arrows). (Scale bar:1 cm); (E) POM photography of the films (Scale bar: 20 µm).

After doing the heat-treatment of the higher AzoCNC solid content films, some samples were washed with water (t~1 to 2 min submersed in water) and then dried at 60 ºC during 6-8 h, still having a yellow appearance but with a smoother surface (Figure 3.5). Also, as observed in Figure 3.5, in the film containing 5 % AzoCNC wt.% was dried at 60 ºC for 15h, and the sample's appearance changed to the color tone orange (Figure 3.5C1). With time (t~5 days), it slowly came back to the transparent yellow tone. In order to see if this color change was due to the presence of the citric acid, the samples of CNC/CA (Figure 3.5A) and CNC/HPC/CA (Figure 3.5B) underwent the same treatment and there was no change after 15h of heating at 60 ºC, so this change was not due to the citric acid incorporation. This result will allow to further explore the photonic characteristics of these composite systems.

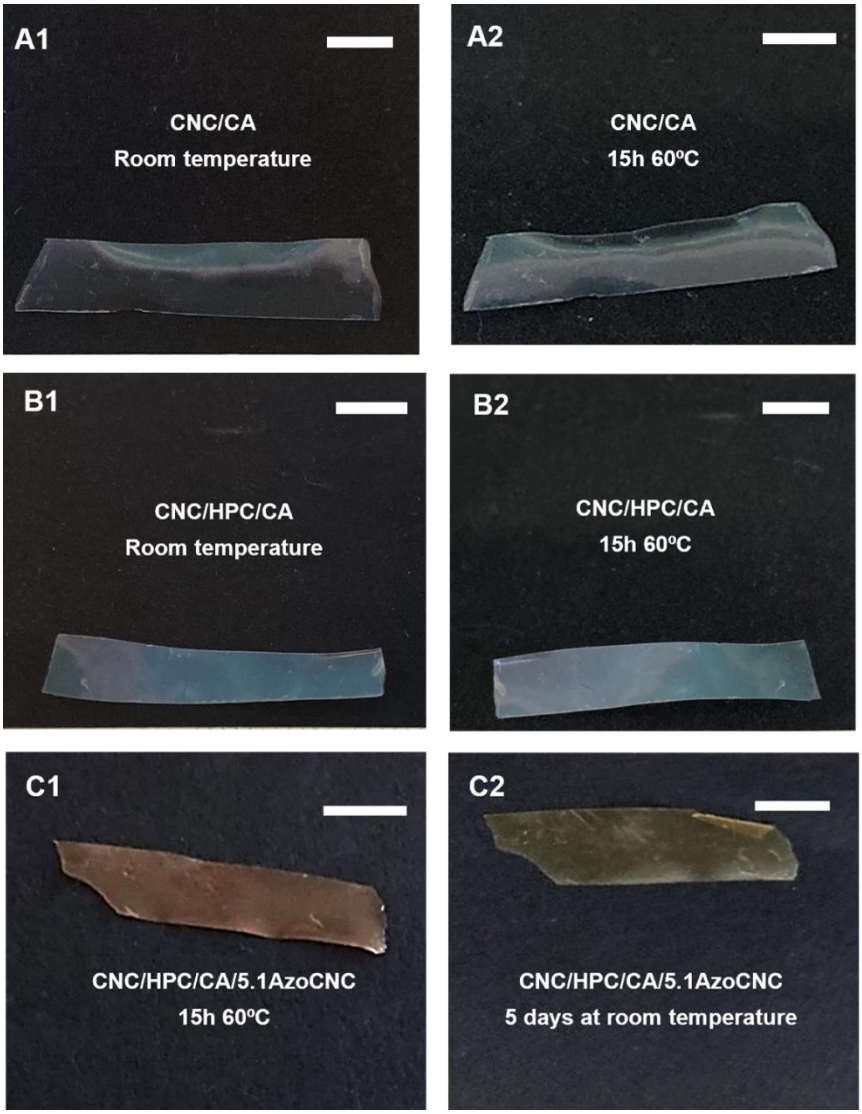

Figure 3.5 — A-B Treated control samples at room temperature and after 15h and 60 ºC; C Treated AzoCNC samples after drying at 60 ºC (Scale bar: 5mm).

3.1.3.1 Attenuated Total Reflectance – Fourier-Transform Infrared

By examining the FTIR spectra, which encompasses a range of infrared wavelengths, it was possible to make inferences about the chemical composition of the composite systems. The study involved the CNC/CA films, both treated and untreated cross-linked CNC, as well as AzoCNC containing samples. The spectral representation in Figure 3.6 revealed distinct absorption bands that correspond to different vibrations within the cellulose molecules. Within this figure, we observed absorption bands

at specific wavenumber values: 3334 cm^{-1}, 2900 cm^{-1}, and 1054 cm^{-1}. These values represent the vibrations of specific chemical bonds in the cellulosic material. For instance, the band at 3334 cm^{-1} indicated the presence of OH groups in the interlinked polymeric chains, the band at 2900 cm^{-1} was related to the stretching of carbon-hydrogen bonds (C-H) and the band at 1054 cm^{-1} was associated with the stretching of specific carbon-oxygen bonds (C-O) [12]. The vibrational band at 896 cm^{-1} is tied to the stretching of C-O-C in glycosidic-β-(1,4) linkages, linked to the amorphous region of cellulose [61], [62]. The band at 811 cm^{-1} is attributed to the stretching of the sulfate linkages (S-O) due to the presence of the ester sulfate that was introduced in the CNC during the acid hydrolysis reaction [63].

An additional band appeared at 1721 cm^{-1} (C=O stretching) in the FTIR spectrum of the CNC/CA and CNC/HPC/CA samples, which may have contributed to the ester bond of the CNC cross-linked with citric acid [64], [65]. The treated and untreated of these samples' FTIR spectra showed this band maybe due to the drying at room temperature, which the temperature might be enough to promote a slow cross-linking reaction. Recalling the ATR-FTIR of the AzoCNC (orange line), the adsorption band at 1743 cm^{-1} is attributed to the presence of the ester carbonyl group (C=O), which would indicate that there's indeed the CNC and the AzoCNC were linked through esterification process. However, as for the samples containing AzoCNC, since the cross-linking with citric acid shares the same type of linkage, the presence of the AzoCNC cannot be evidenced in the low concentrations by ATR-FTIR (Figure 3.6).

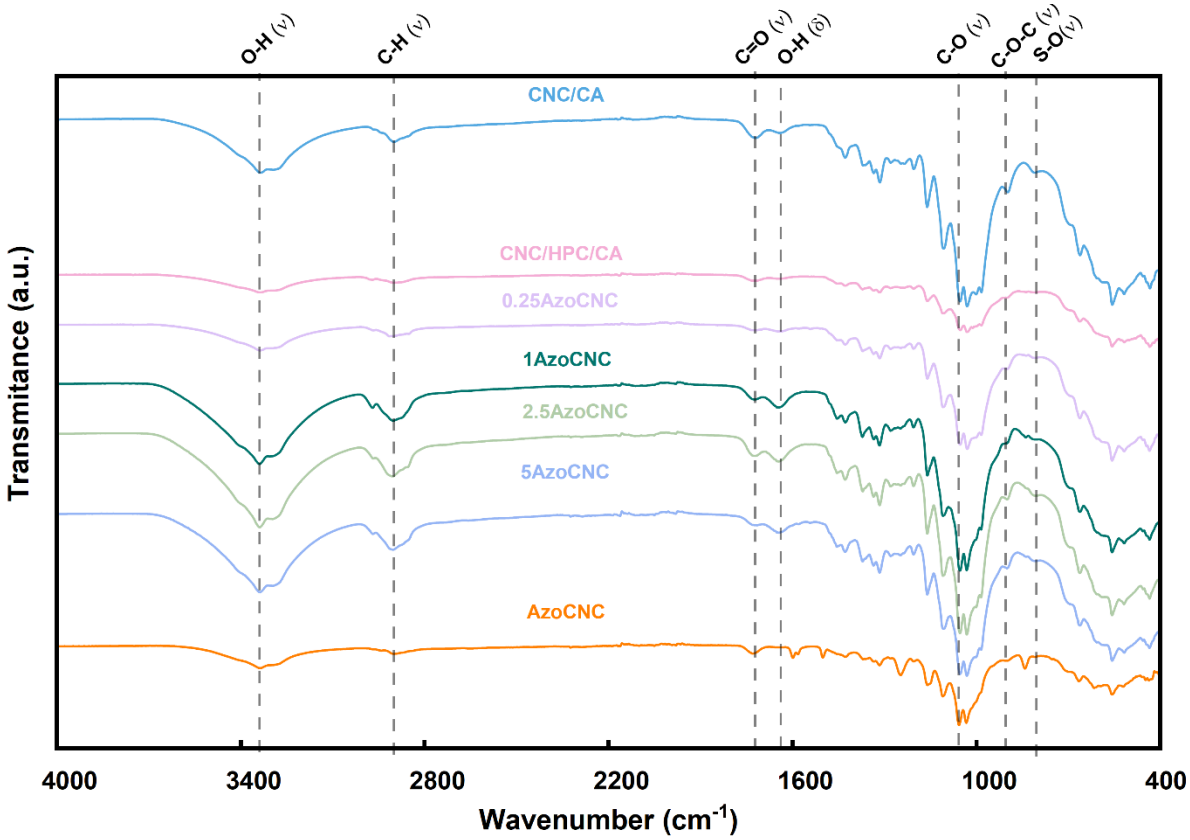

Figure 3.6 — ATR-FTIR spectra of the CNC, CNC/HPC and AzoCNC containing samples, highlighted the vibration bands of cellulose and cross-linker.

3.1.3.2 Scanning Electron Microscopy and Circular Dichroism

In order to confirm that the cholesteric organization from the CNC aqueous suspension was retained in the solid structure, cross-section images of the films were observed by SEM. In Figure 3.7 images of control samples of CNC/CA (Figure 3.7A1 and B1), CNC/HPC/CA (Figure 3.7A2 and B2), and with different ratios of AzoCNC: 0.1 %, 0.25 %, 1 %, 2.5 % and 5 % wt.% (A3-A8 to B3-B8) are

shown. In all the samples, the layered structure, and mainly in the close-up images, the helicoidal structure is observed in the nanocomposite systems. This structural preservation indicates that the helicoidal arrangement of the CNC remains intact within the matrix despite the presence of CA and AzoCNC at the solid content established (Figure 3.7).

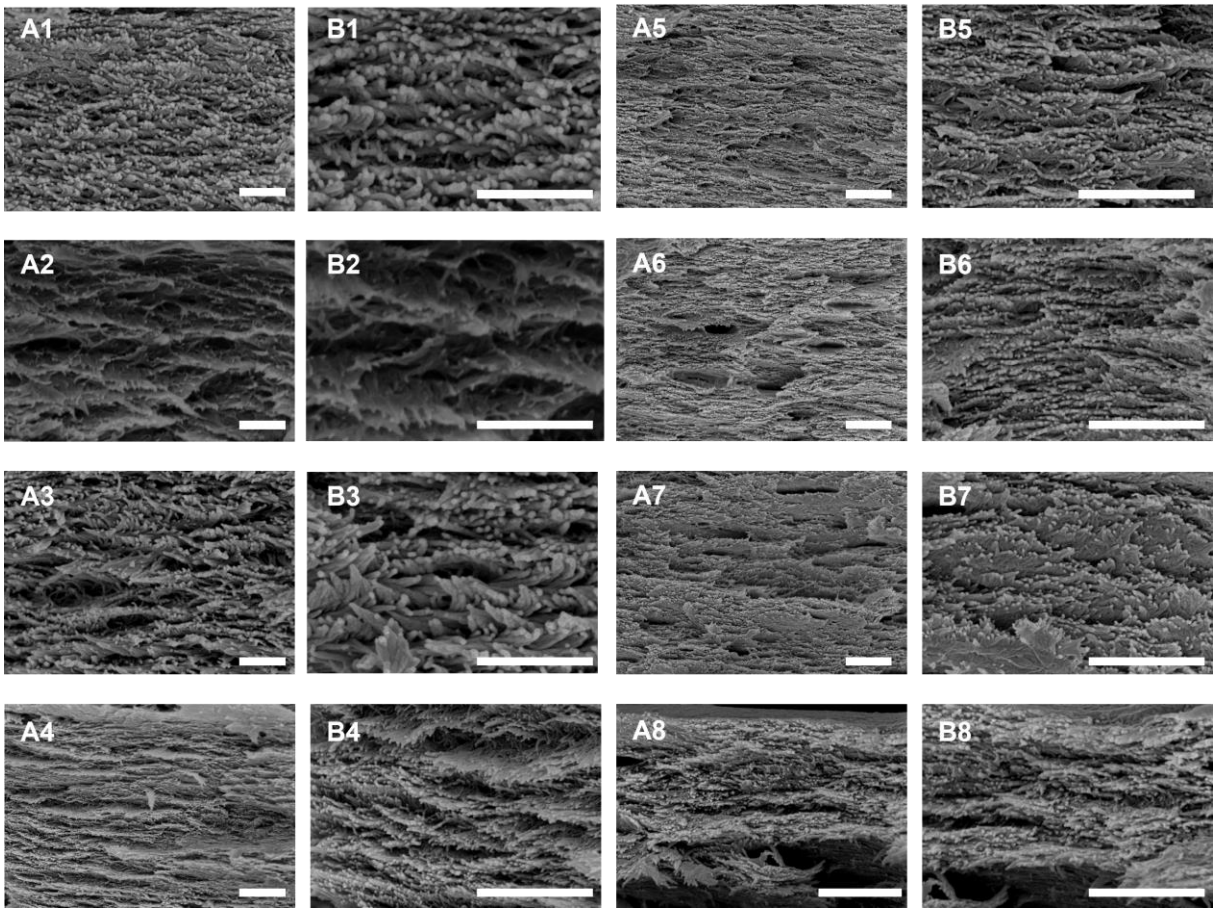

Figure 3.7 — SEM photography of the cross-section (A) and close-ups (B) of each film : 1- CNC/CA ;2- CNC/HPC/CA; 3 to 8 - CNC/HPC/CA/xAzoCNC (x= 0.1; 0.25; 1; 2.5; 5) (Scale bar: 1 μm).

To confirm the handedness direction of the cholesteric structure retained in the nanocomposite films, the central zones of each film and a CNC suspension casted film were analyzed with Circular Dichroism (CD). This technique allows to infer the chirality of the composite system.

In the Figure 3.8A-B, it is represented the CD spectra of each sample, where is possible to see that every sample presented positive values in the range of wavelengths from 190 and 750 nm. These results allow to conclude that the cholesteric structure in all films is left-handed, the same helicoidal orientation of pristine CNC films, and all the spectra of nanocomposites are wide. As observed in Figure 3.8C, it shows a graphic representation of normalized spectra to better access the information about the maximum peak wavelengths of each sample. So, CNC film (Figure 3.1) presented a maximum peak wavelength of 254 nm. With the incorporation of CA on the film, there's a 6 nm red shift of the maximum peak wavelength. While with the CNC/HPC/CA sample, the maximum peak wavelength had a much more significant red shift to the wavelength of 493 nm, which is in accordance with the observation of the photographs on Figure 3.4, that appear yellow. A similar sort of increment was observed by Saraiva et al. for a different CNC source but the same HPC, where the authors saw that the maximum wavelength double when 30% wt.% of HPC was added to the CNC LC-based matrix [6]. The authors attributed the possibility of the HPC macromolecules to interact with CNC forming H bonding, increasing the distance between nanocrystals, affecting its electrostatic interaction and so the pitch value.

With the small increments of AzoCNC concentration on the films, there were small incremental blue shifts of the maximum peak wavelengths. According to Figure 3.6, the AzoCNC samples with concentrations of 0.06 %~0.25 % wt.% presented similar and wider spectra like the CNC/HPC/CA sample, which is according to the yellow appearance of the films seen in the images above (Figure 3.4). As stated in subchapter 3.1.3, the 0.06 %~0.19 % wt.% AzoCNC films displayed a yellow appearance which is in accordance with the maximum wavelength values that varied between 507-468 nm. Compared to these samples, the 0.25 % wt.% AzoCNC sample had a higher blue-shift of the maximum peak wavelength of 394 nm, which in the Figure 3.4 appeared to have a structural coloration ranging from blue to green. Increasing the concentration up to 1% AzoCNC wt.%, the sample showed the largest single band, similar to the AzoCNC films mentioned above, that covers the entire Visible region and with a peak at the wavelength 363 nm. However, when we observed to the spectra of the composite with higher content of AzoCNC, 2.5 % and 5 % wt.%, the difference can be noticed as the spectra are not wide, and other positive bands appear at around wavelength 209, 350 and 420 nm, due to the high content of AzoCNC. The positive signal might indicate that this CNC functionalized with azobenzene acquire a chiral organization within this matrix, however in other to confirm that further studies should be done, and mainly improving the dispersion of this AzoCNC prior to its addition in the composite.

It is possible to estimate the pitch value of the cholesteric organization with the maximum wavelength value (λ_0 of CD spectrum), by recurring to the equation *de Vries* Equation, which relates the pitch value (P) to the maximum wavelength:

$$\lambda_0 = n \cdot P \cdot cos\theta \qquad \text{Eq. 1}$$

where n is the average refractive index of the mesophase (in this case, the solid film) and θ the angle of incident light with the helix axis. The average refractive index was estimated considering the one for CNC, 1.56, HPC, 1.33 (Saraiva et al., 2020) and CA, 1.50 [51], while for AzoCNC average n was assumed to be an approximate value of CNC. The λ_0 and estimated pitch P values are plotted in Figure 3.8D and all the values are presented in annex A.6 (Table 4.1).

Adding CA and HPC to the CNC films caused the estimated pitch value to increase. And with the incremental increase of AzoCNC solid content on the films, from 0.06 % to 5.1 % wt.%, there's a decrease of the pitch value almost proportional up to 2.5 % wt.% AzoCNC, decreasing drastically on the highest content of AzoCNC nanocomposite film produced.

With these results, its demonstrates that the nanocomposite films produced maintained the left-handed orientation of the chiral nematic structure of the CNC film.

3.1.3.3 Thermogravimetric Analysis/ Differential Scanning Calorimetry

TGA/DSC can be particularly useful if you have complex composite materials with various constituents, as it shows the thermal decomposition profiles and offers insights into heat flow and thermal transitions. The thermal degradation of CNC consisted of three moments of the degradation process: dehydration, depolymerization, and decomposition of glucopyranose units, followed by residue formation [66]. The graphics representation shown on the Figure 3.9A-C, represent the TGA, DTG and DSC curves of the nanocomposite films, respectively.

For the determination of the temperature values, it was used auxiliary lines (blue dashed- lines, found in Figure 4.1, in the annex A.1) and those values are tabled in Table 3.2.The degradation temperature is assumed to be the primary peak of the DTG curve, which is the maximum peak of the DTG curves. Additionally, some nanocomposite films presented secondary peaks that were observed on the DTG curves.

All the TGA curves presented a slight weight loss (<4 %) on the low-temperature range (<124 ºC), which alludes to the evaporation of water that was absorbed due to the greater affinity to water due to OH groups of CNC, the citrate groups [53] and HPC [50].

In terms of mass loss, as seen in Figure 3.9A, CNC film had 3 step degradation. Firstly, a small percentage is lost until the onset temperature 220 ºC due to a slight evaporation of physically bound moisture due to the hydrophilic behavior of CNC; the onset temperature (220 ºC) indicates the start of the second step and is associated with a variety of degradation, transformation processes and depolymerization of the glycosidic units [66]. This step is characterized by a wide dip (263 ºC) that represents a high mass loss (25.56 %) in the cellulosic pyrolysis reaction, and this can be evidenced by two endothermic peaks of DSC curve (Figure 3.9C, red dash line); then a small amount of weight is lost (10.16 %); followed by another 26.30 % in between 300 and 550 ºC, leaving a significantly high residue quantity at 550 ºC (33.65 %).

Comparing the CNC sample cross-linked with CA (green line, Figure 3.9) with the CNC sample, the CNC/CA showed a similar TGA curve, meaning that there is almost no influence on the incorporation of the CA, under the conditions of production, in the CNC films. However, the of HPC incorporation to the CNC/CA, presented higher mass loss at the pyrolysis step (51.10 %).

The AzoCNC (black dashed line) showed a different 2 step degradation process: a distinct degradation in about 317–390 ºC with 65.2 % weight loss with its maximum weight-loss temperature at 350 ºC, and the second weight loss of 9.62 % till 550 ºC.

Comparing the nanocomposite films with the previously mentioned, every CNC/HPC/CA/AzoCNC film had a similar 3-step degradation. However, the incremental mass loss is proportional to the increase in the increments of AzoCNC solid content (up to 5 % wt.% :CNC) on the nanocomposite films (from 21 % CNC/HPC to 11 % CNC/HPC/5AzoCNC, as an example). Additionally, the increment of AzoCNC's solid content on the films, showed more similarities with the AzoCNC's TGA curve, as TGA curves revealed different degradation profiles (Figure 3.9A). Besides this, the degradation temperatures also increased with the increment of AzoCNC solid content on the films (from 276 ºC CNC/HPC to 302 ºC CNC/HPC/5AzoCNC).

Moreover, on the DTG curves (Figure 3.9B), we see there is a secondary peak of the graphic representations of CNC, CNC/CA and CNC/HPC/CA/1AzoCNC. However, the exception was the 5 % AzoCNC wt.% (light red line) .This film presented 2-step degradation, likewise to the AzoCNC (black dashed line), leaving almost to no char residue left at the end of the test and presented a single endothermic peak at 301 ºC , as seen in the Figure 3.9C. In general, the DSC curves all films containing AzoCNC DSC curves that showed that the process is endothermic at high temperature values.

Similar cases were reported by Ruiz-Caldas et al. study, where the citrated CNC also showed 2 step degradation process [53]. Besides this, Liu et al. stated an example of an azobenzene compound (MMAZO) that was added to the CNC, whereas also displayed a greater value of degradation temperature up to 318 ºC, meaning that improved the thermal resistance of the CNC film [41].

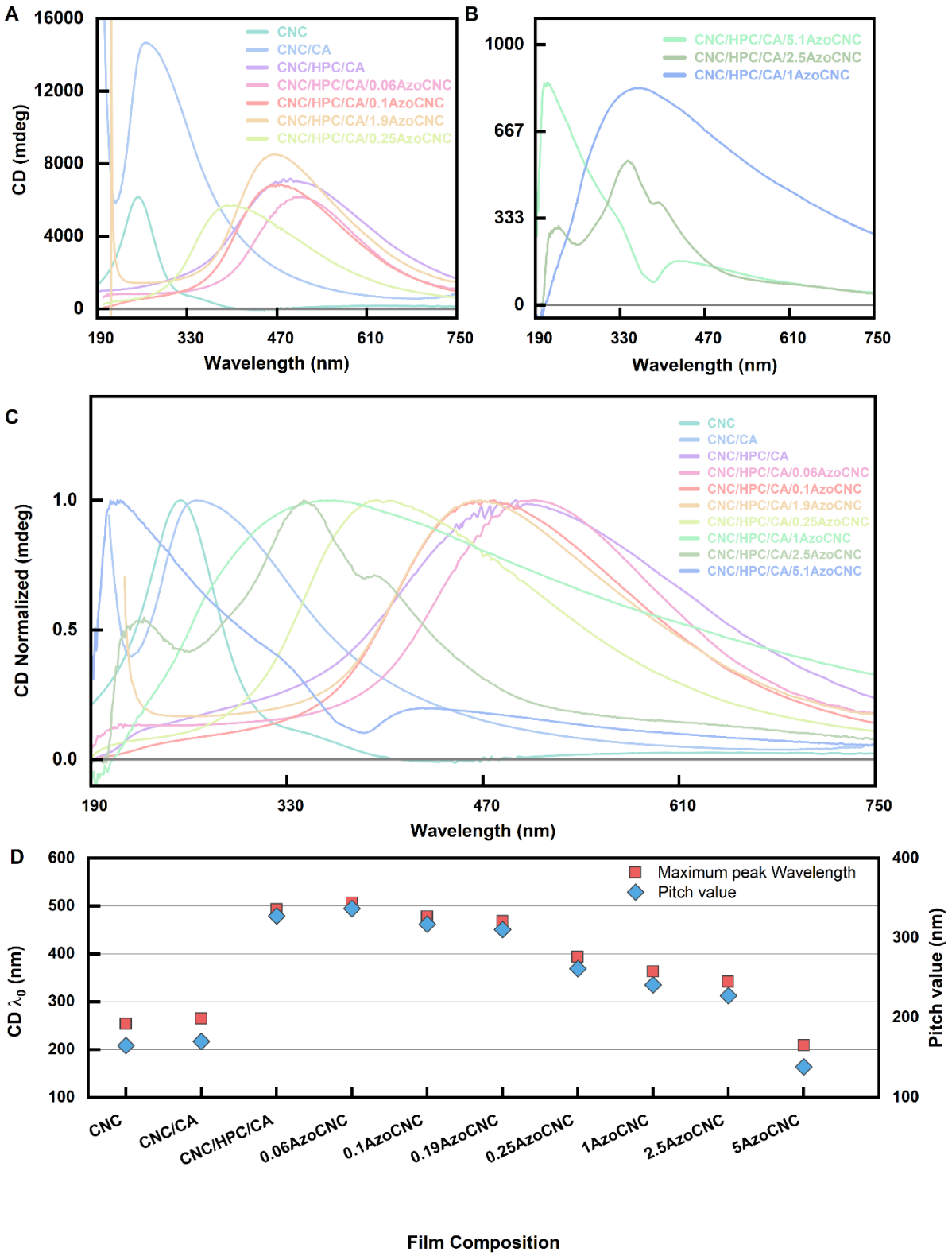

Figure 3.8 — CD spectra normalized graphic representations of the nanocomposite systems in the wavelengths 190-750nm. (ABC); D – estimated pitch value by using the estimated index refractive values of the nanocomposite films and the maximum CD peak wavelength, using the *de Vries* equation.

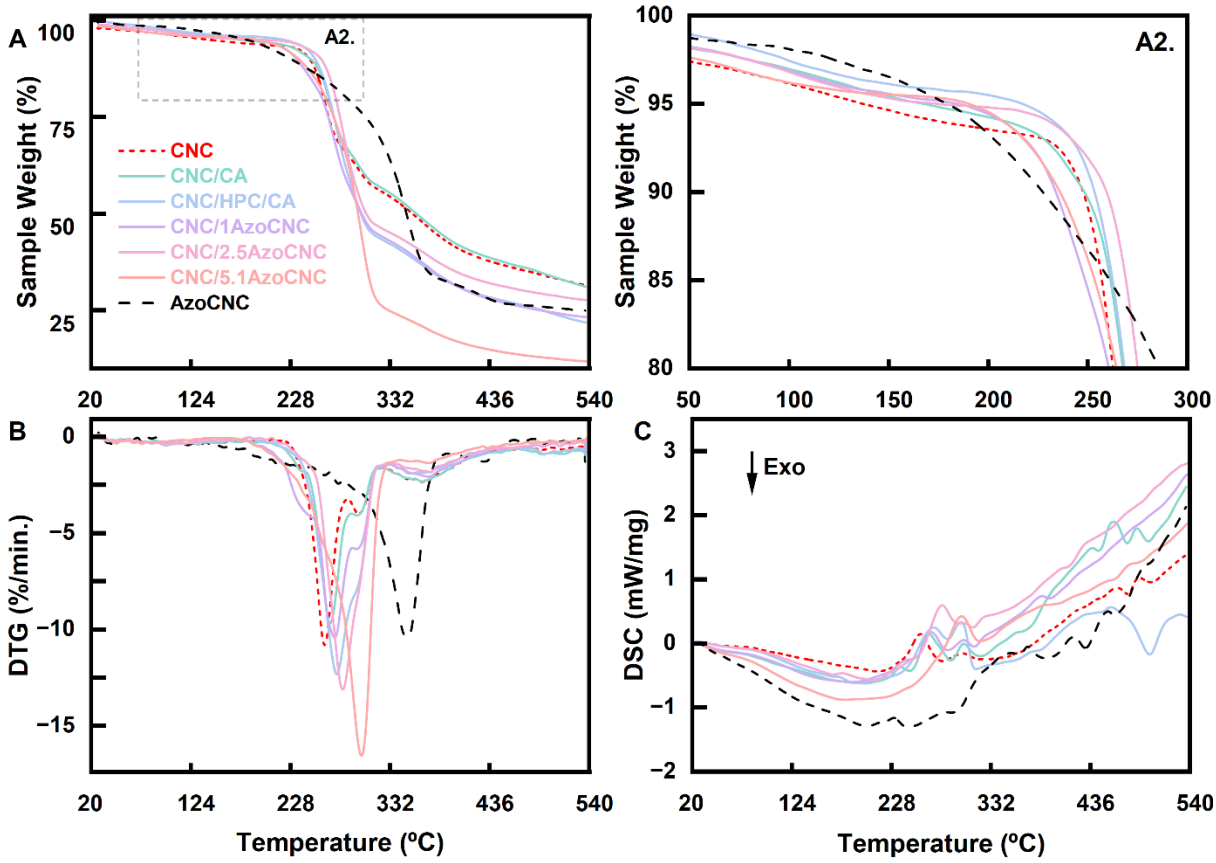

Figure 3.9 — Graphic representations of: A-A2. TGA curve; B. DTG curve; C. DSC curve of the nanocomposite systems, CNC, and AzoCNC.

Table 3.2 — Values of the onset, offset, and degradation temperatures from the termogravimetric analysis. The estimation was done by auxiliary lines for the curves of TGA and DTG.

Film Composition	**CNC**	**CNC/CA**	**CNC/HPC/CA**	**CNC/HPC/CA/xAzoCNC**			**AzoCNC**
				x= 1	**x= 2.5**	**x= 5**	
T_{onset} (ºC)	243	242	246	239	256	261	286
T_{deg} (ºC)	263 287	269 291	276	274 292	282	302	350
T_{offset} (ºC)	315	331	332	327	327	326	382

3.2 Stimuli-Response Tests

3.2.1 Isomerization phenomenon on the Nanocomposite Films

To access the responsive properties of the produced nanocomposite films, the isomerization study was carried out. With isomerization study and by using UV/Vis spectrophotometer, it is possible to have knowledge on the isomerization, if is reversible or not, and the time that it takes to isomerize between from *trans* to *cis* and from the *cis* and *trans*-conformations The isomerization on solid samples were tested on sample with lower AzoCNC solid content (0.06 %-0.25 % wt.%), which can be observed in the Annex A.5. With this, it was not visible major differences in the UV/Vis spectra even after 3h of UV exposure. So, the amount of AzoCNC was very low to produce any effect, and one can assume that the AzoCNC is highly embedded within the matrix to change its conformation.

The isomerization of 1 %-5 % AzoCNC wt.% samples were analyzed (Figure 3.10A-C), while the backswitch was only possible to do on the samples with 2.5 % and 5 % AzoCNC wt.% due to the long time required (Figure 3.11 and Figure 3.12, respectively.).

Generally, after 8 minutes of UV irradiation, the AzoCNC film spectra did not change, showing that the cis photo stationary state is achieved, independently of the AzoCNC solid content used (1 %-5 %: wt.%), as seen in Figure 3.10A-C. In the mentioned figure, the isosbestic points at 280, 300 and 420 nm decrease, and the close-ups of the graphic representations (Figure 3.10A1-C2) showed that the absorption bands are more prominent during the first isomerization (trans-to-cis), making an uplift of the peak at 450 nm of the smaller absorption band, that corresponds to the cis state for all the AzoCNC samples containing concentrations of 1%-5 % wt.%.

The graphic representations of the backswitch of 2.5 % AzoCNC is displayed in the Figure 3.11 and the backswitch of 5 % AzoCNC is evidenced in Figure 3.12. The backswitch from cis to trans-conformation was proceeded in three different ways: in the dark, with exposure of visible light, and temperature, and acquired spectra each time.

For the backswitch in the dark of the 2.5 % wt.% AzoCNC sample, the graphic representation of the spectra is in Figure 3.11A, whereas 19.4 hours were required to achieve the trans-conformation. While with the 5 % wt.% AzoCNC sample is kept in the spectrometer for up to 480 minutes, as evidenced in Figure 3.12A. However, for longer periods of time, it was necessary to remove it and, although it was protected from light by an aluminum sheet, there was always some manipulation to put it back into the spectrometer and absorption of light, due to the need for other colleagues to use the device. For this sample and under these conditions, it appears that time values greater than 1920 minutes will be necessary for total reversibility from the cis-to-trans conformation to occur.

With relaxation on visible light (Figure 3.11B), the *trans*-state of the AzoCNC samples with 2.5 % and 5 % wt.% wasn't achieved. The 2.5 % wt.% AzoCNC sample showed reverse transitions from 5-50 minutes and at 140 minutes, having the opposite direction at a time value of 100 minutes of relaxation, which means a decrease of the peak wavelength towards the *cis*-state. Continuing the time measurement on the backswitch test 2.5 % wt.% with visible light, there's a leap of the peak wavelength towards the reverse direction and it maintains relatively at the same photo stationary state, never reaching the *trans*-state. The measurement with visible light was done until 480 minutes, which, under these conditions, it would be necessary time periods greater than 480 minutes to reach total reversibility. On the other hand, a reverse isomerization process on the 5 % wt.% AzoCNC sample can be observed as the exposure time to visible light increases from 5 to 15 minutes. Although, at 30 minutes, it is possible to observe a decrease in the peak corresponding to the trans-conformation (Figure 3.12B). The use of visible light (derived from LED lamps and sunlight) causes several wavelengths of light to fall on our sample, which include 365 nm. Therefore, for this test, visible light needs to be adapted like using another source of sunlight that excludes the contribution of the UVA wavelength (315-400 nm).

Nevertheless, it is known that in solid form, the nanocomposite system tends to be 100 times slower [67], it may be because of the helicoidal structure of the CNC or the cross-linking might introduce steric hindrance effects, making the isomerization rate back to *trans* be smaller than it is to isomerize to cis. Besides this, the nanocomposite has 4 elements, which might have steric hindrance effects as it creates energy barriers that slow down or inhibit the isomerization process.

Apart from the isomerization study, it was also tested covering a side of a sample of 5 % wt.% AzoCNC before UV exposure with aluminum foil to observe if there is any visual difference. After 20 minutes of UV exposure, there was a change in the hue tone, as seen in Figure 3.12D. This behavior is typical in the azobenzene systems, as observed by Pinto et al. for azobenzene-cellulosic materials [68].

Since the reversible isomerization from *cis*- to *trans*-conformation showed to be to slow or to dependent on the light used, it was relevant to analyze the backswitch with temperature on the 2.5 % and 5 % wt.% AzoCNC samples. As observed in Figure 3.5, there was a change of yellow to orange tone after heating the 5 % wt.% AzoCNC sample at 60 ºC for 15 h. So, for this reason, it was tested the

impact of this temperature value on the isomerization and measured the time and acquire spectra. As evidenced in Figure 3.11C and Figure 3.12C, the *trans*-conformation for the 2.5 % and 5 % wt.% AzoCNC samples was achieved in relatively fast pace 15 mins.

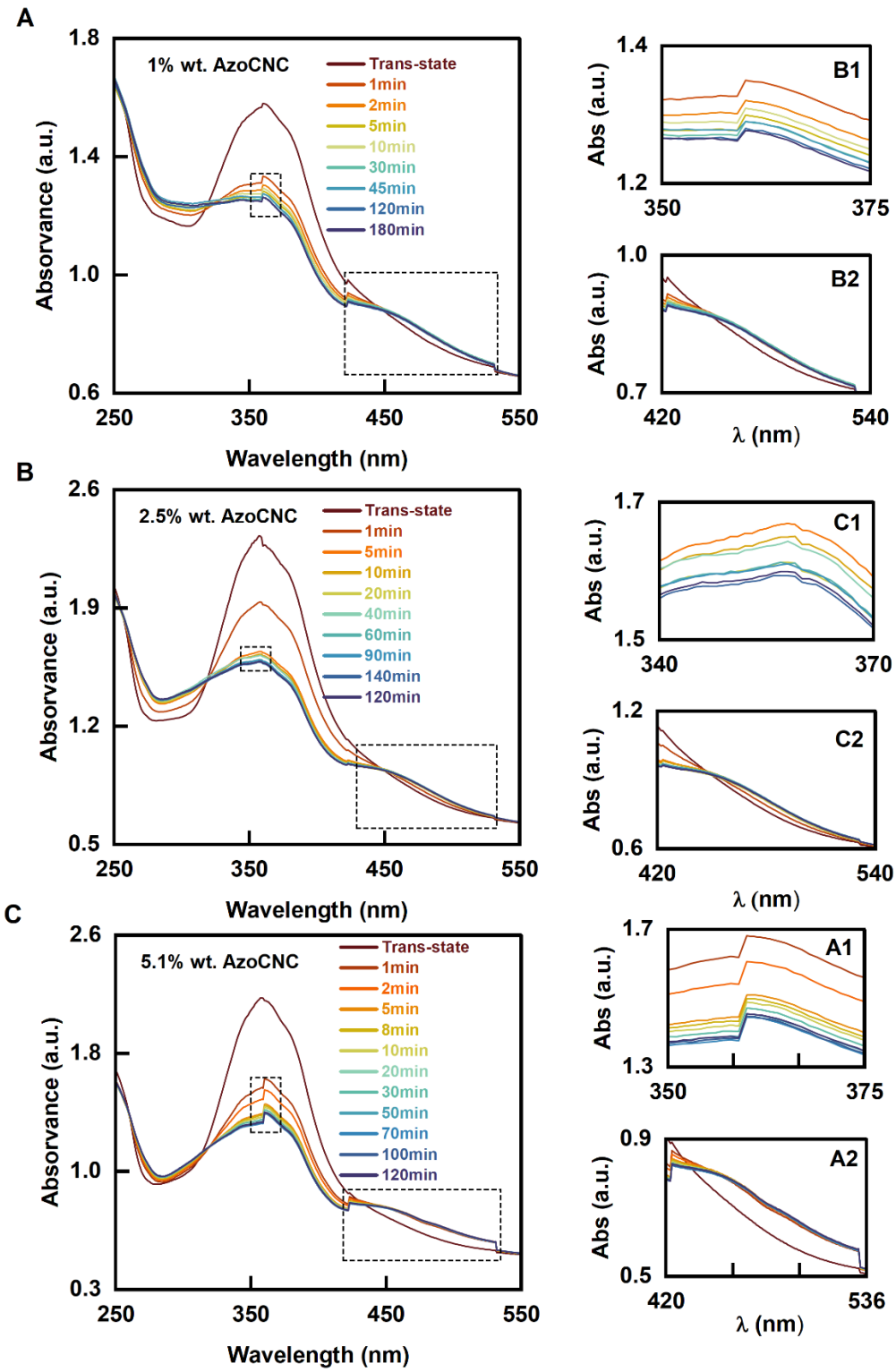

Figure 3.10 — Isomerization from trans- to cis-conformation with UV exposure (ABC) of samples with AzoCNC with the 1%, 2.5 % and 5 % wt.% with close-ups on the right side, respectively.

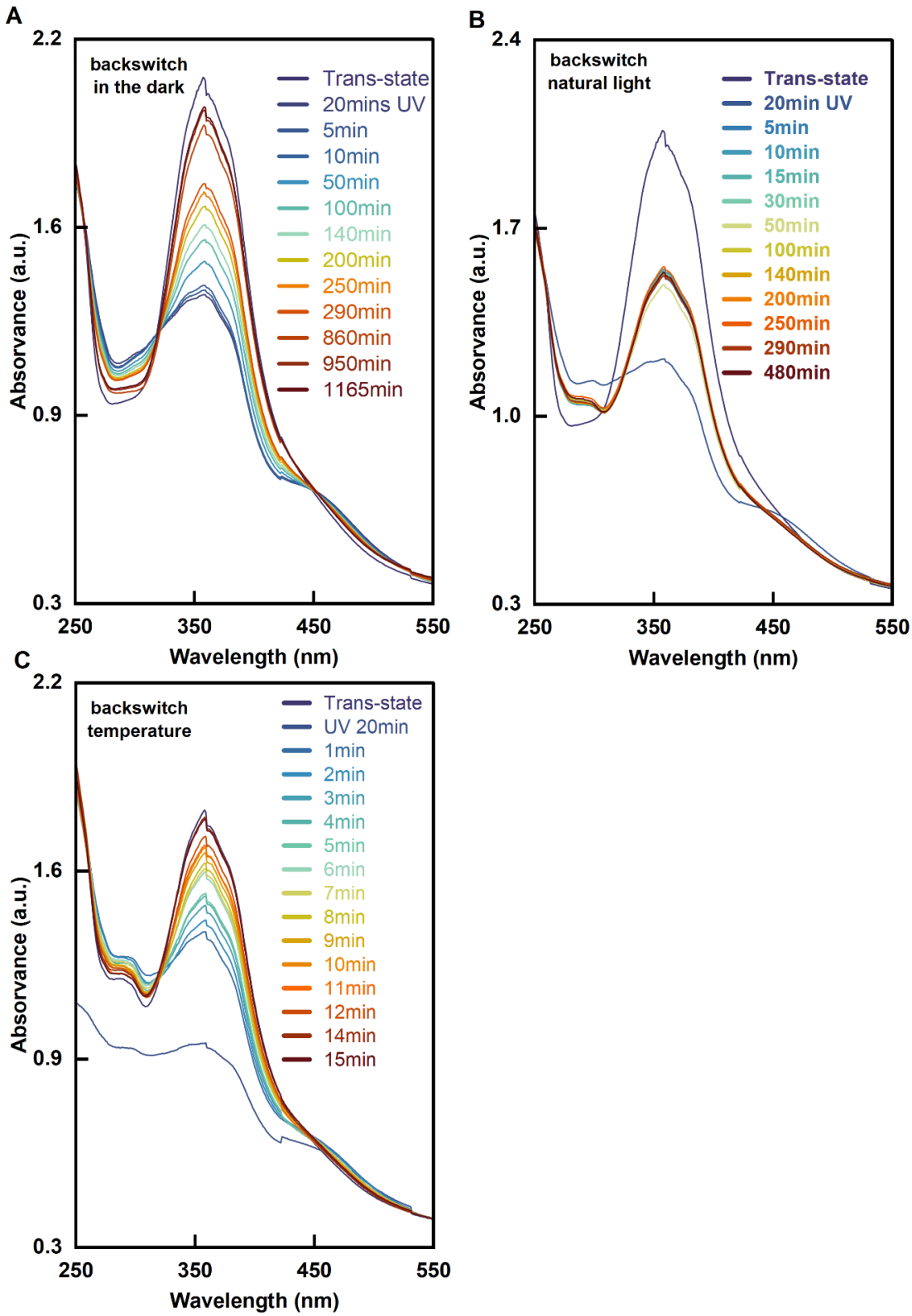

Figure 3.11 — Back switch from cis to trans conformation UV/Vis curves of sample with AZoCNC with 2.5 % AzoCNC (wt.%): in the dark (A) and with visible light (B); of with temperature (C).

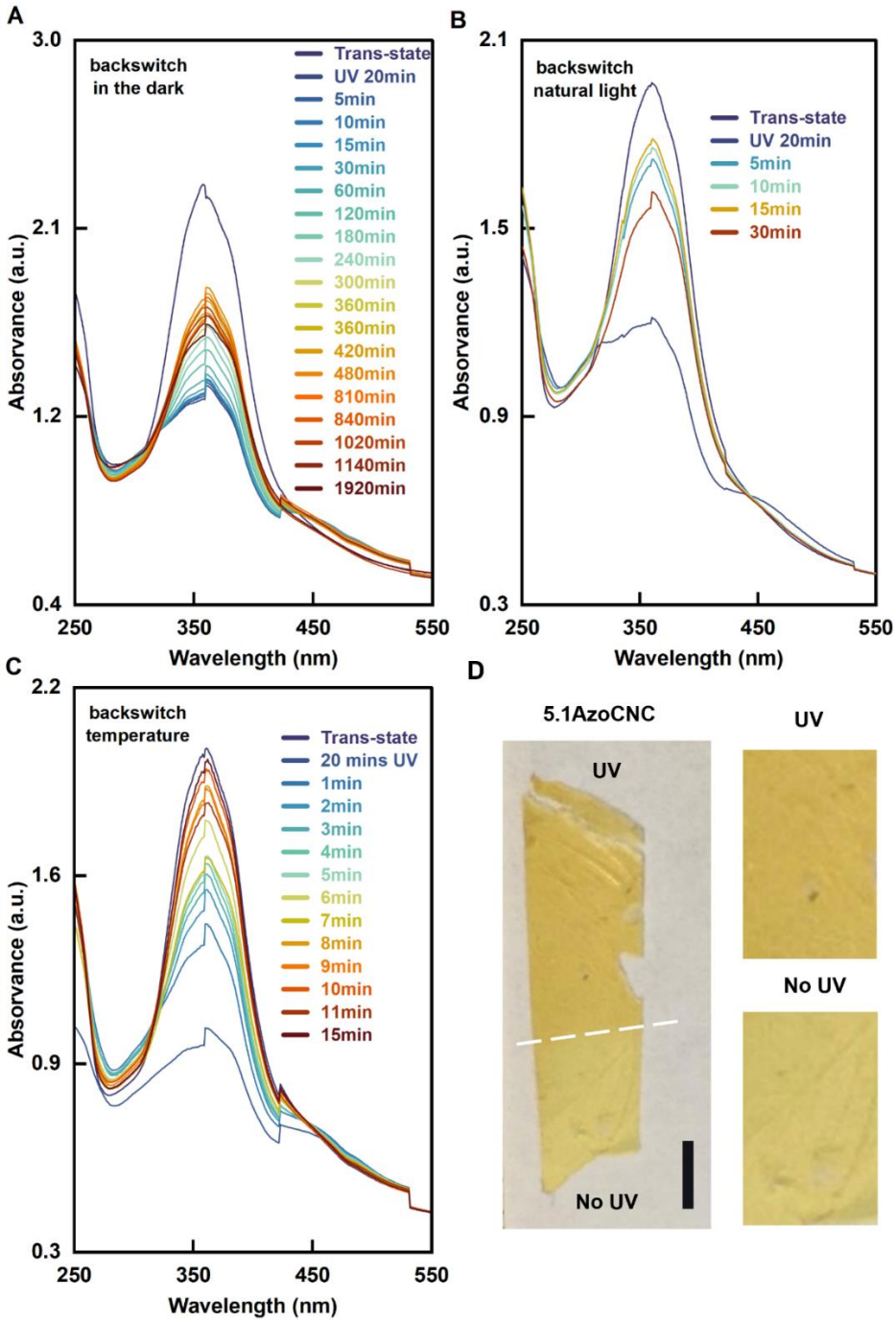

Figure 3.12 — Back switch from *cis to trans* conformation UV/Vis curves of sample with 5 % AzoCNC (wt.%): in the dark (A); and with visible light (B); of with temperature (C). D. photographs of the UV exposure effect on the appearance of a 5 % wt.% AzoCNC sample.

An example of a material that had a relative fast switch and slow back switch was the study done by Yang et al., where a functionalized azobenzene compound, that has a methoxy terminal group, to di-block polymers. Their isomerization study showed that the material had the same wavelength peaks (358 nm and 450 nm), and the *cis* conformation was reached in seconds while the backswitch in the dark was reached 13h later. So, it was suggested that the incorporation of the azo block into a polymeric system reduces the *cis*-to-*trans* isomerization rate of the azo chromophores [69], due to the azo monomer used a rotation mechanism with a high potential energy barrier to achieve a slower isomerization rate [69], [70].

3.2.2 Wettability Tests

The wettability properties offer valuable insights into potential applications [42], [71]. In accordance with Dankovich et al. study, the authors reported that the casted CNC films present, on average, a static contact angle of 32.5º±1.8º [56]. Particularly, the surface free energy can be calculated from the average value of intrinsic contact angle (θc) measurements, resourcing to the Young-Laplace equation (Eq. 2), which γ_{SV}, γ_{SL} and γ represents the surface tensions between the interfaces of solid-vapor phases, solid-liquid phases, and liquid-vapor phases, respectively:

$$cos\ \theta c\ = \frac{\gamma_{SV} - \gamma_{SL}}{\gamma} \qquad \text{(Eq. 2)}$$

This study was divided by first having several measurements involving the CNC-based films with the cross-linking agent and the combined thermal treatment effect. On the other hand, the effect on AzoCNC films while exposed to cycles of UV/Vis was also to analyzed. The static contact angle measurements were obtained from sessile droplets deposited onto the surface of the samples and the SCA20 software that uses the Young-Laplace equation automatically to calculate the value of θc. Besides this, the contact angle measurement was also done on the GA films, which it can be found in the annex A.3.

3.2.2.1 Wettability tests with UV/Vis cycles

A recent study was conducted on the effect of the CA on the CNC-based films whereas, Csiszár et al. concluded that at a 30% concentration of CA, the degree of cross-linking becomes significant due to the reduction of available OH groups on the surface, leading to a decrease of the surface free energy [71]. By looking at how the CNC and CNC/HPC films react to the heat treatment, it is possible to figure out how heat treatment affects the energy of the surface, as it is expected for CNC/CA films to be more hydrophobic than CNC films. Csiszár et al. also studied the CNC/CA film surface with water droplets. The static contact angle value increased with the increase of CA solid content on the CNC film. Besides that, the contact angle value also increased significantly on the treated samples at 160 ºC, compared to the untreated samples.[71]

Figure 3.13A shows a graphic containing the average values of 10 measurements retrieved at 2 seconds of settle time of a 2 µL water droplet deposit on the surface of the treated and untreated control samples. All the control samples showed a hydrophilic behavior (<90 ºC), as the heat-treated counterparts showed higher values, although the increase was not significant. Besides, these values are in accordance with data from other working groups [71], [72], as the CNC with CA may have values between 30~37º (untreated) or 36~48 º (treated at 160 ºC).

Wettability tests were accessed in order to infer about effect of the isomerization has on the wettability properties of the nanocomposite films produced.

The contact angles measurements were done onto the samples with a solid content of 1 % and 5 % wt.% AzoCNC as described in chapter 2.3. The measurements were taken initially at *trans*-state (t= 0 min) and then measured after 20 minutes of UV light exposure and after 20 minutes of relaxation with visible light (1 phase), at room temperature (20-25 ºC) (Figure 3.13B).

The test was considered done after the 2nd cycle, although the static contact angle values of the 3rd to 8th cycle of the films containing concentrations of 1 %/5 % wt.% and 0.06 %~0.19% wt.% AzoCNC are found in the annex A.4, particularly in the Figure 4.5 and Figure 4.6, respectively. For concentrations of AzoCNC (0.06 %-5.1 % AzoCNC wt.%, presented no tendency on wettability character (Figure 3.13B). However, the contact angle variation is almost 20º between cycles. In general, all the samples presented, in most of the measures after the UV exposure, lower contact values compared to the measurement after the relaxation in visible light. This means that the samples when displayed in *cis*-conformation are predisposed to hydrophilic character, while in the *trans*-conformation, the samples have a predisposition towards a hydrophobic behavior.

The test was considered finished after the 2nd cycle due to denoted torsions on the samples. This was caused by the consecutive water droplets and UV exposure. To have a visual observation of this phenomenon, in the Figure 3.13C an image was added with the state of a sample after 8 cycles.

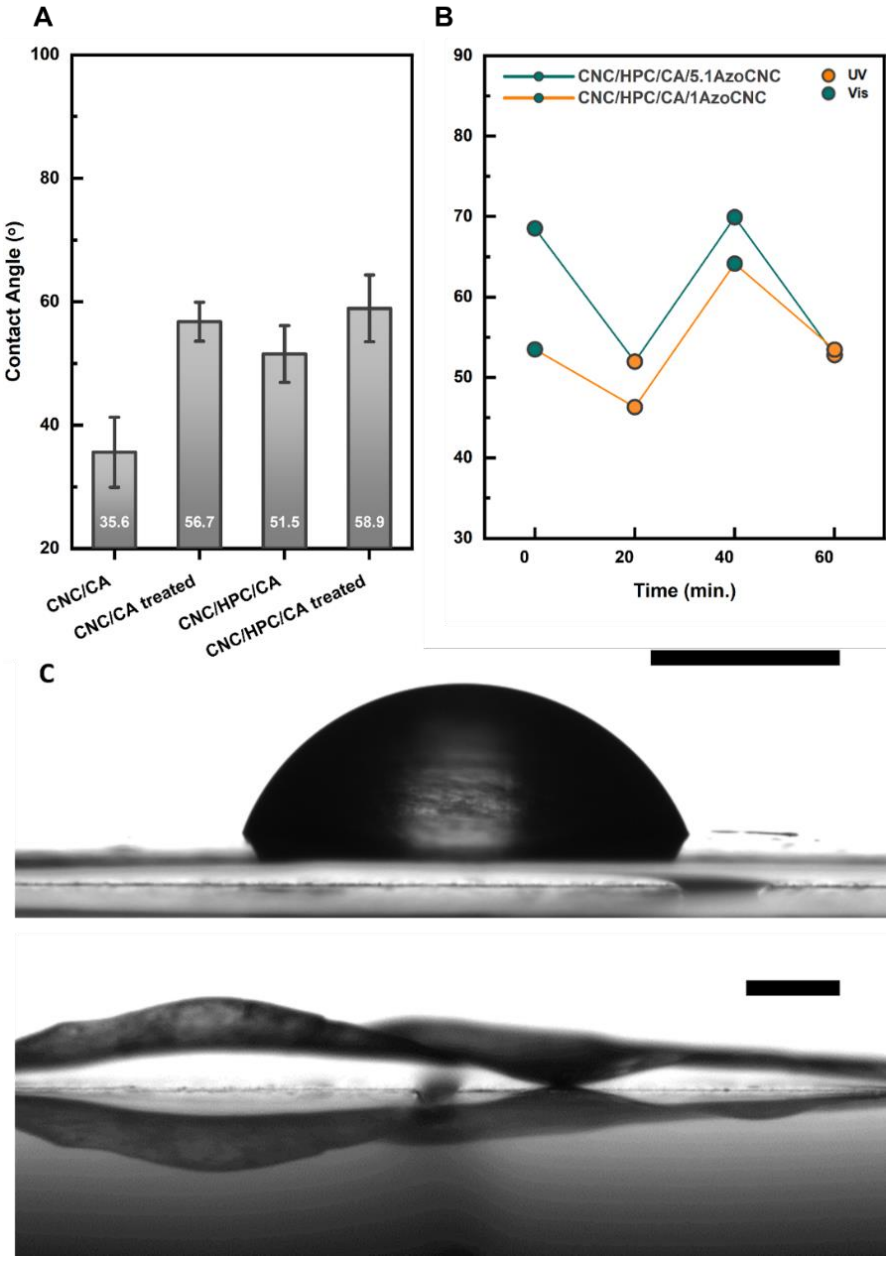

Figure 3.13 — A. Contact Angle measurement of the treated and non-treated control samples and the respective contact angle values. (n=12); B. 5 % AzoCNC sample after 2 cycles of UV/Vis; C. 5 % AzoCNC sample state before UV exposure and after 8 cycles of UV/Vis (Scale bar: 1 mm).

In the literature, it's been known that azobenzene-functionalizing cellulosic materials had a particular effect on its surface free energy [42], emphasizing the change of wettability, as it's characteristic of azobenzene moieties to turn the surface more hydrophobic, on the *trans*-state, after the relaxation, which means after a certain time period of the film not absorbing UV light.

4

CONCLUSION

Initially, the preparation of the CNC, AzoCNC, and CNC/HPC suspensions were conducted, with the aim of producing films that comprised the interesting properties of each material. Additionally, a cross-linker agent was needed to produce the films, which preliminary tests were conducted to choose between glutaraldehyde and citric acid, which the latter was chosen due to the fast thermal cross-linking reaction and its non-toxicity. With the cross-linker selected, the isomerization of the AzoCNC suspension was study before use. So, with this, the main goal of this work was the production of a stimuli-responsive material. The nanocomposite films produced were also the target of a variety of characterization techniques, such as POM, CD, SEM, and stimuli-responsive tests, like isomerization study on the film's samples and wettability test, which involved the contact angle measurements with UV/Vis cycles.

With POM photography, Circular Dichroism and SEM images we were able to demonstrate that the nanocomposite films produced maintained the left-handed orientation of the chiral nematic structure of the CNC film.

While TGA analysis indicate that the degradation of the films initiate at values higher than 200 ºC, and between studies, it was observed the samples of the nanocomposite films produced changing tones of the films overexposure of long periods of a low-temperature value (60 ºC) (turning yellow to orange tone), hinting that the films and may have colorimetric properties.

The isomerization showed that the relaxation rate was slower than what is found in the literature for simple cellulose materials functionalized with azobenzene moieties, taking almost a day to back switch in the dark with the suspension and the films, concluding that the *cis* isomer is retained. The isomerization in visible light of the suspension showed to be reversible while in the films it was not, as the back switch of *cis* to *trans* isomer wasn't reached. This might be due to the UV contribution on the visible light. A particularity is that the 5 % did not present a reversible isomerization, always transitioning between two photostacionary positions and never reaching the *trans*-conformation. Nevertheless, the composite film that underwent this UV exposure were photosensitive.

The contact angles measurements with UV/Vis cycles (40 mins each cycle) were ensued, and after 2 cycles the samples had torsions due to the consecutive combined effect of the water droplets and UV exposure. The incorporation of AzoCNC into this nanocomposite system, after irradiation with UV, turned out to reduce the hydrophobic properties of AzoCNC because of the high dipole moment of *cis* isomer. The wettability results are in conformity with the isomerization study as the time of relaxation was not enough to fully return to the *trans*-state in all the cycles, with more hydrophobic properties of AzoCNC.

While with the visible light or even in the dark, it was not enough to reverse the AzoCNC conformation to the *trans*-state, a test with temperature was done. Using 60 ºC, the Azo moiety was able to show a full conversion into the *trans* conformation after just 15 minutes. However, the temperature to be used should be optimized.

The propositions for future studies would be the optimization of the dispersion of AzoCNC, in order to obtain a more stable suspension where no aggregation could be seen. Besides this, it would be interesting to also compare to CNC/HPC/AzoCNC to have inferences of the cross-linking effect on the isomerization.

Further studies would be needed to confirm if the nanocomposite system produced has other multi-responsive properties and analyze its colorimetric, bending, wettability properties: with pH, humidity as citric acid and HPC is known for its pH and humidity-responsive properties, respectively [73], whereas per example CA-cross-linked CNC showed different behaviors in solutions with different pH [51].

Besides this, it would be important to do a contact angle measurement with UV/ temperature cycles to assess the effect of the rapid isomerization of the nanocomposite systems with other temperature values and study the backswitch isomerization with an LED light with $\lambda \approx 450$ nm. Furthermore this, it would be interesting to see the effect of the isomerization on the CD spectra as well.

It is also suggested to further study the GA-cross-linked films. For example, to perform contact angle measurement and isomerization study of heat-treated and/or HCl-treated CNC/HPC/AzoCNC/GA films.

REFERENCES

[1] H. E. P. P. de J. Almeida, “Aplicação de polímeros sensíveis a estímulos em sistemas de libertação modificada de fármacos para uso oftálmico.,” Doctoral Thesis, Faculty of Farmacy of the University of Porto, 2016.

[2] R. Nasseri, C. P. Deutschman, L. Han, M. A. Pope, and K. C. Tam, “Cellulose nanocrystals in smart and stimuli-responsive materials: a review,” *Mater Today Adv*, vol. 5, p. 100055, 2020, doi: 10.1016/j.mtadv.2020.100055.

[3] N. H. A. A. Halim and K. N. M. Amin, “Rheological properties of cellulose nanocrystals isolated via mechanical methods in thermoplastic polyurethane matrix,” *Mater Today Proc*, vol. 57, pp. 1021–1026, Jan. 2022, doi: 10.1016/j.matpr.2021.08.273.

[4] B. M. de Abreu, “Bio-inspired nanocellulose composites systems with structural coloration as optical security features,” Master Thesis, Faculty of Science and Technology of NOVA University of Lisbon, 2019. Accessed: Dec. 03, 2022. [Online]. Available: https://run.unl.pt/handle/10362/91293

[5] P. G. de Gennes, J. Prost, and R. Pelcovits, “*The Physics of Liquid Crystals*,” *Phys Today*, vol. 48, no. 5, pp. 70–71, May 1995, doi: 10.1063/1.2808028.

[6] D. V. Saraiva *et al.*, “Flexible and Structural Coloured Composite Films from Cellulose Nanocrystals/Hydroxypropyl Cellulose Lyotropic Suspensions,” *Crystals (Basel)*, vol. 10, no. 2, p. 122, Feb. 2020, doi: 10.3390/cryst10020122.

[7] H. Oguzlu, C. Danumah, and Y. Boluk, “Colloidal behavior of aqueous cellulose nanocrystal suspensions,” *Curr Opin Colloid Interface Sci*, vol. 29, pp. 46–56, May 2017, doi: 10.1016/j.cocis.2017.02.002.

[8] R. M. Parker *et al.*, “The Self-Assembly of Cellulose Nanocrystals: Hierarchical Design of Visual Appearance.,” *Adv Mater*, vol. 30, no. 19, p. e1704477, May 2018, doi: 10.1002/adma.201704477.

[9] S. N. Fernandes, L. F. Lopes, and M. H. Godinho, “Recent advances in the manipulation of circularly polarised light with cellulose nanocrystal films,” *Curr Opin Solid State Mater Sci*, vol. 23, no. 2, pp. 63–73, Apr. 2019, doi: 10.1016/j.cossms.2018.11.004.

[10] D. Qu, O. J. Rojas, B. Wei, and E. Zussman, “Responsive Chiral Photonic Cellulose Nanocrystal Materials,” *Adv Opt Mater*, vol. 10, no. 22, p. 2201201, Nov. 2022, doi: 10.1002/adom.202201201.

[11] C. S. N. Gouveia, “Elementos oticamente variáveis para sistemas de anti falsificação originários de celulose nanocristalina,” Master Thesis, Faculty of Science and Technology of NOVA University of Lisbon, 2018. Accessed: Dec. 02, 2022. [Online]. Available: https://run.unl.pt/handle/10362/41283

[12] A. R. G. L. de Almeida, “Stimuli-Responsive Cellulose Nanocrystals based Materials,” Master Thesis, Faculty of Science and Technology of NOVA University of Lisbon, 2020. Accessed: Dec. 31, 2022. [Online]. Available: http://hdl.handle.net/10362/104027

[13] A. F. P. Lopes, “Development of New Cellulose Nanocrystal-based materials with high added value,” Master Thesis, Faculty of Science and Technology of NOVA University of Lisbon, 2018. Accessed: Dec. 03, 2022. [Online]. Available: http://hdl.handle.net/10362/40171

[14] Y. bo Wei, Q. Tang, C. Bin Gong, and M. H. W. Lam, “Review of the recent progress in photoresponsive molecularly imprinted polymers containing azobenzene chromophores,” *Anal Chim Acta*, vol. 900, pp. 10–20, Nov. 2015, doi: https://doi.org/10.1016/J.ACA.2015.10.022.

[15] J. García-Amorós and D. Velasco, “Recent advances towards azobenzene-based light-driven real-time information-transmitting materials,” *Beilstein journal of organic chemistry*, vol. 8, Jul. 2012, doi: https://doi.org/10.3762/BJOC.8.113.

[16] A. Abdollahi, H. Roghani-Mamaqani, and B. Razavi, “Stimuli-chromism of photoswitches in smart polymers: Recent advances and applications as chemosensors,” *Prog Polym Sci*, vol. 98, p. 101149, Nov. 2019, doi: 10.1016/j.progpolymsci.2019.101149.

[17] I. Otsuka and C. Barrett, “Electrospinning of photo-responsive Azo-Cellulose: towards smart fibrous materials,” *Cellulose*, vol. 26, Jul. 2019, doi: https://doi.org/10.1007/s10570-019-02585-9.

[18] B. R. Donovan, V. M. Matavulj, S. kyun Ahn, T. Guin, and T. J. White, “All-Optical Control of Shape,” *Advanced Materials*, vol. 31, no. 2, p. 1805750, Jan. 2019, doi: https://doi.org/10.1002/ADMA.201805750.

[19] C. Echeverria, S. Fernandes, M. Godinho, J. Borges, and P. Soares, “Functional Stimuli-Responsive Gels: Hydrogels and Microgels,” *Gels*, vol. 4, no. 2, p. 54, Jun. 2018, doi: 10.3390/gels4020054.

[20] G. A. Mandl, P. A. Rojas-Gutierrez, and J. A. Capobianco, “A NIR-responsive azobenzene-based supramolecular hydrogel using upconverting nanoparticles,” *Chemical Communications*, vol. 54, no. 46, pp. 5847–5850, 2018, doi: 10.1039/C8CC03101K.

[21] H. Kim *et al.*, “Shape morphing smart 3D actuator materials for micro soft robot,” *Materials Today*, vol. 41, pp. 243–269, Dec. 2020, doi: 10.1016/j.mattod.2020.06.005.

[22] M. Pilz da Cunha, S. Ambergen, M. G. Debije, E. F. G. A. Homburg, J. M. J. den Toonder, and A. P. H. J. Schenning, “A Soft Transporter Robot Fueled by Light,” *Advanced Science*, vol. 7, no. 5, p. 1902842, Mar. 2020, doi: 10.1002/advs.201902842.

[23] L. Dong and Y. Zhao, “Photothermally driven liquid crystal polymer actuators,” *Mater Chem Front*, vol. 2, no. 11, pp. 1932–1943, Oct. 2018, doi: 10.1039/C8QM00363G.

[24] S. N. Fernandes *et al.*, “Cellulose-based nanostructures for photoresponsive surfaces,” *Cellulose*, vol. 23, no. 1, pp. 465–476, Feb. 2016, doi: 10.1007/s10570-015-0815-8.

[25] L. Zhang, J. Li, and H. Liu, “Thermal inverse phase transition of azobenzene hydroxypropylcellulose in aqueous solutions,” *Cellulose*, vol. 23, no. 2, pp. 1177–1188, Apr. 2016, doi: 10.1007/s10570-016-0878-1.

[26] Y. Kim, D. Jeong, V. V. Shinde, Y. Hu, C. Kim, and S. Jung, “Azobenzene-grafted carboxymethyl cellulose hydrogels with photo-switchable, reduction-responsive and self-healing properties for a controlled drug release system,” *Int J Biol Macromol*, vol. 163, pp. 824–832, Nov. 2020, doi: 10.1016/j.ijbiomac.2020.07.071.

[27] X. Pang, J. Lv, C. Zhu, L. Qin, and Y. Yu, “Photodeformable Azobenzene-Containing Liquid Crystal Polymers and Soft Actuators,” *Advanced Materials*, vol. 31, no. 52, p. 1904224, Dec. 2019, doi: 10.1002/adma.201904224.

[28] J. R. McKee, E. A. Appel, J. Seitsonen, E. Kontturi, O. A. Scherman, and O. Ikkala, “Healable, Stable and Stiff Hydrogels: Combining Conflicting Properties Using Dynamic and Selective Three-Component Recognition with Reinforcing Cellulose Nanorods,” *Adv Funct Mater*, vol. 24, no. 18, pp. 2706–2713, May 2014, doi: 10.1002/adfm.201303699.

[29] E. Gicquel, “Development of stimuli-responsive cellulose nanocrystals hydrogels for smart applications,” 2017. Accessed: Jan. 05, 2023. [Online]. Available: https://www.theses.fr/2017GREAI105.pdf

[30] J. Kim, J. W. Kim, H. C. Kim, L. Zhai, H.-U. Ko, and R. M. Muthoka, “Review of Soft Actuator Materials,” *International Journal of Precision Engineering and Manufacturing*, vol. 20, no. 12, pp. 2221–2241, Dec. 2019, doi: 10.1007/s12541-019-00255-1.

[31] J. Hu, Y. Zhu, H. Huang, and J. Lu, “Recent advances in shape–memory polymers: Structure, mechanism, functionality, modeling and applications,” *Prog Polym Sci*, vol. 37, no. 12, pp. 1720–1763, Dec. 2012, doi: 10.1016/j.progpolymsci.2012.06.001.

[32] D. Y. Wu, S. Meure, and D. Solomon, “Self-healing polymeric materials: A review of recent developments,” *Prog Polym Sci*, vol. 33, no. 5, pp. 479–522, May 2008, doi: 10.1016/j.progpolymsci.2008.02.001.

[33] O. Kose, A. Tran, L. Lewis, W. Y. Hamad, and M. J. MacLachlan, “Unwinding a spiral of cellulose nanocrystals for stimuli-responsive stretchable optics,” *Nat Commun*, vol. 10, no. 1, p. 510, Jan. 2019, doi: 10.1038/s41467-019-08351-6.

[34] L. Cao, J. Fan, J. Huang, and Y. Chen, “A robust and stretchable cross-linked rubber network with recyclable and self-healable capabilities based on dynamic covalent bonds,” *J Mater Chem A Mater*, vol. 7, no. 9, pp. 4922–4933, Feb. 2019, doi: 10.1039/C8TA11587G.

[35] G. Wu *et al.*, “Multi-stimuli responsive shape memory behavior of dual-switch TPU/CB/CNC hybrid nanocomposites as triggered by heat, water, ethanol, and pH,” *Chemical Engineering Journal*, vol. 450, p. 138253, Dec. 2022, doi: 10.1016/j.cej.2022.138253.

[36] Q. Meng and J. Hu, “A review of shape memory polymer composites and blends,” *Compos Part A Appl Sci Manuf*, vol. 40, no. 11, pp. 1661–1672, Nov. 2009, doi: 10.1016/j.compositesa.2009.08.011.

[37] Q. Zheng, C. Xu, Z. Jiang, M. Zhu, C. Chen, and F. Fu, “Smart Actuators Based on External Stimulus Response,” *Front Chem*, vol. 9, 2021, doi: 10.3389/fchem.2021.650358.

[38] L. A. E. Müller *et al.*, “Functionalized Cellulose Nanocrystals as Active Reinforcements for Light-Actuated 3D-Printed Structures,” *ACS Nano*, vol. 16, no. 11, pp. 18210–18222, Nov. 2022, doi: 10.1021/acsnano.2c05628.

[39] W. Yuan, C. Wang, S. Lei, J. Chen, S. Lei, and Z. Li, “Ultraviolet light-, temperature- and pH-responsive fluorescent sensors based on cellulose nanocrystals,” *Polym Chem*, vol. 9, no. 22, pp. 3098–3107, Jun. 2018, doi: 10.1039/C8PY00613J.

[40] Q. Xu, J. Yi, X. Zhang, and H. Zhang, “A novel amphotropic polymer based on cellulose nanocrystals grafted with azo polymers,” *Eur Polym J*, vol. 44, no. 9, pp. 2830–2837, Sep. 2008, doi: 10.1016/j.eurpolymj.2008.06.010.

[41] X. Liu, M. Li, X. Zheng, E. Retulainen, and S. Fu, “Dual Light- and pH-Responsive Composite of Polyazo-Derivative Grafted Cellulose Nanocrystals,” *Materials*, vol. 11, no. 9, p. 1725, Sep. 2018, doi: 10.3390/ma11091725.

[42] Z. Xu, S. Peng, G. Zhou, and X. Xu, “Highly Hydrophobic, Homogeneous Suspension and Resin by Graft Copolymerization Modification of Cellulose Nanocrystal (CNC),” *Journal of Composites Science*, vol. 4, no. 4, p. 186, Dec. 2020, doi: 10.3390/jcs4040186.

[43] S. Peng, Q. Luo, G. Zhou, and X. Xu, “Recent Advances on Cellulose Nanocrystals and Their Derivatives,” *Polymers (Basel)*, vol. 13, no. 19, p. 3247, Sep. 2021, doi: 10.3390/polym13193247.

[44] O. Kose, C. E. Boott, W. Y. Hamad, and M. J. MacLachlan, “Stimuli-Responsive Anisotropic Materials Based on Unidirectional Organization of Cellulose Nanocrystals in an Elastomer,” *Macromolecules*, vol. 52, no. 14, pp. 5317–5324, Jul. 2019, doi: 10.1021/acs.macromol.9b00863.

[45] C. M. Walters, C. E. Boott, T.-D. Nguyen, W. Y. Hamad, and M. J. MacLachlan, “Iridescent Cellulose Nanocrystal Films Modified with Hydroxypropyl Cellulose,” *Biomacromolecules*, vol. 21, no. 3, pp. 1295–1302, Mar. 2020, doi: 10.1021/acs.biomac.0c00056.

[46] D. v. Saraiva *et al.*, “Flexible and Structural Coloured Composite Films from Cellulose Nanocrystals/Hydroxypropyl Cellulose Lyotropic Suspensions,” *Crystals 2020, Vol. 10, Page 122*, vol. 10, no. 2, p. 122, Feb. 2020, doi: https://doi.org/10.3390/CRYST10020122.

[47] P. R. Anusuyadevi *et al.*, “Photoresponsive and Polarization-Sensitive Structural Colors from Cellulose/Liquid Crystal Nanophotonic Structures,” *Advanced Materials*, vol. 33, no. 36, p. 2101519, Sep. 2021, doi: 10.1002/adma.202101519.

[48] Z. Hanif, D. Choi, M. Z. Tariq, M. La, and S. J. Park, “Water-Stable Flexible Nanocellulose Chiral Nematic Films through Acid Vapor Cross-Linked Glutaraldehyde for Chiral Nematic Templating,” *ACS Macro Lett*, vol. 9, no. 2, pp. 146–151, Feb. 2020, doi: 10.1021/acsmacrolett.9b00826.

[49] L. Bai, Z. Wang, Y. He, F. Song, X. Wang, and Y. Wang, “Flexible Photonic Cellulose Nanocrystal Films as a Platform with Multisensing Functions,” *ACS Sustain Chem Eng*, vol. 8, no. 50, pp. 18484–18491, Dec. 2020, doi: 10.1021/acssuschemeng.0c06174.

[50] R. R. da Rosa, S. N. Fernandes, M. Mitov, and M. H. Godinho, “Cellulose and Chitin Twisted Structures: From Nature to Applications,” *Adv Funct Mater*, p. 2304286, Aug. 2023, doi: 10.1002/adfm.202304286.

[51] C. Verma, M. Chhajed, S. Singh, M. Sathwane, and P. K. Maji, “Bioinspired structural color sensors based on self-assembled cellulose nanocrystal/citric acid to distinguish organic solvents,” *Colloids Surf A Physicochem Eng Asp*, vol. 655, p. 130206, Dec. 2022, doi: 10.1016/j.colsurfa.2022.130206.

[52] P. Spiliopoulos *et al.*, “Native Structure of the Plant Cell Wall Utilized for Top-Down Assembly of Aligned Cellulose Nanocrystals into Micrometer-Sized Nanoporous Particles,” *Macromol Rapid Commun*, vol. 41, no. 15, Aug. 2020, doi: 10.1002/marc.202000201.

[53] M.-X. Ruiz-Caldas *et al.*, “Citrated cellulose nanocrystals from post-consumer cotton textiles,” *J Mater Chem A Mater*, vol. 11, no. 13, pp. 6854–6868, Mar. 2023, doi: 10.1039/D2TA09456H.

[54] C. L. C. Chan *et al.*, “Visual Appearance of Chiral Nematic Cellulose-Based Photonic Films: Angular and Polarization Independent Color Response with a Twist,” *Advanced Materials*, vol. 31, no. 52, p. 1905151, Dec. 2019, doi: 10.1002/adma.201905151.

[55] T. Balcerowski, B. Ozbek, O. Akbulut, and A. G. Dumanli, “Hierarchical Organization of Structurally Colored Cholesteric Phases of Cellulose via 3D Printing,” *Small*, vol. 19, no. 8, p. 2205506, Feb. 2023, doi: 10.1002/smll.202205506.

[56] T. A. Dankovich and D. G. Gray, “Contact Angle Measurements on Smooth Nanocrystalline Cellulose (I) Thin Films,” *J Adhes Sci Technol*, vol. 25, no. 6–7, pp. 699–708, Jan. 2011, doi: 10.1163/016942410X525885.

[57] P. Spiliopoulos *et al.*, “Native Structure of the Plant Cell Wall Utilized for Top-Down Assembly of Aligned Cellulose Nanocrystals into Micrometer-Sized Nanoporous Particles,” *Macromol Rapid Commun*, vol. 41, no. 15, 2020, doi: 10.1002/marc.202000201.

[58] W. Park and D. K. Yoon, “Orientation control of helical nanofilament phase and its chiroptical applications,” *Crystals*, vol. 10, no. 8. 2020. doi: 10.3390/cryst10080675.

[59] S. A. A. Sanches, W. C. Costa, I. H. Bechtold, R. A. P. Halfen, A. A. Merlo, and L. F. Campo, “Bromine-terminated azobenzene liquid crystals,” *Liq Cryst*, vol. 46, no. 5, pp. 655–665, Apr. 2019, doi: 10.1080/02678292.2018.1517226.

[60] N. Łukasik, K. Hemine, I. Anusiewicz, P. Skurski, and E. Paluszkiewicz, “Photoresponsive Amide-Based Derivatives of Azobenzene-4,4′-Dicarboxylic Acid—Experimental and Theoretical Studies,” *Materials*, vol. 14, no. 14, p. 3995, Jul. 2021, doi: 10.3390/ma14143995.

[61] V. Hospodarova, E. Singovszka, N. Stevulova, V. Hospodarova, E. Singovszka, and N. Stevulova, “Characterization of Cellulosic Fibers by FTIR Spectroscopy for Their Further Implementation to Building Materials,” *Am J Analyt Chem*, vol. 9, no. 6, pp. 303–310, Jun. 2018, doi: 10.4236/AJAC.2018.96023.

[62] D. Ciolacu, F. Ciolacu, and V. I. Popa, “Amorphous Cellulose-Structures and Characterization,” *Cellulose Chemistry and Technology*, vol. 45, no. 2, pp. 13–21, 2011.

[63] D. Gaspar *et al.*, “Nanocrystalline cellulose applied simultaneously as the gate dielectric and the substrate in flexible field effect transistors,” *Nanotechnology*, vol. 25, no. 9, p. 094008, Feb. 2014, doi: 10.1088/0957-4484/25/9/094008.

[64] Y. Zhou, Y. Li, F. Dundar, K. R. Carter, and J. J. Watkins, “Fabrication of patterned cellulose film via solvent-assisted soft nanoimprint lithography at a submicron scale,” *Cellulose*, vol. 25, no. 9, 2018, doi: 10.1007/s10570-018-1920-2.

[65] S. Spinella *et al.*, “Concurrent Cellulose Hydrolysis and Esterification to Prepare a Surface-Modified Cellulose Nanocrystal Decorated with Carboxylic Acid Moieties,” *ACS Sustain Chem Eng*, vol. 4, no. 3, pp. 1538–1550, Mar. 2016, doi: 10.1021/acssuschemeng.5b01489.

[66] H. Yu, Z. Qin, B. Liang, N. Liu, Z. Zhou, and L. Chen, “Facile extraction of thermally stable cellulose nanocrystals with a high yield of 93% through hydrochloric acid hydrolysis under hydrothermal conditions,” *J Mater Chem A Mater*, vol. 1, no. 12, p. 3938, Feb. 2013, doi: 10.1039/c3ta01150j.

[67] G. Smets, “Photochromic phenomena in the solid phase,” in *Unusual Properties of New Polymers*, 2005. doi: 10.1007/bfb0025248.

[68] L. F. V. Pinto *et al.*, “Cellulose-based liquid crystalline photoresponsive films with tunable surface wettability,” *Langmuir*, vol. 27, no. 10, 2011, doi: 10.1021/la200422q.

[69] P.-C. Yang, C.-Y. Li, H.-C. Chen, and R.-S. Juang, “Synthesis, photochemical properties, and self-assembly of diblock copolymer bearing azobenzene moieties,” *J Taiwan Inst Chem Eng*, vol. 54, pp. 155–164, Sep. 2015, doi: 10.1016/j.jtice.2015.03.008.

[70] C. Ho, K. Yang, and S. Lee, “Mechanistic study of trans⇆cis isomerization of the substituted azobenzene moiety bound on a liquid-crystalline polymer,” *J Polym Sci A Polym Chem*, vol. 39, no. 13, pp. 2296–2307, Jul. 2001, doi: 10.1002/pola.1206.

[71] E. Csiszár, I. Herceg, and E. Fekete, “Effect of Heating and Citric Acid on the Performance of Cellulose Nanocrystal Thin Films,” *Polymers (Basel)*, vol. 15, no. 7, p. 1698, Mar. 2023, doi: 10.3390/polym15071698.

[72] M. Nuruddin *et al.*, “Gas and Water Vapor Barrier Performance of Cellulose Nanocrystal–Citric Acid-Coated Polypropylene for Flexible Packaging,” *ACS Appl Polym Mater*, vol. 2, no. 11, pp. 4405–4414, Nov. 2020, doi: 10.1021/acsapm.0c00483.

[73] S. Krukowski, M. Karasiewicz, and W. Kolodziejski, “Convenient UV-spectrophotometric determination of citrates in aqueous solutions with applications in the pharmaceutical analysis of oral electrolyte formulations,” *J Food Drug Anal*, vol. 25, no. 3, pp. 717–722, Jul. 2017, doi: 10.1016/j.jfda.2017.01.009.

A

MATERIALS AND EQUIPMENTS

A.1 Characterization Techniques

Thermogravimetric Analysis coupled with Differential Scanning Calorimetry (TGA-DSC) was conducted on 8 mg of AzoCNC and 15 mg of heat-treated samples using a Thermogravimetric Analyzer (Setaram Labsys EVO) and a Differential Scanning Calorimeter (DSC 131, Setaram). Each sample was heated from 20°C to 540°C at a rate of 10°C per minute, under an inert atmosphere. To determine the values of onset, offset temperatures it was used secondary lines (blue lines) for the TGA curve (red line) while the determination of the values of degradation temperatures were done with the wavelength value of the DTG curve (black line), as seen in the Figure 4.1.

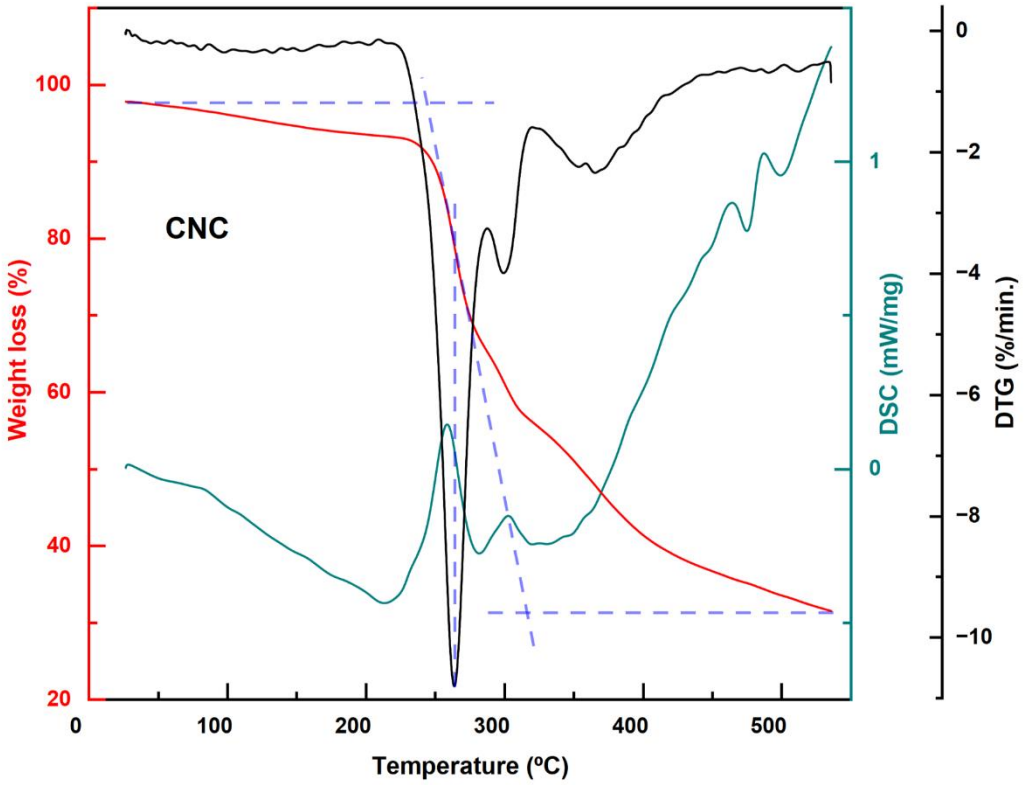

Figure 4.1 — Representation of TGA/DSC/DTG curves and the secondary lines (blue dashed lines) for the determination of the onset and offset temperatures values.

To observe the textures of the films, it was collected POM images in transmission mode of the samples, with or without crossed polarizers and circular polarizers, the films were observed on the polarized optical microscope (Olympus BX-51 connected to Schott KL2500 light source, with Olympus Stream Basic software Version 1.9 and camera Olympus DP73).

The photographs obtained of the casted samples and the suspension samples were obtained with polarized white light, using a Canon camera (EOS 550D with a macro lens EF-S 60 mm), a Nikkon J5 (Nikkor 10-30mm 1:3.5-5.6 VR) or an iPhone SE (2nd generation).

Static contact angles were measured on the surface through the sessile drop method using an OCA20 contact angle measuring instrument (DataPhysics Instruments, GmbH). Ultrapure water microdroplets (2 µL) were generated with an electronic micrometric syringe and deposited on the substrate's surface. Contact angles were determined in a settled time (2 s) after the droplet deposition. Image acquisition, analysis, and contact angle determination were performed using the SCA20 v.4.3.12 software (DataPhysics Instruments GmbH). A total of 12 measurements were taken, each in a different region of the control samples and GA-contained samples surface.

The isomerization study of the suspension and nanocomposite films was done by UV/Vis spectroscopy. It was obtained absorbance spectra, ranging between wavelengths 190-600 nm with a step of 1 nm, using a spectrophotometer with a double-beam system from G Instruments T90+, and software UVWin Version 5.2.0.

To confirm the cholesteric structure's handedness in each nanocomposite film, Circular Dichroism spectroscopy was performed with a CD spectrometer (Chirascan qCD AppliedPhotoPhysics, Chirascan software version 4.5.1825.0). All data retrieved covered wavelengths between 190-750 nm with a bandwidth of 1 nm and a scanning rate of 200 nm/s.

To observe the structure of nanocomposite films, cross-sections of the films were examined using a Scanning Electron Microscope (HITACHI Regulus 8220 in SE mode).

The samples' preparation consisted of irregular cut of each film and fixating those smaller samples onto the aluminum substrate with conductive double-sided carbon adhesive strip and then layed a thin 20 nm iridium coating (Q150T ES Quorum Sputter Coater). Images were captured in different magnifications and (8.2-20.9 mm) with 3-5 kV acceleration voltage.

To make inferences of the chemical composition of the AzoCNC and the composite films and prove if the cross-linking was successful, it was used Attenuated Total Reflectance-Fourier Transform-Infrared Spectroscopy (ATR-FTIR). All spectra were obtained in the range of wavenumbers 4000 to 500 cm^{-1}, with a 1 cm^{-1} resolution, recurring an FT-IR spectrometer (Thermo Nicolet 6700) equipped attenuated total reflectance (ATR) cell.

To measure the CNC concentration value in the suspension, a study was carried out, a gravimetric method, in which aliquots of aqueous suspensions were placed in Eppendorf's to dry at a constant temperature of 60 ºC and proceeded to dryness until the mass value numbers were constant.

A.2 CNC/CA Films

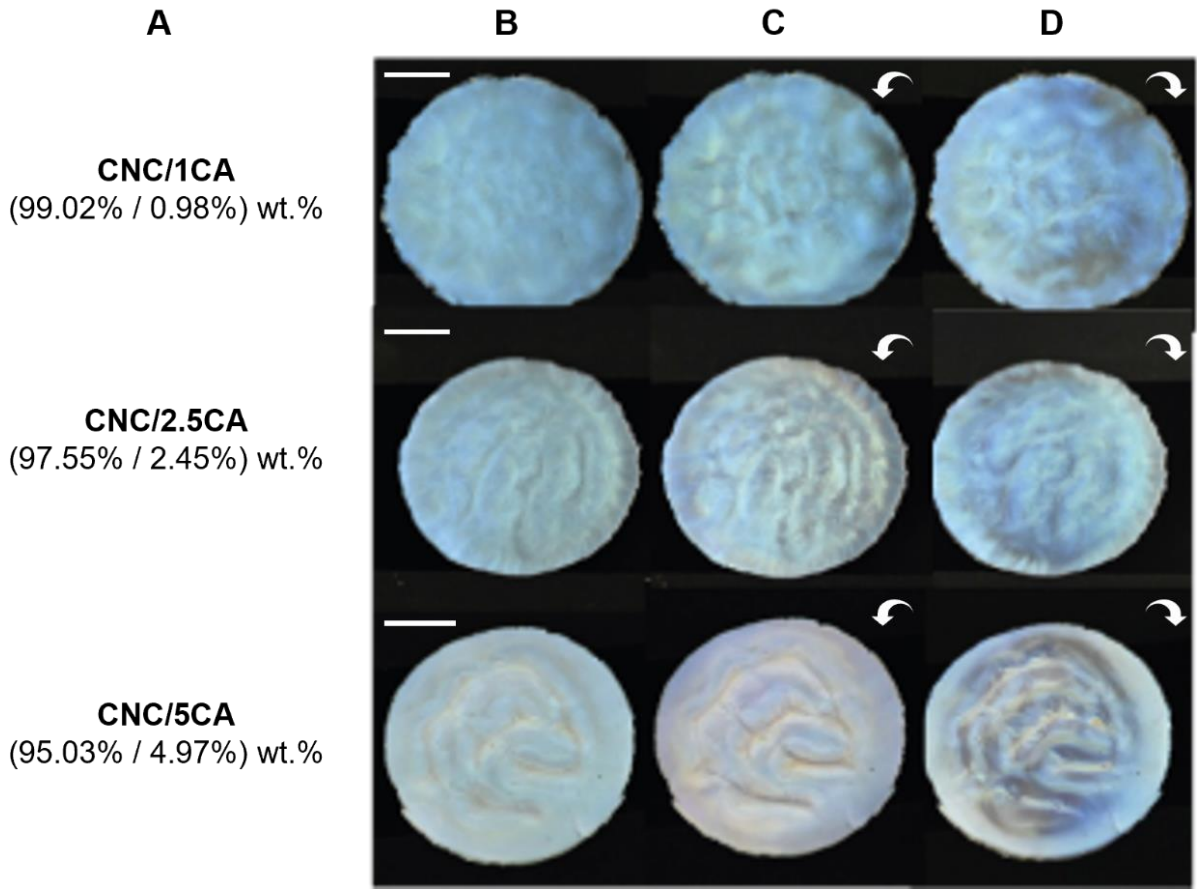

Figure 4.2 — A. Information of the films casted of the composite system of CNC/CA: composition, solid content (wt.%); B-D. Photographs with cold white light (Scale bar: 1cm): B. without polarizer; C. LCPL (left-handed arrow); D with RCPL (right-handed arrow).

A.3 CNC/HPC/GA Films

A	B	C	D
CNC/HPC **(77.02% / 22.98%) wt.%** (64 ± 8) µm			
CNC/HPC/GA 1 **(76.46% / 22.79% / 0.76%) wt.%** (106 ± 20) mm			
CNC/HPC/GA 2 **(75.73% / 22.75% / 1.52%) wt.%** (99 ± 70) mm			
CNC/HPC/GA 3 **(75.27% / 22.48% / 2.26%) wt.%** (72 ± 21) mm			
CNC/HPC/GA 4 **(74.53% / 22.51% / 2.96%) wt.%** (62 ± 16) mm			

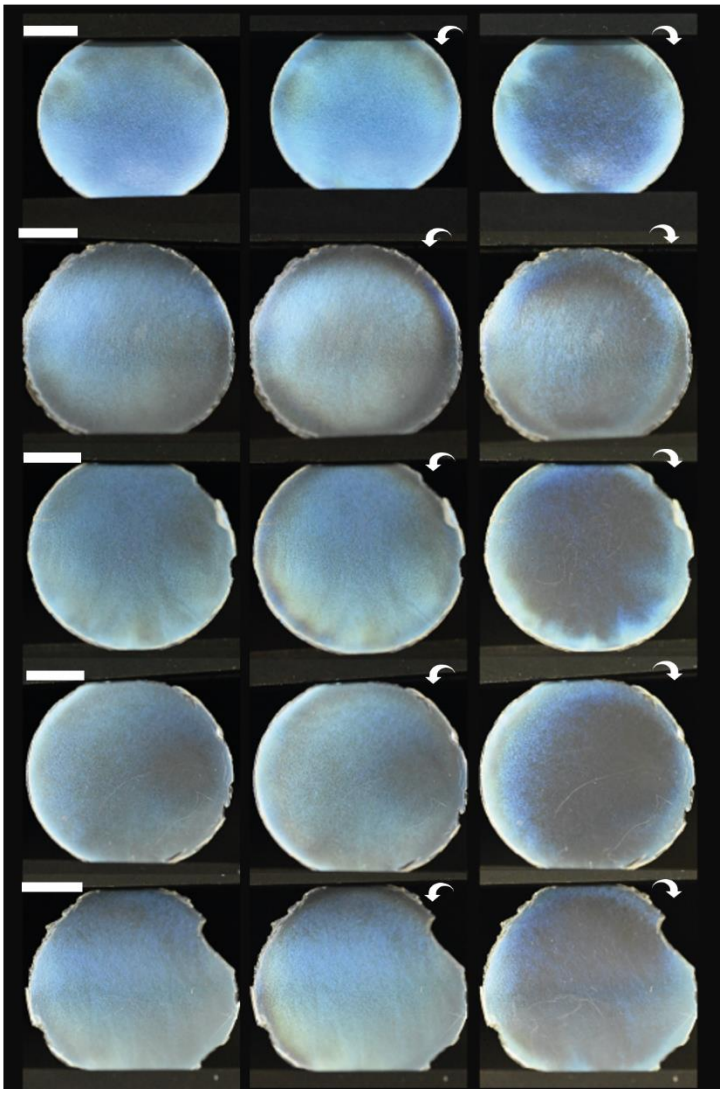

Figure 4.3 — A. Information of the films casted of the composite system of CNC/HPC/GA: composition, solid content (wt.%) and average thickness (n=10); B-D. Photographs with cold white light (Scale bar: 1cm): B. without polarizer; C. LCPL (left-handed arrow); D with RCPL (right-handed arrow).

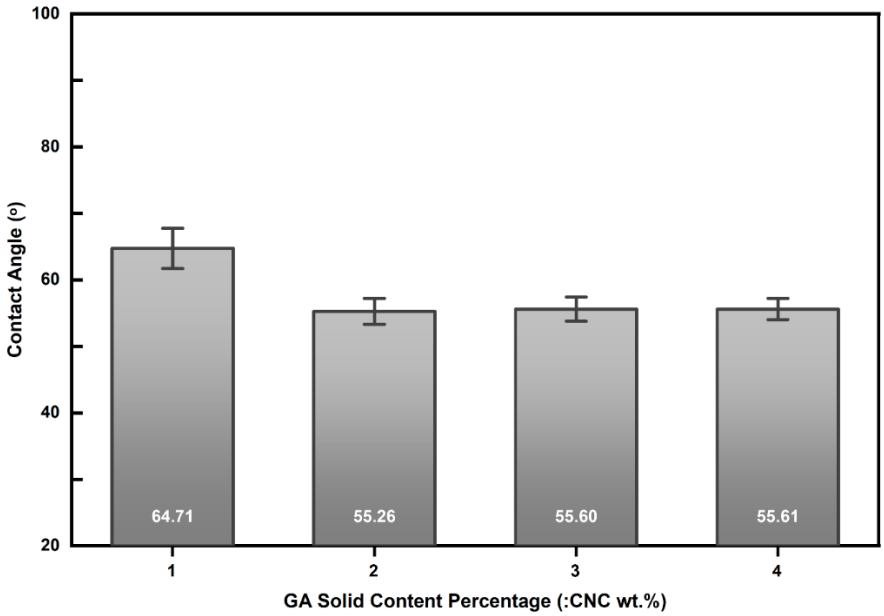

Figure 4.4 — Contact angles measurement done in CNC/HPC/CA films containing 1-4 % wt.% of GA (n=8).

A.4 Contact Angle Measurements Test with UV/Vis cycles

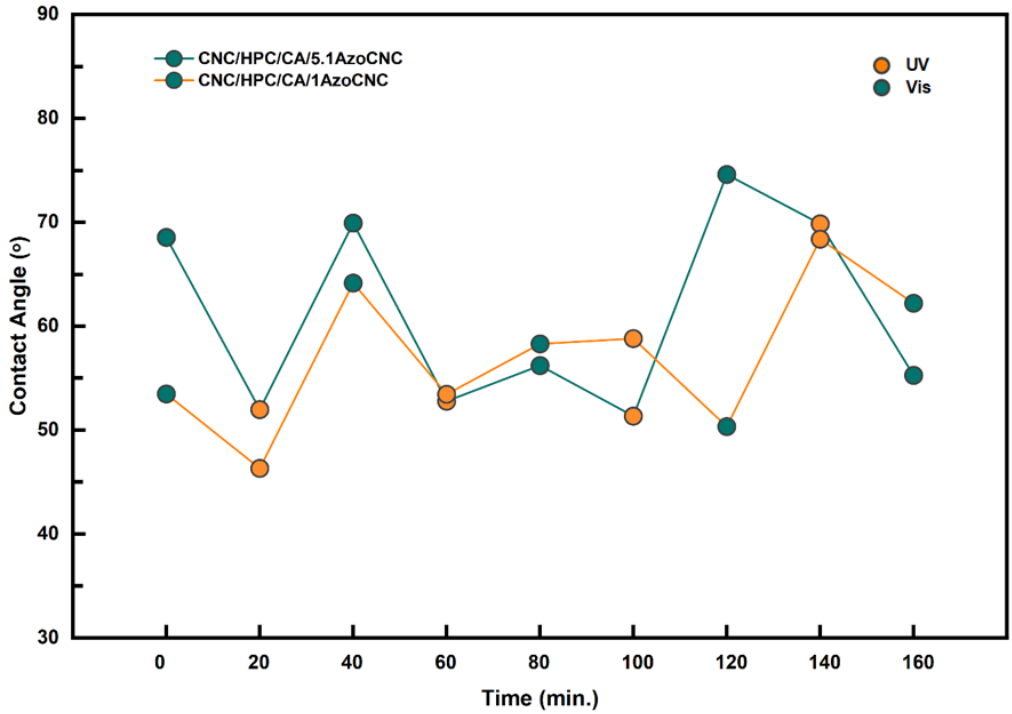

Figure 4.5 — Static Contact Angle measurements done onto the nanocomposite films with high concentrations of 1~5,1% wt.% AzoCNC.This measurements were done until the 8th cycle, measuring the static contact angle after 20 minutes UV exposure (yellow symbols) and after 20 minutes relaxation of the films, alternatively.

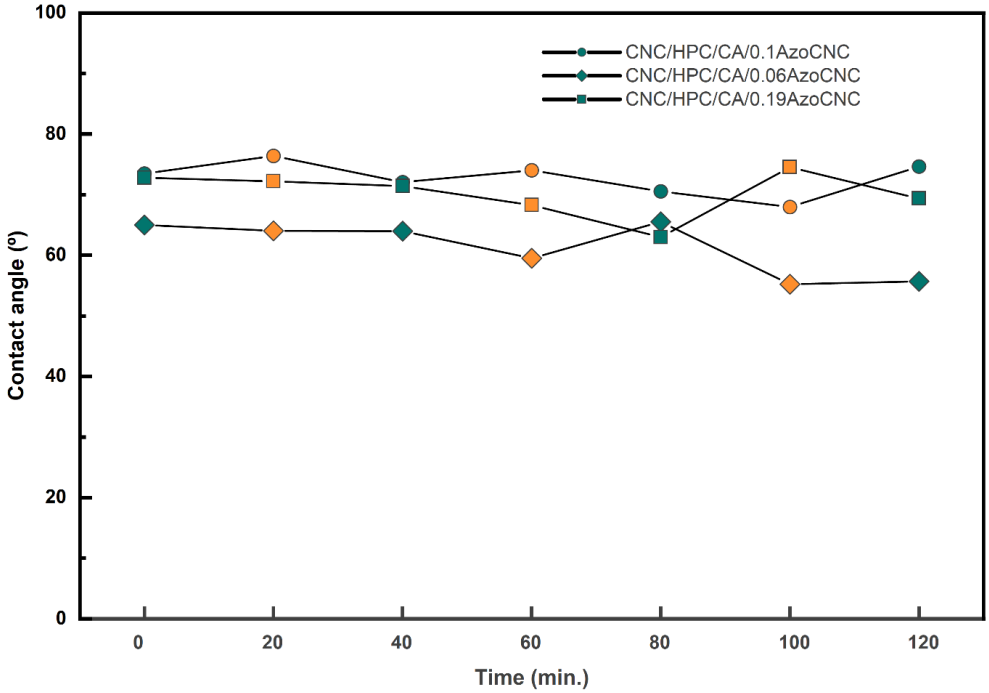

Figure 4.6 — Static Contact Angle measurements done onto the nanocomposite films with low concentrations of 0.1 %~0.19 % wt.% AzoCNC.This measurements were done until the 8th cycle,measuring the static contact angle after 20 minutes UV exposure (yellow symbols) and after 20 minutes relaxation of the films, alternatively.

A.5 UV/Vis Spectrophotometry

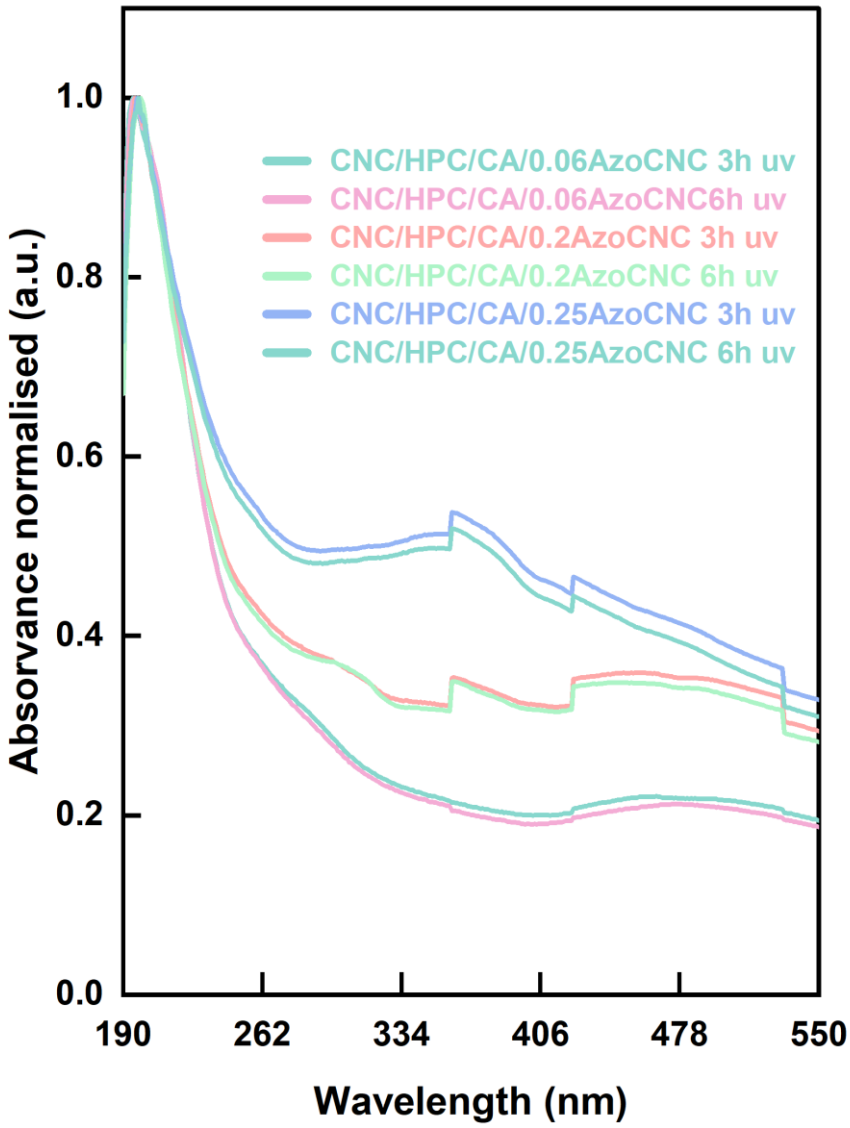

Figure 4.7 — UV/Vis spectra of the isomerization study of the nanocomposite films with low concentrations of 0.06 %~0.25 % wt.% AzoCNC.

A.6 Circular Dichroism

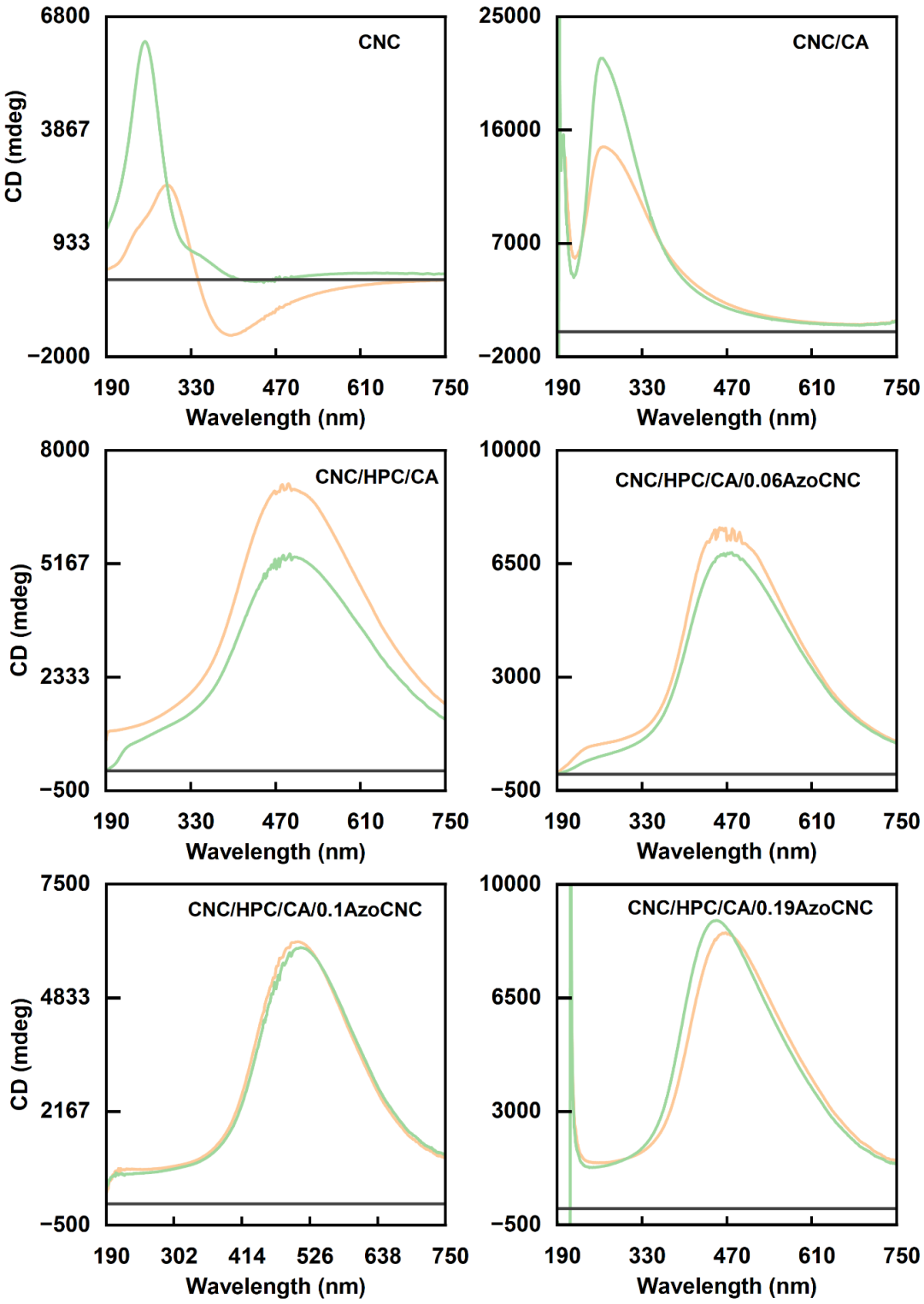

Figure 4.8 — CD spectra from both sides of each sample of CNC, CNC/CA, CNC/HPC/CA and films containing concentrations between 0.06 %~0.19 % wt.% AzoCNC.

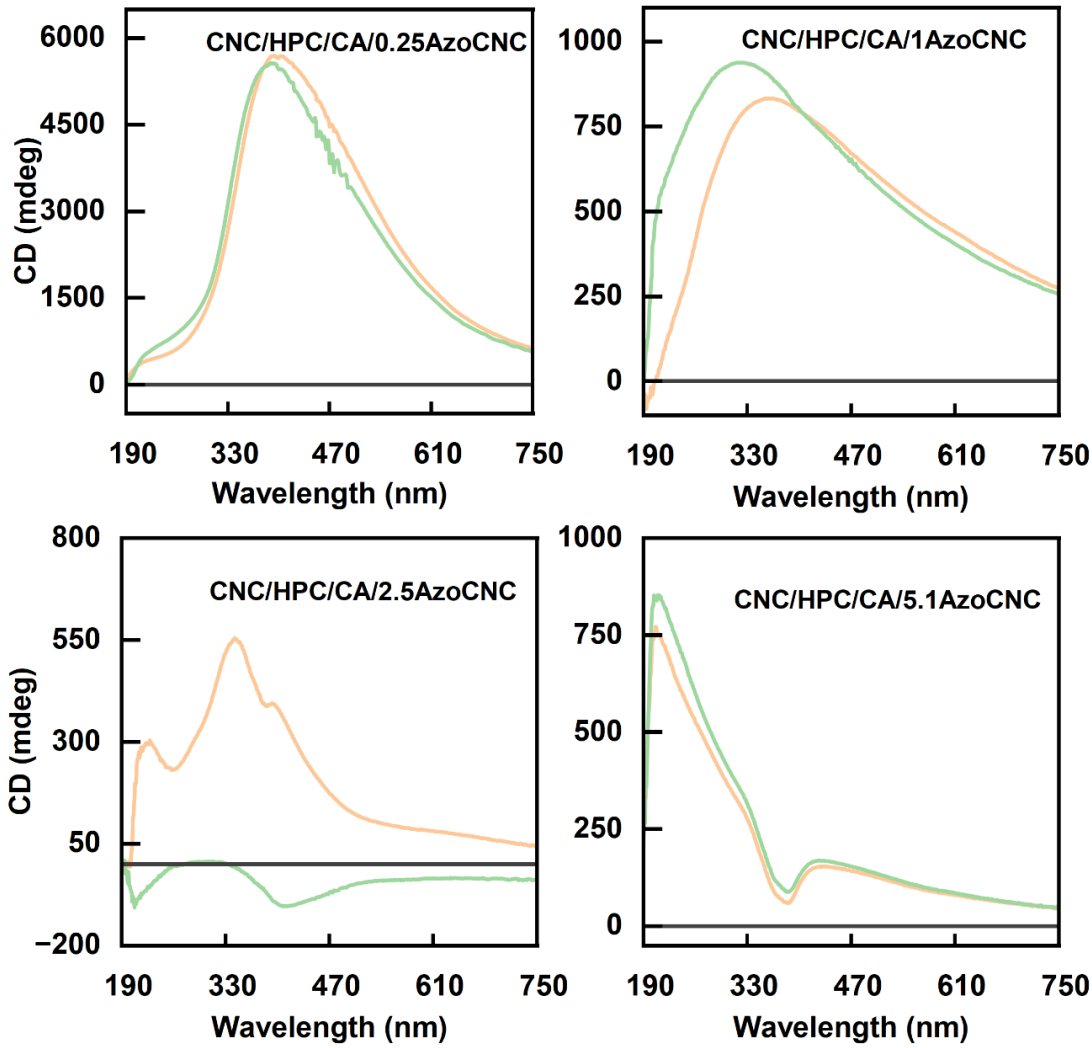

Figure 4.9 — CD spectra from both sides of each film samples containing between 0.25 %~5.1 % wt.% AzoCNC.

Table 4.1 — Estimated *n* values in accordance with the real percentages of each nanocomposite film. By the application of the *de Vries* Equation with the tabled CD maximum peak wavelengths, the estimated pitch values are obtained.

Composition	**CNC**	**CNC/CA**	**CNC/HPC/CA**	**CNC/HPC/CA/XAzoCNC**						
				X=0.06	**X=0.1**	**X=0.19**	**X=0.25**	**X=1**	**X=2.5**	**X=5**
Estimated n	1.54	1.56	1.51	1.50	1.51	1.52	1.51	1.50	1.50	1.51
CD λ_0	254	265	493	507	478	468	394	363	342	209
Estimated Pitch value	165	170	327	337	317	310	317	241	227	138

JOHN WILEY AND SONS LICENSE
TERMS AND CONDITIONS
Jan 13, 2024

This Agreement between Ms. Inês Esteves dos Santos ("You") and John Wiley and Sons ("John Wiley and Sons") consists of your license details and the terms and conditions provided by John Wiley and Sons and Copyright Clearance Center.

License Number	5707110113141
License date	Jan 13, 2024
Licensed Content Publisher	John Wiley and Sons
Licensed Content Publication	Advanced Materials
Licensed Content Title	Photodeformable Azobenzene-Containing Liquid Crystal Polymers and Soft Actuators
Licensed Content Author	Yanlei Yu, Lang Qin, Chongyu Zhu, et al
Licensed Content Date	Oct 9, 2019
Licensed Content Volume	31
Licensed Content Issue	52
Licensed Content Pages	26
Type of use	Dissertation/Thesis
Requestor type	University/Academic
Format	Electronic
Portion	Figure/table
Number of figures/tables	1
Will you be translating?	No
Title of new work	Smart and stimuli-responsive materials based on nanocellulose
Institution name	NOVA School of Sciences and Technology of Lisbon
Expected presentation date	Jan 2024
Portions	Figure 1.a)
Publisher Tax ID	EU826007151
Total	0.00 EUR

TERMS AND CONDITIONS

This copyrighted material is owned by or exclusively licensed to John Wiley & Sons, Inc. or one of its group companies (each a"Wiley Company") or handled on behalf of a society with which a Wiley Company has exclusive publishing rights in relation to a particular work (collectively "WILEY"). By clicking "accept" in connection with completing this licensing transaction, you agree that the following terms and conditions apply to this transaction (along with the billing and payment terms and conditions established by the Copyright Clearance Center Inc., ("CCC's Billing and Payment terms and conditions"), at the time that you opened your RightsLink account (these are

available at any time at http://myaccount.copyright.com).

Terms and Conditions

- The materials you have requested permission to reproduce or reuse (the "Wiley Materials") are protected by copyright.
- You are hereby granted a personal, non-exclusive, non-sub licensable (on a stand-alone basis), non-transferable, worldwide, limited license to reproduce the Wiley Materials for the purpose specified in the licensing process. This license, **and any CONTENT (PDF or image file) purchased as part of your order,** is for a one-time use only and limited to any maximum distribution number specified in the license. The first instance of republication or reuse granted by this license must be completed within two years of the date of the grant of this license (although copies prepared before the end date may be distributed thereafter). The Wiley Materials shall not be used in any other manner or for any other purpose, beyond what is granted in the license. Permission is granted subject to an appropriate acknowledgement given to the author, title of the material/book/journal and the publisher. You shall also duplicate the copyright notice that appears in the Wiley publication in your use of the Wiley Material. Permission is also granted on the understanding that nowhere in the text is a previously published source acknowledged for all or part of this Wiley Material. Any third party content is expressly excluded from this permission.
- With respect to the Wiley Materials, all rights are reserved. Except as expressly granted by the terms of the license, no part of the Wiley Materials may be copied, modified, adapted (except for minor reformatting required by the new Publication), translated, reproduced, transferred or distributed, in any form or by any means, and no derivative works may be made based on the Wiley Materials without the prior permission of the respective copyright owner.**For STM Signatory Publishers clearing permission under the terms of the STM Permissions Guidelines only, the terms of the license are extended to include subsequent editions and for editions in other languages, provided such editions are for the work as a whole in situ and does not involve the separate exploitation of the permitted figures or extracts,** You may not alter, remove or suppress in any manner any copyright, trademark or other notices displayed by the Wiley Materials. You may not license, rent, sell, loan, lease, pledge, offer as security, transfer or assign the Wiley Materials on a stand-alone basis, or any of the rights granted to you hereunder to any other person.
- The Wiley Materials and all of the intellectual property rights therein shall at all times remain the exclusive property of John Wiley & Sons Inc, the Wiley Companies, or their respective licensors, and your interest therein is only that of having possession of and the right to reproduce the Wiley Materials pursuant to Section 2 herein during the continuance of this Agreement. You agree that you own no right, title or interest in or to the Wiley Materials or any of the intellectual property rights therein. You shall have no rights hereunder other than the license as provided for above in Section 2. No right, license or interest to any trademark, trade name, service mark or other branding ("Marks") of WILEY or its licensors is granted hereunder, and you agree that you shall not assert any such right, license or interest with respect thereto
- NEITHER WILEY NOR ITS LICENSORS MAKES ANY WARRANTY OR REPRESENTATION OF ANY KIND TO YOU OR ANY THIRD PARTY, EXPRESS, IMPLIED OR STATUTORY, WITH RESPECT TO THE MATERIALS OR THE ACCURACY OF ANY INFORMATION CONTAINED IN THE MATERIALS, INCLUDING, WITHOUT LIMITATION, ANY IMPLIED WARRANTY OF MERCHANTABILITY, ACCURACY, SATISFACTORY QUALITY, FITNESS FOR A PARTICULAR PURPOSE, USABILITY, INTEGRATION OR NON-INFRINGEMENT AND ALL SUCH WARRANTIES ARE HEREBY EXCLUDED BY WILEY AND ITS LICENSORS AND WAIVED BY YOU.
- WILEY shall have the right to terminate this Agreement immediately upon breach of this Agreement by you.
- You shall indemnify, defend and hold harmless WILEY, its Licensors and their respective directors, officers, agents and employees, from and against any actual or threatened claims, demands, causes of action or proceedings arising from any breach of this Agreement by you.

- IN NO EVENT SHALL WILEY OR ITS LICENSORS BE LIABLE TO YOU OR ANY OTHER PARTY OR ANY OTHER PERSON OR ENTITY FOR ANY SPECIAL, CONSEQUENTIAL, INCIDENTAL, INDIRECT, EXEMPLARY OR PUNITIVE DAMAGES, HOWEVER CAUSED, ARISING OUT OF OR IN CONNECTION WITH THE DOWNLOADING, PROVISIONING, VIEWING OR USE OF THE MATERIALS REGARDLESS OF THE FORM OF ACTION, WHETHER FOR BREACH OF CONTRACT, BREACH OF WARRANTY, TORT, NEGLIGENCE, INFRINGEMENT OR OTHERWISE (INCLUDING, WITHOUT LIMITATION, DAMAGES BASED ON LOSS OF PROFITS, DATA, FILES, USE, BUSINESS OPPORTUNITY OR CLAIMS OF THIRD PARTIES), AND WHETHER OR NOT THE PARTY HAS BEEN ADVISED OF THE POSSIBILITY OF SUCH DAMAGES. THIS LIMITATION SHALL APPLY NOTWITHSTANDING ANY FAILURE OF ESSENTIAL PURPOSE OF ANY LIMITED REMEDY PROVIDED HEREIN.
- Should any provision of this Agreement be held by a court of competent jurisdiction to be illegal, invalid, or unenforceable, that provision shall be deemed amended to achieve as nearly as possible the same economic effect as the original provision, and the legality, validity and enforceability of the remaining provisions of this Agreement shall not be affected or impaired thereby.
- The failure of either party to enforce any term or condition of this Agreement shall not constitute a waiver of either party's right to enforce each and every term and condition of this Agreement. No breach under this agreement shall be deemed waived or excused by either party unless such waiver or consent is in writing signed by the party granting such waiver or consent. The waiver by or consent of a party to a breach of any provision of this Agreement shall not operate or be construed as a waiver of or consent to any other or subsequent breach by such other party.
- This Agreement may not be assigned (including by operation of law or otherwise) by you without WILEY's prior written consent.
- Any fee required for this permission shall be non-refundable after thirty (30) days from receipt by the CCC.
- These terms and conditions together with CCC's Billing and Payment terms and conditions (which are incorporated herein) form the entire agreement between you and WILEY concerning this licensing transaction and (in the absence of fraud) supersedes all prior agreements and representations of the parties, oral or written. This Agreement may not be amended except in writing signed by both parties. This Agreement shall be binding upon and inure to the benefit of the parties' successors, legal representatives, and authorized assigns.
- In the event of any conflict between your obligations established by these terms and conditions and those established by CCC's Billing and Payment terms and conditions, these terms and conditions shall prevail.
- WILEY expressly reserves all rights not specifically granted in the combination of (i) the license details provided by you and accepted in the course of this licensing transaction, (ii) these terms and conditions and (iii) CCC's Billing and Payment terms and conditions.
- This Agreement will be void if the Type of Use, Format, Circulation, or Requestor Type was misrepresented during the licensing process.
- This Agreement shall be governed by and construed in accordance with the laws of the State of New York, USA, without regards to such state's conflict of law rules. Any legal action, suit or proceeding arising out of or relating to these Terms and Conditions or the breach thereof shall be instituted in a court of competent jurisdiction in New York County in the State of New York in the United States of America and each party hereby consents and submits to the personal jurisdiction of such court, waives any objection to venue in such court and consents to service of process by registered or certified mail, return receipt requested, at the last known address of such party.

WILEY OPEN ACCESS TERMS AND CONDITIONS

Wiley Publishes Open Access Articles in fully Open Access Journals and in Subscription journals offering Online Open. Although most of the fully Open Access journals publish open access articles under the terms of the Creative Commons Attribution (CC BY) License only, the subscription journals and a few of the Open Access Journals offer a choice of Creative Commons Licenses. The license type is clearly identified on the article.

The Creative Commons Attribution License
The Creative Commons Attribution License (CC-BY) allows users to copy, distribute and transmit an article, adapt the article and make commercial use of the article. The CC-BY license permits commercial and non-
Creative Commons Attribution Non-Commercial License
The Creative Commons Attribution Non-Commercial (CC-BY-NC)License permits use, distribution and reproduction in any medium, provided the original work is properly cited and is not used for commercial purposes.(see below)
Creative Commons Attribution-Non-Commercial-NoDerivs License
The Creative Commons Attribution Non-Commercial-NoDerivs License (CC-BY-NC-ND) permits use, distribution and reproduction in any medium, provided the original work is properly cited, is not used for commercial purposes and no modifications or adaptations are made. (see below)
Use by commercial "for-profit" organizations
Use of Wiley Open Access articles for commercial, promotional, or marketing purposes requires further explicit permission from Wiley and will be subject to a fee.
Further details can be found on Wiley Online Library http://olabout.wiley.com/WileyCDA/Section/id-410895.html

---

JOHN WILEY AND SONS LICENSE
TERMS AND CONDITIONS

Jan 13, 2024

This Agreement between Ms. Inês Esteves dos Santos ("You") and John Wiley and Sons ("John Wiley and Sons") consists of your license details and the terms and conditions provided by John Wiley and Sons and Copyright Clearance Center.

License Number	5707110476352
License date	Jan 13, 2024
Licensed Content Publisher	John Wiley and Sons
Licensed Content Publication	Advanced Functional Materials
Licensed Content Title	Healable, Stable and Stiff Hydrogels: Combining Conflicting Properties Using Dynamic and Selective Three-Component Recognition with Reinforcing Cellulose Nanorods
Licensed Content Author	Olli Ikkala, Oren A. Scherman, Eero Kontturi, et al
Licensed Content Date	Mar 4, 2014
Licensed Content Volume	24
Licensed Content Issue	18
Licensed Content Pages	8
Type of use	Dissertation/Thesis
Requestor type	University/Academic
Format	Electronic
Portion	Figure/table
Number of figures/tables	2

Will you be translating?	No
Title of new work	Smart and stimuli-responsive materials based on nanocellulose
Institution name	NOVA School of Sciences and Technology of Lisbon
Expected presentation date	Jan 2024
Portions	Fig.1c-b; Fig.7a-b
Publisher Tax ID	EU826007151
Total	0.00 EUR

TERMS AND CONDITIONS
This copyrighted material is owned by or exclusively licensed to John Wiley & Sons, Inc. or one of its group companies (each a"Wiley Company") or handled on behalf of a society with which a Wiley Company has exclusive publishing rights in relation to a particular work (collectively "WILEY"). By clicking "accept" in connection with completing this licensing transaction, you agree that the following terms and conditions apply to this transaction (along with the billing and payment terms and conditions established by the Copyright Clearance Center Inc., ("CCC's Billing and Payment terms and conditions"), at the time that you opened your RightsLink account (these are available at any time at http://myaccount.copyright.com).

Terms and Conditions

- The materials you have requested permission to reproduce or reuse (the "Wiley Materials") are protected by copyright.
- You are hereby granted a personal, non-exclusive, non-sub licensable (on a stand-alone basis), non-transferable, worldwide, limited license to reproduce the Wiley Materials for the purpose specified in the licensing process. This license, **and any CONTENT (PDF or image file) purchased as part of your order,** is for a one-time use only and limited to any maximum distribution number specified in the license. The first instance of republication or reuse granted by this license must be completed within two years of the date of the grant of this license (although copies prepared before the end date may be distributed thereafter). The Wiley Materials shall not be used in any other manner or for any other purpose, beyond what is granted in the license. Permission is granted subject to an appropriate acknowledgement given to the author, title of the material/book/journal and the publisher. You shall also duplicate the copyright notice that appears in the Wiley publication in your use of the Wiley Material. Permission is also granted on the understanding that nowhere in the text is a previously published source acknowledged for all or part of this Wiley Material. Any third party content is expressly excluded from this permission.
- With respect to the Wiley Materials, all rights are reserved. Except as expressly granted by the terms of the license, no part of the Wiley Materials may be copied, modified, adapted (except for minor reformatting required by the new Publication), translated, reproduced, transferred or distributed, in any form or by any means, and no derivative works may be made based on the Wiley Materials without the prior permission of the respective copyright owner.**For STM Signatory Publishers clearing permission under the terms of the STM Permissions Guidelines only, the terms of the license are extended to include subsequent editions and for editions in other languages, provided such editions are for the work as a whole in situ and does not involve the separate exploitation of the permitted figures or extracts,** You may not alter, remove or suppress in any manner any copyright, trademark or other notices displayed by the Wiley Materials. You may not license, rent, sell, loan, lease, pledge, offer as security, transfer or assign the Wiley Materials on a stand-alone basis, or any of the rights granted to you hereunder to any other person.
- The Wiley Materials and all of the intellectual property rights therein shall at all times remain the exclusive property of John Wiley & Sons Inc, the Wiley Companies, or their respective licensors, and your interest therein is only that of having possession of and the right to reproduce the Wiley Materials pursuant to Section 2 herein during the continuance of this Agreement. You agree that you own no right, title or interest in or to the Wiley

Materials or any of the intellectual property rights therein. You shall have no rights hereunder other than the license as provided for above in Section 2. No right, license or interest to any trademark, trade name, service mark or other branding ("Marks") of WILEY or its licensors is granted hereunder, and you agree that you shall not assert any such right, license or interest with respect thereto

- NEITHER WILEY NOR ITS LICENSORS MAKES ANY WARRANTY OR REPRESENTATION OF ANY KIND TO YOU OR ANY THIRD PARTY, EXPRESS, IMPLIED OR STATUTORY, WITH RESPECT TO THE MATERIALS OR THE ACCURACY OF ANY INFORMATION CONTAINED IN THE MATERIALS, INCLUDING, WITHOUT LIMITATION, ANY IMPLIED WARRANTY OF MERCHANTABILITY, ACCURACY, SATISFACTORY QUALITY, FITNESS FOR A PARTICULAR PURPOSE, USABILITY, INTEGRATION OR NON-INFRINGEMENT AND ALL SUCH WARRANTIES ARE HEREBY EXCLUDED BY WILEY AND ITS LICENSORS AND WAIVED BY YOU.
- WILEY shall have the right to terminate this Agreement immediately upon breach of this Agreement by you.
- You shall indemnify, defend and hold harmless WILEY, its Licensors and their respective directors, officers, agents and employees, from and against any actual or threatened claims, demands, causes of action or proceedings arising from any breach of this Agreement by you.
- IN NO EVENT SHALL WILEY OR ITS LICENSORS BE LIABLE TO YOU OR ANY OTHER PARTY OR ANY OTHER PERSON OR ENTITY FOR ANY SPECIAL, CONSEQUENTIAL, INCIDENTAL, INDIRECT, EXEMPLARY OR PUNITIVE DAMAGES, HOWEVER CAUSED, ARISING OUT OF OR IN CONNECTION WITH THE DOWNLOADING, PROVISIONING, VIEWING OR USE OF THE MATERIALS REGARDLESS OF THE FORM OF ACTION, WHETHER FOR BREACH OF CONTRACT, BREACH OF WARRANTY, TORT, NEGLIGENCE, INFRINGEMENT OR OTHERWISE (INCLUDING, WITHOUT LIMITATION, DAMAGES BASED ON LOSS OF PROFITS, DATA, FILES, USE, BUSINESS OPPORTUNITY OR CLAIMS OF THIRD PARTIES), AND WHETHER OR NOT THE PARTY HAS BEEN ADVISED OF THE POSSIBILITY OF SUCH DAMAGES. THIS LIMITATION SHALL APPLY NOTWITHSTANDING ANY FAILURE OF ESSENTIAL PURPOSE OF ANY LIMITED REMEDY PROVIDED HEREIN.
- Should any provision of this Agreement be held by a court of competent jurisdiction to be illegal, invalid, or unenforceable, that provision shall be deemed amended to achieve as nearly as possible the same economic effect as the original provision, and the legality, validity and enforceability of the remaining provisions of this Agreement shall not be affected or impaired thereby.
- The failure of either party to enforce any term or condition of this Agreement shall not constitute a waiver of either party's right to enforce each and every term and condition of this Agreement. No breach under this agreement shall be deemed waived or excused by either party unless such waiver or consent is in writing signed by the party granting such waiver or consent. The waiver by or consent of a party to a breach of any provision of this Agreement shall not operate or be construed as a waiver of or consent to any other or subsequent breach by such other party.
- This Agreement may not be assigned (including by operation of law or otherwise) by you without WILEY's prior written consent.
- Any fee required for this permission shall be non-refundable after thirty (30) days from receipt by the CCC.
- These terms and conditions together with CCC's Billing and Payment terms and conditions (which are incorporated herein) form the entire agreement between you and WILEY concerning this licensing transaction and (in the absence of fraud) supersedes all prior agreements and representations of the parties, oral or written. This Agreement may not be amended except in writing signed by both parties. This Agreement shall be binding upon and inure to the benefit of the parties' successors, legal representatives, and authorized assigns.
- In the event of any conflict between your obligations established by these terms and conditions and those established by CCC's Billing and Payment terms and conditions, these terms and conditions shall prevail.

- WILEY expressly reserves all rights not specifically granted in the combination of (i) the license details provided by you and accepted in the course of this licensing transaction, (ii) these terms and conditions and (iii) CCC's Billing and Payment terms and conditions.
- This Agreement will be void if the Type of Use, Format, Circulation, or Requestor Type was misrepresented during the licensing process.
- This Agreement shall be governed by and construed in accordance with the laws of the State of New York, USA, without regards to such state's conflict of law rules. Any legal action, suit or proceeding arising out of or relating to these Terms and Conditions or the breach thereof shall be instituted in a court of competent jurisdiction in New York County in the State of New York in the United States of America and each party hereby consents and submits to the personal jurisdiction of such court, waives any objection to venue in such court and consents to service of process by registered or certified mail, return receipt requested, at the last known address of such party.

WILEY OPEN ACCESS TERMS AND CONDITIONS

Wiley Publishes Open Access Articles in fully Open Access Journals and in Subscription journals offering Online Open. Although most of the fully Open Access journals publish open access articles under the terms of the Creative Commons Attribution (CC BY) License only, the subscription journals and a few of the Open Access Journals offer a choice of Creative Commons Licenses. The license type is clearly identified on the article.

The Creative Commons Attribution License

The Creative Commons Attribution License (CC-BY) allows users to copy, distribute and transmit an article, adapt the article and make commercial use of the article. The CC-BY license permits commercial and non-

Creative Commons Attribution Non-Commercial License

The Creative Commons Attribution Non-Commercial (CC-BY-NC)License permits use, distribution and reproduction in any medium, provided the original work is properly cited and is not used for commercial purposes.(see below)

Creative Commons Attribution-Non-Commercial-NoDerivs License

The Creative Commons Attribution Non-Commercial-NoDerivs License (CC-BY-NC-ND) permits use, distribution and reproduction in any medium, provided the original work is properly cited, is not used for commercial purposes and no modifications or adaptations are made. (see below)

Use by commercial "for-profit" organizations

Use of Wiley Open Access articles for commercial, promotional, or marketing purposes requires further explicit permission from Wiley and will be subject to a fee.

Further details can be found on Wiley Online Library http://olabout.wiley.com/WileyCDA/Section/id-410895.html

Other Terms and Conditions.

v1.10 Last updated September 2015

Questions? customercare@copyright.com.